AD-A094 791 CALIFORNIA INST OF TECH PASADENA GRADUATE AERONAUTIC--ETC F/G 6/16
HYGROVISCOELASTICITY OF THE HUMAN INTERVERTEBRAL DISC.(U)
JUL 80 W G KNAUSS AFOSR-77-3139
UNCLASSIFIED GALCIT-SM-80-18 AFOSR-TR-81-0084 NL

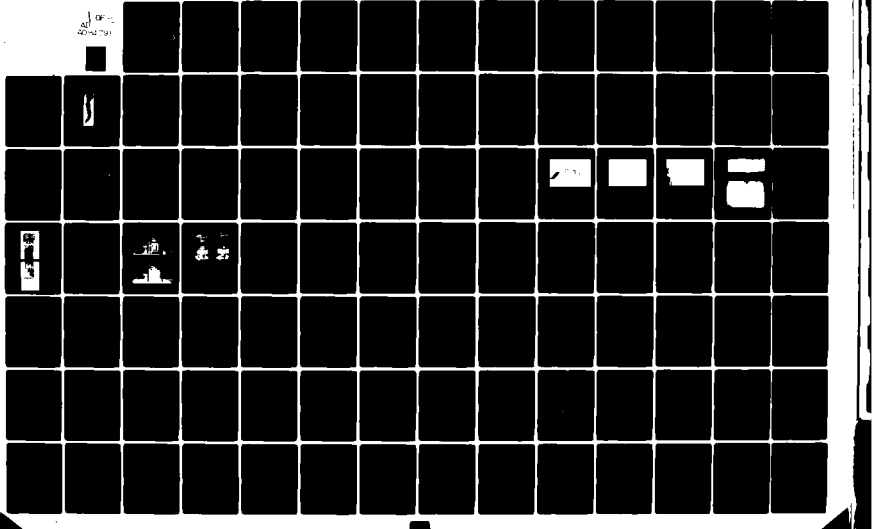

SECURITY CLASSIFICATION OF THIS PAGE (When Data Entered)

REPORT DOCUMENTATION PAGE

READ INSTRUCTIONS BEFORE COMPLETING FORM

1. REPORT NUMBER: AFOSR-TR-81-0084	2. GOVT ACCESSION NO.
3. RECIPIENT'S CATALOG NUMBER	
4. TITLE (and Subtitle): HYGROVISCOELASTICITY OF THE HUMAN INTERVERTEBRAL DISC	5. TYPE OF REPORT & PERIOD COVERED: Final
6. PERFORMING ORG. REPORT NUMBER: GALCIT-SM-80-17	
7. AUTHOR(s): W. G. Knauss	8. CONTRACT OR GRANT NUMBER(s): AFOSR-77-3139
9. PERFORMING ORGANIZATION NAME AND ADDRESS: California Institute of Technology, Graduate Aeronautical Laboratories, 105-50, Pasadena, CA 91125	10. PROGRAM ELEMENT, PROJECT, TASK AREA & WORK UNIT NUMBERS: 61102F, 2312/A2
11. CONTROLLING OFFICE NAME AND ADDRESS: Air Force Office of Scientific Research (NL), Bolling Air Force Base, Washington, D.C. 20332	12. REPORT DATE: July 1980
	13. NUMBER OF PAGES: 117
14. MONITORING AGENCY NAME & ADDRESS (if different from Controlling Office)	15. SECURITY CLASS. (of this report): Unclassified
	15a. DECLASSIFICATION/DOWNGRADING SCHEDULE

16. DISTRIBUTION STATEMENT (of this Report)

Approved for public release; distribution unlimited.

17. DISTRIBUTION STATEMENT (of the abstract entered in Block 20, if different from Report)

18. SUPPLEMENTARY NOTES

19. KEY WORDS (Continue on reverse side if necessary and identify by block number)

viscoelastic behavior, human intervertebral disc, spine shock

20. ABSTRACT (Continue on reverse side if necessary and identify by block number)

In an effort to develop non-invasive diagnostic tools such as x-ray tomography the mechanical properties of human disc material were studied. Special attention was given to the anisotropic layer structure of the disc annulus in studying lamella behavior as well as multi-layer averaging relaxation properties. Viscoelastic response is significantly affected by water concentration in the material, a fact that is of utmost importance for control in laboratory testing.

DD FORM 1 JAN 73 1473 EDITION OF 1 NOV 65 IS OBSOLETE

Unclassified 157700

SECURITY CLASSIFICATION OF THIS PAGE (When Data Entered)

AFOSR-TR- 81-0084

Final Report

to the

Air Force Office of Scientific Research

on

Hygroviscoelasticity of the Human Intervertebral Disc

by

W. G. Knauss

California Institute of Technology

Pasadena, California

91125

July 1980

Approved for public release;
distribution unlimited.

Graduate Aeronautical Laboratories - Report GALCIT SM 80-18

SUMMARY

In order to gain an improved understanding of the behavior of human intervertebral disc material under various kinds of loads the viscoelastic properties of small specimens excised from human L4-L5 discs were examined. Excisions were made from donated spine segments procured a few hours after death and then frozen. Material examined was in the form of single lamellar specimens as well as specimens containing several lamellae.

Tensile relaxation tests were performed on single lamellae prepared such that the collagen fibers were a) aligned with the tension axis, b) normal to the tension axis and c) at an angle of about 30° with that axis. The multi-lamellar specimens were excised from the disc such that one set produced the tensile axis to run parallel to the disc circumference (surrounding the spinal axis) while another set caused the tensile axis to run parallel to the spinal axis.

It was found early in the study that the water content of the disc material has a profound effect on its mechanical response. Consequently the diffusion and swelling characteristics of the material in different water environments were studied. Primarily air of differing relative humidity and various concentrated solutions of NaCl were used to provide for different water concentrations in the material.

For the relaxation studies the same environments were used. This allowed achieving water concentrations ranging from virtually dry to in-vivo conditions.

The main findings of this work are:

1) Water affects the relaxation time in a sensitive way. A few percent change in water content can change the relaxation time by an order of magnitude or more. This fact is important when one is concerned with laboratory testing without being able to control the water content at all times.
2) Diffusion is a surprisingly slow process taking place over several hours (2-3) in specimens only ½mm thick. The amount of water take-up is controlled by the environment (distilled water destroys samples into fissures) and by constraints offered by the fiber structure and the stresses it engenders (see point 5) below).
3) The stiffness of the disc material is on the order of 3 to 10 x 10^{-6} N/m^2; relaxation occuring, on the whole rather slowly, i.e., on the order of 10% per decade. The relaxation modulus at right angles to the collagen fibers is about 1/3 that of the modulus along the fiber direction.
4) The relaxation modulus of multi-layer specimens cut from the disc in a circumferential and a spine-axial direction are very nearly the same; the modulus for the circumferential material is slightly higher. The consequence of this would be that although one would expect a markedly

anisotropic behavior of the disc material on the basis of its fiber and lamellar construction, the disc material does not deviate very strongly from isotropic response. (Isotropy as referred to a plane that is tangent to the disc perimetric surface.)

5) Stress affects the equilibrium concentration of water in the material. The implication - and test result - is that once the stress has changed the equilibrium of water content with the environment is disturbed and the concentration changes. That change, in turn, causes a change in relaxation behavior such that tensile stresses cause an acceleration of relaxation or creep (softening), while compression would cause the opposite affect (hardening). The material responds thus to stress as a system that is open to the environment.

1. PUBLICATIONS AND REPORTS

1. Panagiotacopulos, N. D., Bloch, R., Knauss, W. G., Harvey, P., and Patzakis, M.; On the Mechanical Properties of the Human Intervertebral Disc; California Institute of Technology, Pasadena, CA 91125; GALCIT SM 78-13; AFOSR-TR-0054; 1978.
2. Panagiotacopulos, N. D., Knauss, W. G., and Bloch, R.; On the Mechanical Properties of Human Intervertebral Disc Material; Biorheology Vol. 16, 317-330; 1979.
3. Knauss, W. G., Kenner, V. H.; A Technique to Measure Poisson Contraction in Small Biological Specimens; California Institute of Technology, Pasadena, CA 91125; GALCIT SM 80-2; 1980.
4. Knauss, W. G.; Hygroviscoelastic Behavior of Human Intervertebral Disc Material; California Institute of Technology, Pasadena, CA 91125; GALCIT SM 80-14; 1980. (in preparation).

2. PROFESSIONAL STAFF ASSOCIATED WITH THIS RESEARCH EFFORT

The program was staffed by several coworkers:

N. Panagiotacopulos, Member of the technical staff at the Jet Propulsion Loboratory of the California Institute of Technology.

Dr. R. Bloch, Research Fellow.

Dr. V. H. Kenner, Senior Research Fellow.

Dr. W. G. Knauss, Professor.

R. Calvet, Graduate student.

S. Chang, Graduate student.

Prof. P. Harvey, Chairman of Orthopedics, USC Medical School, Los Angeles, CA.

Prof. M. Patzakis, Orthopedics, USC Medical School, Los Angeles, CA.

3. INTRODUCTION

The spine is a lineal assembly of vertebrae which are connected to each other via intervertebral "discs"; this assembly is sheathed in ligaments and muscles. The main function of the spine is to support the weight of the body and to transmit it to the legs. The flexibility of the spine is provided solely by the "discs" which make up, in total, about 1/4 of the length of the spine. In the human body the cumulative weight of the erect body loads the discs in the lumbar region most highly which fact is recognized to lead to a relatively large number of back disorders. In fact, a recent article in Time magazine [1] reports that "In the U.S. alone, as many as 75 million Americans have back problems, and there are 7 million new victims each year. Of these, 5 million are partly disabled and 2 million are unable to work at all."

While these estimates seem on the high side [2,3] they nevertheless point up the seriousness and prevalence of the problem for individuals in all walks of life; obviously, certain professions generate still higher percentages of back problems amongst which all those associated with high spine-axial accelerations (jumping by paratroopers, aircraft seat ejection, horseback riding) and/or spinal twist (certain sports) are particularly prone to lead to mechanical problems of the spine.

A recurring problem is that of the "herniated disc" often improperly called a "slipped disc"; this condition results from the extrusion of the jelly-like material (nucleus pulposus) from the center of the disc (vide infra) through the "disc wall" (annulus fibrous). This extrusion occurs most frequently in the posterior portion of the disc and results often in painful pressure on the spinal nerves.

When high mechanical loads act on a "disc" it is also possible that the jelly-like nucleus penetrates into one or both of the adjacent vertebral bodies giving rise to Schmorl's nodes. This type of damage does not generally, per se, lead to pain symptoms, but because the phenomenon can change the overall stiffness of the disc, spinal deformation may localize at this damaged junction; thus it can readily lead to the deterioration of the disc and subsequent severe problems.

Because present diagnostic tools (myelography, discography, electromyography) are not without detrimental side effects it was deemed desirable to examine alternate methods. In particular, low intensity x-ray coupled with computer aided image enhancement seemed a promising avenue. Because such a method would play directly on the deformation of a disc under differing body attitudes and loads it appeared mandatory to better understand the deformation properties of disc material in order to distinguish between the deformations of healthy and defective discs. It was this basic thought which motivated this work from the beginning.

The special problem of disc herniation is primarily a mechanical problem of failure and the proclivity to herniation with age depends on the biochemical changes that occur in the material of the disc during its maturation process. However, a careful machanics-based analysis of failures adequate to the need is not available today. It seems to us that the treatment, as well as the possible prevention of the disc herniation problems, would be greatly aided by an improved understanding of the mechanical behavior of the human intervertebral disc under various modes of deformations of the human spine.

A review of the work done in this field has shown that, so far, experimental work on the human intervertebral disc has been carried out on autopsy specimens, such as segments of the spine consisting of two vertebral bodies with their intervening disc or small sections of the annulus fibrosus (Ref. 2). Most of these experiments were intended to obtain mechanical properties of the <u>total disc</u>, assuming that the disc material exhibits <u>elastic</u> behavior. However, to the best of our knowledge, only three experiments (Refs. 4-6) not including our experiments, recognize the viscoelastic behavior of the disc. To date, no use has been made of this observation in performing structural analyses of the disc.

In studying the viscoelastic properties of the disc, we observed that the water content of the disc material is important in that it controls the relaxation behavior of the material. This was done by subjecting small sections of the disc's

lamellae to simple tension tests. Based on these requirements, as well as on data obtained from a literature review, and on the fact that the water content of the disc decreases with age (Refs. 7-11), a qualitative hydrorheological model for the behavior of the disc's material has been proposed. [Ref. 12, Appendix I] This model, although qualitative, provides a possible basis for discussing the maturation of the disc. In the follow-on work presented here we check the validity of this model.

A principal effect of water on the disc material is to influence its viscoelastic response; in addition varying amounts of water concentration provoke dimensional changes. Because the total disc is a rather inhomogeneous structure this latter effect will produce signigicant inhomogeneous stress distributions when complete discs attached to adjacent vertebrae are hydrated as observed by a number of investigators [13-15]. Since laboratory work is always conducted with artificially hydrated material we have studied here some of these characteristics.

The present work covers several topics germane to the hygromechanical behavior of the disc materials. Accordingly we divide this report into several sections that deal with specific issues.

Following a brief anatomical review of the disc structure we delineate some special problems associated with the testing of the very small specimen samples used in this study and the next section is concerned with the interaction of the stress

free disc material with water. The major section is concerned with the viscoelastic response of the hydrated disc material and a section on an approximate stress analysis of the disc concludes the body of this report.

Because a portion of this work has already appeared in the open literature or has been submitted for publication those presentations are attached in the form of appendices rather than report them again in a different form.

4. ANATOMICAL AND BIOCHEMICAL REVIEW

The human vertebral column is formed by a series of 33 vertebrae:

(1) 7 cervical (neck region)

(2) 12 thoracic (chest region)

(3) 5 lumbar (low back region)

(4) 5 sacral

(5) 4 coc‹ gal.

The cervical, thoracic, and lumbar vertebrae remain distinct and separate from each other throughout life. They are considered as movable vertebrae and are separated from each other by intervertebral discs. In contrast, adult sacral and coccygeal vertebrae are fused with each other to form two bones, the sacrum and the coccyx. Figure 1 shows a lateral view of the vertebral column in the erect position together with the names and locations of its basic constituents.

It is customary to distinguish three domains of the disc, though the demarkation of these domains is not sharp:

(1) The annulus fibrosus

(2) The nucleus pulposus

(3) The cartilaginous end plates.

Each disc is named by the two surrounding vertebrae; for example, the disc L4-L5 is surrounded by vertebrae L4 and L5.

The Annulus Fibrosus: The annulus fibrosus is the outer fibrous part of the intervertebral disc (Figures 2(a) and 2(b)).

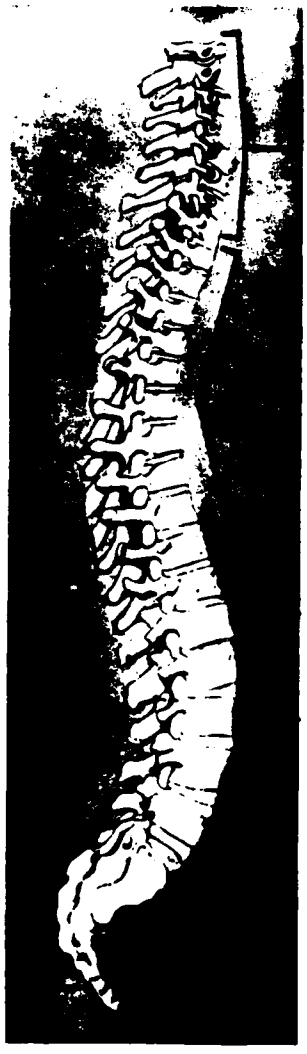

FIGURE 1 Lateral View of Vertebral Column

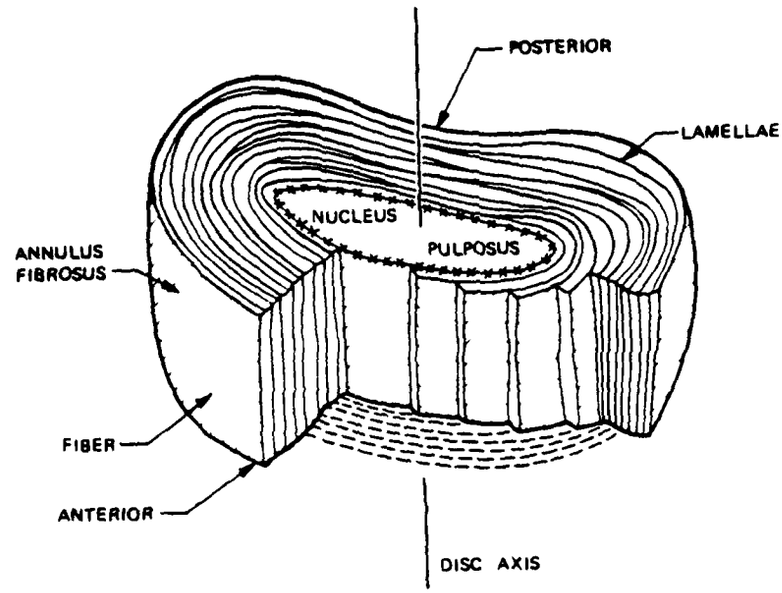

(a)

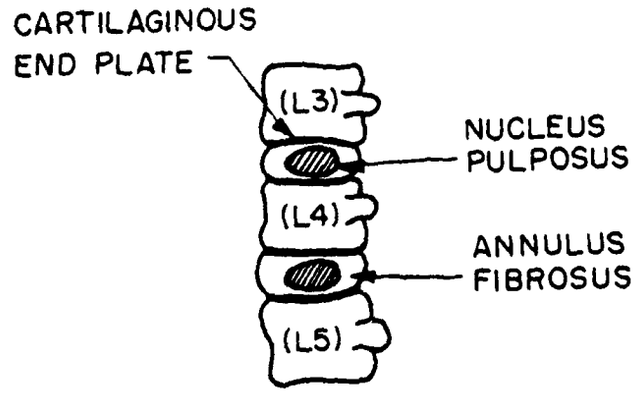

(b)

FIGURE 2 Schematic Representation of the Human Intervertebral Disc and Vertebral Bodies

Although it has been reported that the annulus fibrosus is formed by 12-14 concentrically arranged lamellae, in our laboratory we have observed that this number may be considerably larger. A lamella is defined as a layer from the disc's annulus fibrosus in which collageneous fibers are contained in a mucopolysaccharide matrix.

In order to give an approximate representation of the lamellar arrangement as far as the direction of the fibers is concerned, let us consider two adjoining lamellae. In each lamella the fibers run approximately parallel to each other. In one the fibers form an angle of approximately $+50^{o}$ to $+60^{o}$ with respect to the disc axis as illustrated in Figure 2(a); in the next one the fibers form an angle -50^{o} to -60^{o}. Figure 2(a) gives a simplified schematic representation of the layered structure of the inhomogenious disc.

In the lumbar region the lamellae vary in thickness from tenths to several millimeters (Ref. 4). It is thicker anteriorly (front of the disc) where the lamellae are more numerous than posteriorly (rear of the disc). It is worth mentioning that some interweaving is present between adjoining posterior lamellae. The outermost lamellae attach themselves to the bony edge of the vertebral body (bony epiphyseal ring) while the rest continue into the cartilaginous plates. (c.f. fig. 2(b)) In the front, intimate connections exist with the anterior longitudinal ligament, while the posterior longitudinal ligament is less firmly attached to the annulus.

The Nucleus Pulposus

The nucleus pulposus is centrally situated (Figures 2(a) and 2(b)) it consists of a three dimensional network of non-oriented collagen fibrils enmeshed in a mucoprotein gel and occupies about 25-50% of the disc volume.

The Cartilaginous End-Plates

The cartilaginous end-plates (Figure 2(b)) connect the disc with the vertebral bodies above and below. Peripherally they are attached to the bony epiphyseal ring.

The Disc Shape and Dimensions

The disc is somewhat kidney-shaped. However, it appears that the pattern of the disc shape varies considerably from individual to individual or even in the same individual. The following parameters shown in Figure 3 are normally used to characterize the disc's geometry. They are its major diameters (B, b), its minor diameters (D, d) and its height (h).

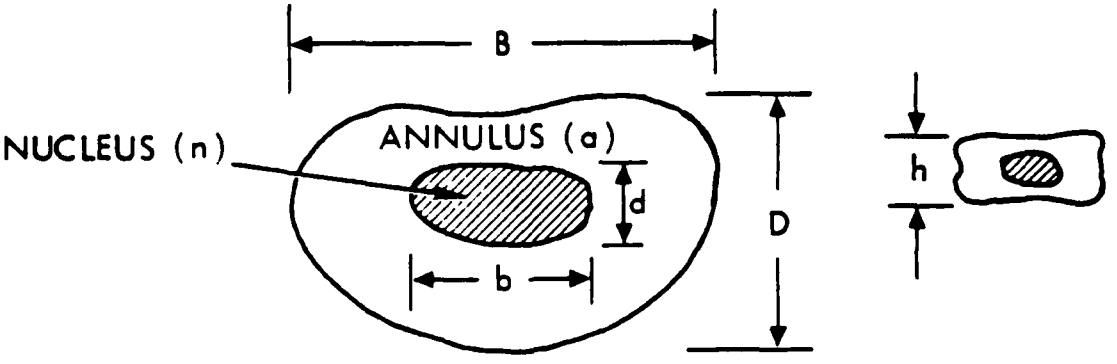

FIGURE 3 Parameters Characterizing the Disc's Geometry

In Table 1. some measurements for these parameters taken from radiographs of lumbar intervertebral discs are presented.

TABLE 1. Typical Lumbar Intervertebral Disc Dimensions

Disc Level	Major Diameter (cm)		Minor Diameter (cm)		Vertical Disc Height (cm)
	Disc	Nucleus	Disc	Nucleus	
L1-L2	5.26	2.83	3.81	1.78	.69
L2-L3	5.46	2.67	3.81	1.55	.87
L3-L4	2.57	2.64	3.58	1.71	.82
L4-L5	5.59	2.54	3.86	1.49	.96

The Vertebral Bodies and the Ligaments

The Vertebral Bodies: The somewhat kidney-shaped vertebral body (Figure 4) consists of an outer shell of dense bone about 0.5 mm thick. The inner portion of the body is composed of trabecular or spongy bone. Its upper and lower flattened, slightly concave surfaces are covered by the vertebral end plates which are approximately 1 mm thick.

The Ligaments: The vertebral bodies and the intervertebral discs are surrounded by fibrous bands in tension called ligaments. The names and locations of these ligaments are shown in Figure 5.

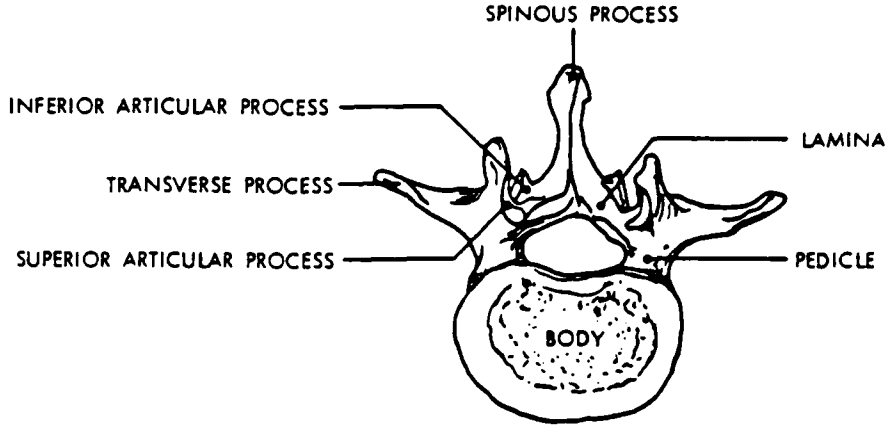

(a) Top View

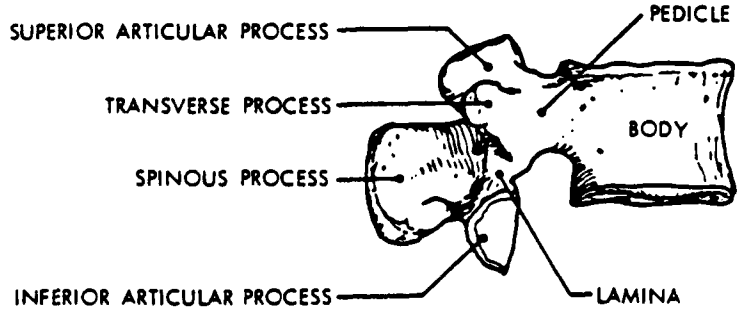

(b) Side View

FIGURE 4 A Typical Lumbar Vertebra

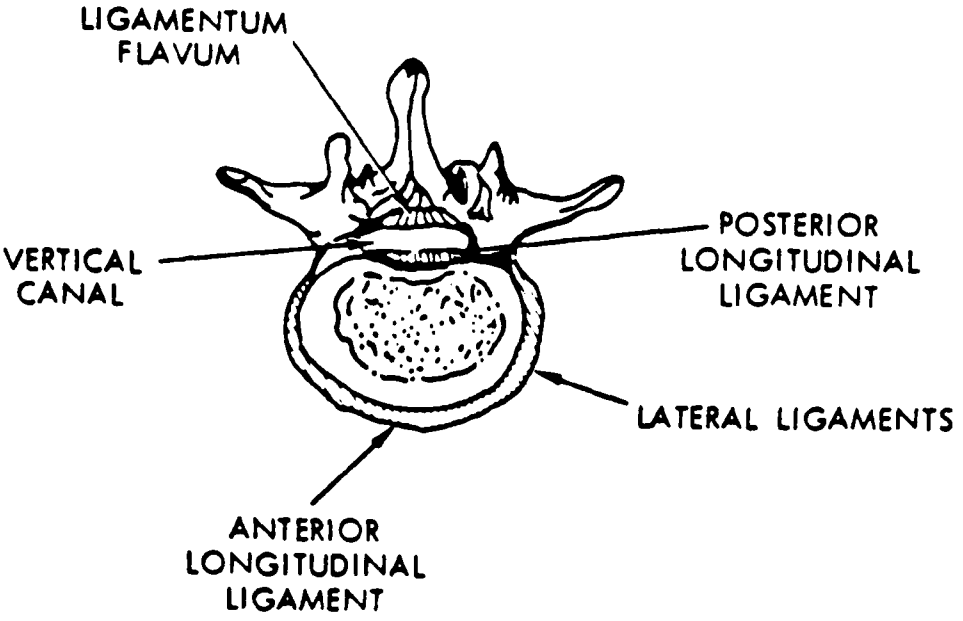

(a) Top View

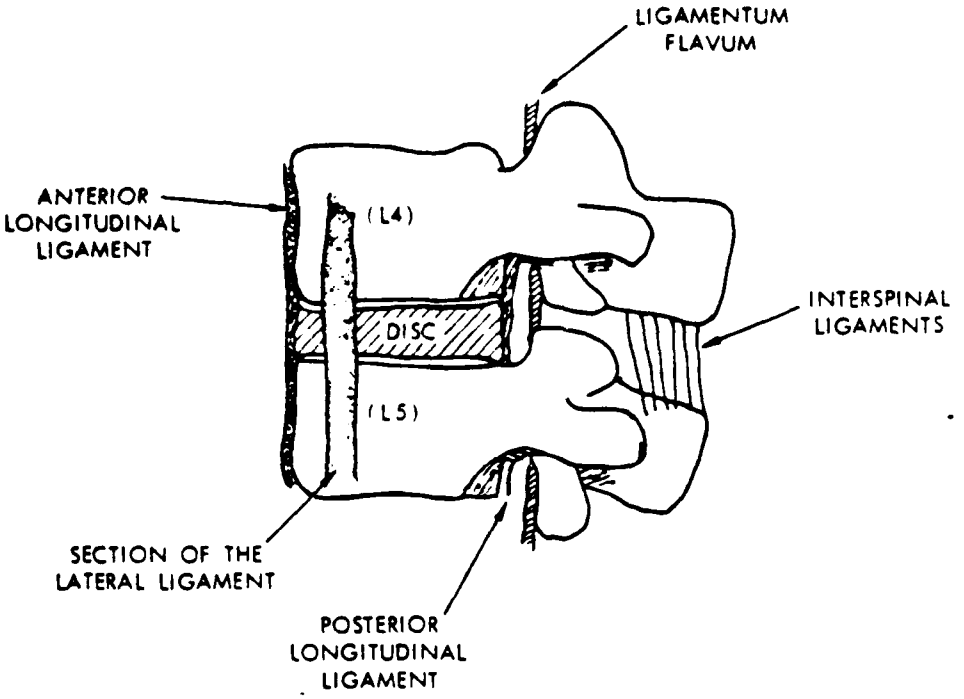

(b) Side View

FIGURE 5 The Ligaments

The Anterior Longitudinal Ligament: The anterior longitudinal ligament (Figure 5) is a broad strong band of fibers extending along the anterior surfaces of the vertebral bodies. Essentially, it consists of 3 layers of dense fibers, all of which run in a longitudinal direction. The innermost layer extends from one vertebra to the next, adhering intimately to the intervertebral discs and the epiphyseal ring. It blends with the outer fibers of the annulus and cannot be separated from it easily. The middle layer extends between 2 or 3 vertebrae, and the outermost is the longest and extends over 4 or 5 vertebrae.

The Posterior Longitudinal Ligament: The posterior longitudinal ligament (Figure 5) lies within the vertebral canal, extending along the posterior surfaces of the vertebral bodies. It consists of 2 layers; the outermost layer extends over 3 or 4 vertebrae, and the inner layer extends between adjacent vertebrae. It is considered to be a much more delicate (thinner) structure than the anterior one.

The Lateral Vertebral Ligament: The lateral vertebral ligaments (Figure 5) are situated between the anterior and posterior longitudinal ligaments. They consist of fibers firmly attached to the intervertebral discs and apparently less firmly to the vertebral bodies.

The Ligamentum Flavum: This is a structure composed of thick (3 mm), strong fibers. It bridges the gap between the

edges of two adjacent laminae as also shown in Figure 5.

The Interspinal Ligaments: These ligaments are fibers which connect the root of one spinous process to the tip of the next. Although they are thin and membranous in the cervical and thoracic areas of the spine, they are thick and well developed in the lumbar region.

In addition various muscles attach to the spinal column, but their function was not considered important in this study.

Blood Supply of the Intervertebral Disc

It has been reported that in children and young adults one can find small blood vessels within the periphery of the cartilaginous end-plates. These vessels gradually disappear so that probably by the beginning of the second decade the intervertebral disc is found to be completely evascular. There are only a few small vessels in the outermost layers of the ligaments, but these vessels never penetrate into the annulus.

The disc's limited nutritional demands are probably fulfilled by the diffusion of lymph from the marrow cavity to the cartilaginous end-plates, which permits some lymph supply to diffuse through the disc.

As was described earlier, the structure of the disc lamella consists of collageneous fibers embedded in a mucopolysaccharide matrix. Next we document some general information regarding the disc's biochemical constituents.

Collagen

The collagen fibers appear as bundles of individual non-branching fibrils. The structure of the fibrils consists of a core and an annulus as is shown in Figure 6.

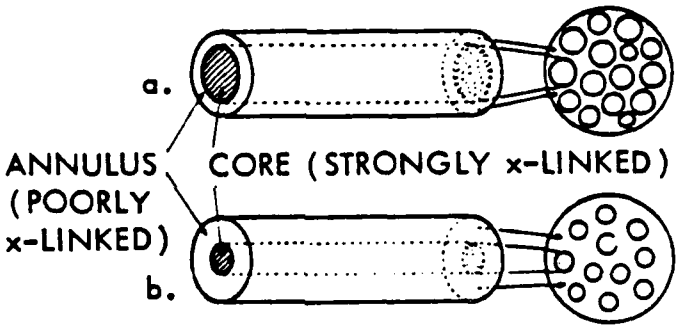

(a) Old Fibril

(b) Young Fibril

FIGURE 6 Structure of a Fibril

Electron microscope studies have shown that in a given fiber the diameter of the fibril's core increases with age at the expense of the fibril's annulus, as shown in Figure 6.

The fibrils are made of tropocollagen molecules. Each tropocollagen molecule is composed of three strands forming a

triple helix. Each strand is made of amino acids with glycine, proline, and hydroxyproline being the primary ones. The amino acid composition of the tropocollagen molecules appears to be almost constant with age. Fibril growth and development occurs by accumulating newly formed tropocollagen molecules on its surfaces. Furthermore, it is accepted that the tropocollagen molecules are strongly bonded between themselves (highly cross-linked) in the core area and more poorly cross-linked in the fibril's annulus. Therefore, the "annulus" will be narrower in older fibrils than in younger ones. It seems to follow that old fibril cores are stiffer than young ones by virtue of the increased crosslink density. As growth continues, the fibril will tend toward complete three-dimensional cross-linking and the "annulus" will decrease until the whole fibril is uniformly cross-linked.

The Mucopolysaccharides

According to Reference 4, mucoploysaccharides are composed of: Hyaloronic Acid, chondroitin sulfate (A, B, C), heparitin sulfate, keratosulfate, and heparin. The majority of these mucopolysaccharides appear to be nonbranched amorphous polymers. They are covalently bound to proteins resulting in a compound called protein-polysaccharides or mucoprotein. To the best of our knowledge, the variation of these compounds with age is not known for the human intervertebral disc material. However, for the case of the skin where similar components are

present, it is known that the percentage of hyaloronic acid decreases and the percentage of chondroitin sulfates increases with age.

Some of the functions of the mucoproteins are:

(1) To Stabilize Mechanically the Collagen Fibrils. The mucoproteins act as the bonding agent between the collagen fibrils as shown in Figure 7.

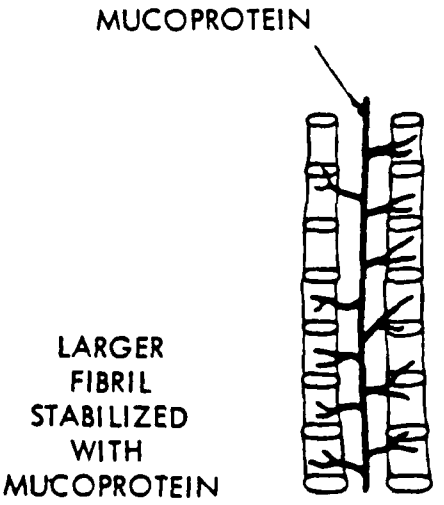

FIGURE 7 Stabilization of Collagen Fibrils (Schematic)

(2) To Bind Water. These high molecular weight polymers trap large amounts of water within their domain, an important factor in determining their physical and mechanical properties.

(3) To Control the Synthesis of Collagen.

The Chemical Constituents of the Human Intervertebral Disc

Dickson, Naylor et al reported the percentage of hydroxyproline, and thus the collagen content, as a function of age (3-89 years) for dry nucleus pulposus and annulus fibrosus (Ref. 7). They found that in the nucleus pulposus, the hydroxyproline content remains fairly constant after the age of 10 until the age of 65 and then decreases slightly. They reported that in the annulus fibrosus the percentage of hydroxyproline decreases until the age of 62 and then remains constant. The mucopolysaccharides are present in larger amount in the nucleus and their highest level is reached in the 30-40 age group, declining to its lowest level in later years. Moreover, they found that for a ruptured disc in a younger man, the hydroxyproline content (or collagen) of both nucleus and annulus was increased and their mucoploysaccharide content was reduced. (Ref. 8). This is consistent with what is found in nonruptured discs from older individuals. Lyons et al felt that disc degeneration represents a premature aging process (Ref. 9). Also there is little doubt that severe damage in the disc material is a manifestation of excessive production and aberrant arrangement of collagen in the affected disc material. Many of the chemical details of the various processes related to the synthesis and deterioration of these constituents are not yet known.

Besides these relatively solid components, the disc contains a large amount of water (trapped by the mucoprotein macro-

molecules as discussed earlier) which influences strongly its mechanical response characteristics. The following table gives the approximate water variations in the disc as a function of age (Ref 4).

TABLE 2. Approximate Water Variations in the Human Intervertebral Disc

Age	At birth	By age 30	By age 75
Nucleus Pulposus	88%	decreased to 65% (gradually)	still 65%
Annulus Fibrosus	78%	decreased to 70% (gradually)	70%

Puschel indicated that the water content of the disc decreases progressively with age (Ref. 10). Later DePukey reported that the average person is one percent shorter at the end of the day than in the morning on first rising (Ref. 11). It was observed that the average daily change in body length is two percent in the first decade and only 0.5 percent in the eighth decade. DePuky attributed this difference in age-related response to the decreasing water content of the disc.

Some Lumbar Intervertebral Disc Problems

Its unique construction and composition enable the disc to withstand stresses varying in duration and magnitude. We may think of the annulus as a flexible pressure vessel with the less structured nucleus as the pressure medium. Its nearly incompressible behavior converts the spine-axial load into (tangential) tension stresses in the annulus. The disc's reaction to pressure is nicely demonstrated in Figure 8.

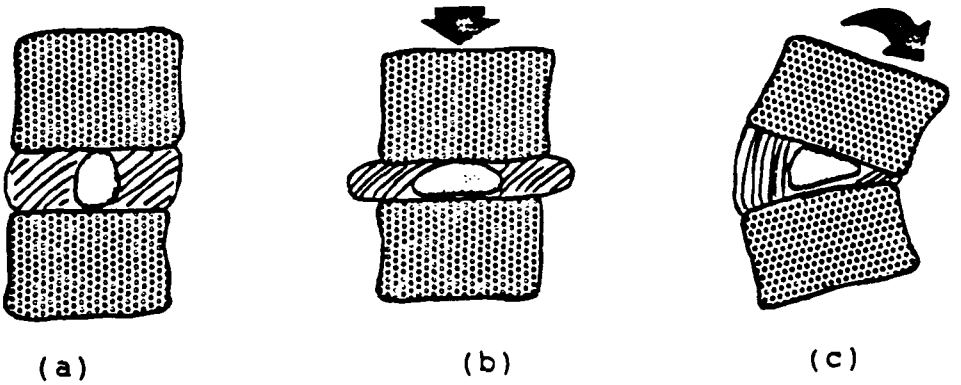

FIGURE 8 The Rection of the Disc to Pressure (After Cailliet)

As one can see, the normal disc has a rounded well-hydrated intact nucleus (Figure 8(a)) and under normal pressure maintains normal vertebral separation. Compression deforms the nucleus and "bulges" the annulus physiologically (Figure 8(b)). Flexion or extension deforms the disc nucleus and permits the motion (Figure 8(c)). Upon release of compression or bending forces, the disc resumes its normal position as a result of the intrinsic intervertebral disc pressure and elasticity of the disc material.

Somehow, in a still unkown way, the above mentioned physiological behavior is perturbed, subsequently allowing the spinal axial load to cause ruptures. Furthermore, biochemical changes due to aging or early maturation of the disc may be the cause of another problem known as disc degeneration.

Ruptures

Annular Rupture: The annular rupture (frequently referred to as disc herniation) of the disc is shown in Figure 9(a). It is the extrusion of material from the nucleus pulposus through the posterior part of the disc. This extrusion can cause pain by pressing on nerve endings in the ligamentous layers surrounding the vertebrae, or on the spinal nerve.

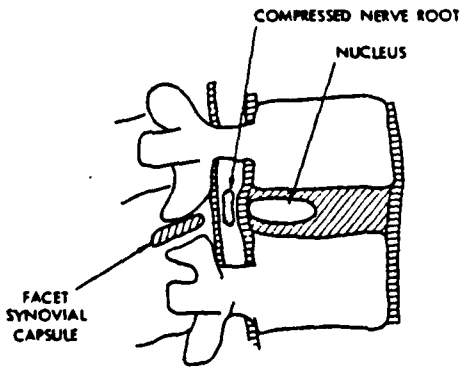

FIGURE 9(a) Annular Disc Rupture (Herniated Disc)

End-Plate Rupture (Schmorl's Node): This pathological occurence is defined as the penetration of nuclear material through the cartilaginous end plates into the spongy bone of the vertebral body (Figure 9(b)).

FIGURE 9(b) Schematic Representation of Schmorl's Node

Disc Degeneration: Degeneration of the disc implies dehydration and fragmentation of the lamellae with some radial tearing. The nucleus material escapes into the adjacent annulus and loses its intradiscal pressure thus allowing the narrowing of the intervertebral space (Figure 10). This narrowing can cause the posterior facets to touch each other producing a crushing of their synovial capsule and consequently pain. This problem may occur as a result of aging or repeated injuries associated with overloading.

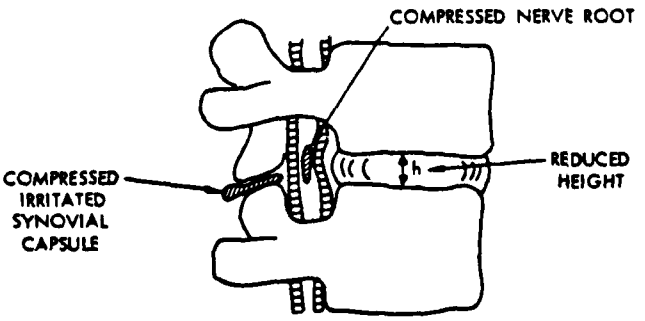

FIGURE 10 Degenerated Disc

Diagnostic Techniques Presently in Use: In combatting the spine problems discussed earlier, reliable diagnostic methods are needed for their identification. Presently, the techniques in use are: exterior physical examination, and conventional radiograms of the spine. Neither of these has proved to be really satisfactory.

Let us briefly now look at these techniques and the problems associated with them.

The exterior physical examination is based on testing joint motions in the back and the legs. In addition, the neurological activity is checked by testing the muscle and sensory response. Although low back pain is a very well-recognized symptom, disc herniation is not always a cause of this pain. On the other hand, disc herniation may occur at sites where nerve roots do not exist, so that pain is not always associated with this problem.

Conventional diagnostic radiograms, necessary in the clinical evaluation of all patients with such problems, are based on measurements of the space between vertebral bodies. Unfortunately, these measurements do not allow a satisfactory diagnosis of the problem. That is, in the majority of patients, the specific cause of low back pain is not always clearly demonstrated by these radiograms. In addition, these radiograms can show, very faintly, some features of the intervertebral disc only if properly taken. Presently, the only way to improve the diagnosis of such problems is by the use of contrast

producing materials. More precisely, a better visualization of the spinal canal, and indirectly of the disc, is usually achieved by means of myelographic studies (Ref 4). When myelography is performed, a radiopaque substance, heavier than the spinal fluid, is introduced via a needle into the subarachnoid or spinal canal space. By tilting the patient up and down under fluoroscopic guidance, one can follow the column of dye along the length of the spine; if, as illustrated in Figure 11, a bulge or other irregularity exists, such occurrence may be taken as evidence of disc herniation. Myelography is used on a routine basis prior to lumbar disc surgery, even though it is not an accurate detection method (it is claimed that the method is 80-85% accurate). For instance, in some cases the myelogram was interpreted as nonrevealing, although surgery revealed a disc protrusion.

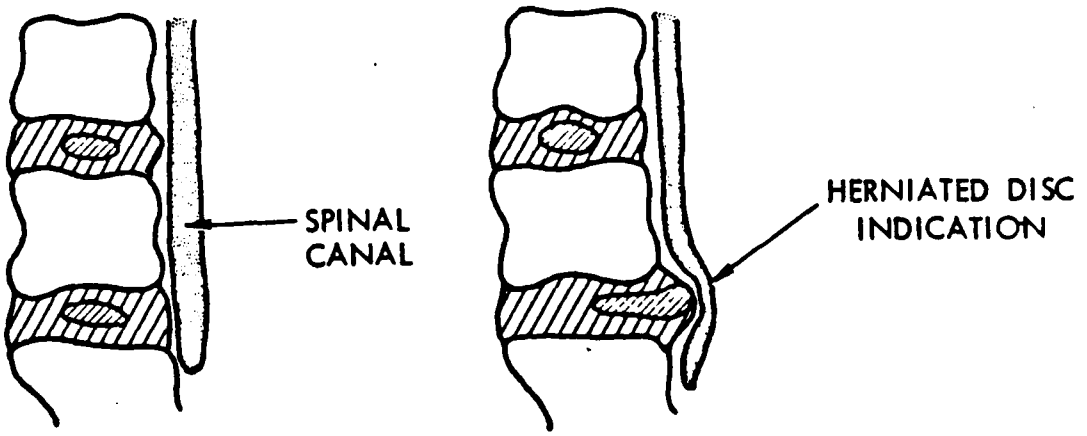

FIGURE 11 Schematic Representation of (a) Normal, and (b) Herniated Disc Myelograms

Furthermore, faulty lumbar puncture techniques used in the myelogram may deposit radiopaque substance outside the sub-aracnoid space making removal much more difficult and at times impossible. Several reports of more severe and even fatal reactions attributed to a unique hypersensitivity to the radiopaque substance have appeared in the literature. As a result of the increased sensitivity to this radiopaque material, a widespread aseptic leptomeningitis may occur, involving not only the spine but extending into the brain, with some cases terminating in death.

The low frequency of occurrence of these tragedies makes it impossible to establish reasonable criteria to prevent similar future complications. Intradermal radiopaque skin tests have been used, but have proven to be unreliable. Until satisfactory guidelines can be developed, patients with a severe allergic background, including a specific allergy to iodine, should probably not have radiopaque myelography. However, at present there is research going on in the development of safer contrast materials which will reduce these dangers.

5. SPECIMEN PREPARATION

Small tensile specimens were cut from discs for different purposes: In order to study the behavior of the material in different humidity environments, relatively large lamellae were cut from the anterior disc circumference. To study the relaxation behavior still smaller specimens were cut from such laminae with fibers running either parallel or perpendicular to the long axis of the specimen. In addition to "single" laminae multilayer specimens were examined. For later reference we use the definitions in figure 12 to identify specimens and their orientation on the disc.

Discs were supplied* from unclaimed bodies within a few hours after death. All specimens used in this study were sectioned from L4-L5 discs. The disc with adjoining vertebral bodies were held in the fixture shown in figure 13 which allowed application of axial tension via a footpedal to the assembly while still permitting rotation around the normal axis; experience showed both capabilities to be necessary for separating off the thin (0.3-0.5 mm) lamina specimens. This microsurgical procedure was carried out under a stereo microscope possessing a long focal length.

In figure 14 we show a sagittal section through the annulus fibrosus of a disc from which specimens for testing have been

---

*We are greatly indebted to Professor P. Harvey and M. Patzakis of the USC Medical School for making the specimens available.

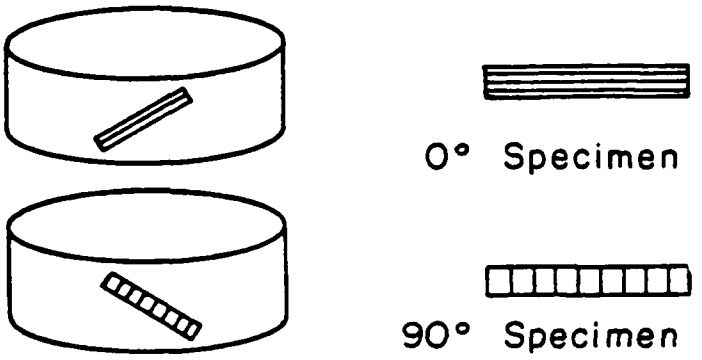

Single Layer (Laminate) Specimens

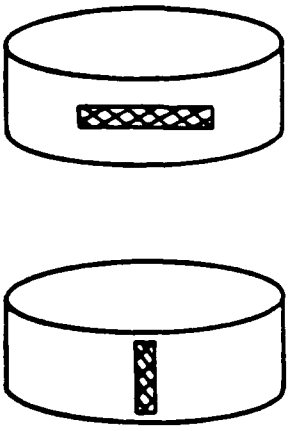

FIG.12 NOMENCLATURE FOR SPECIMEN ORIENTATION IN DISCS

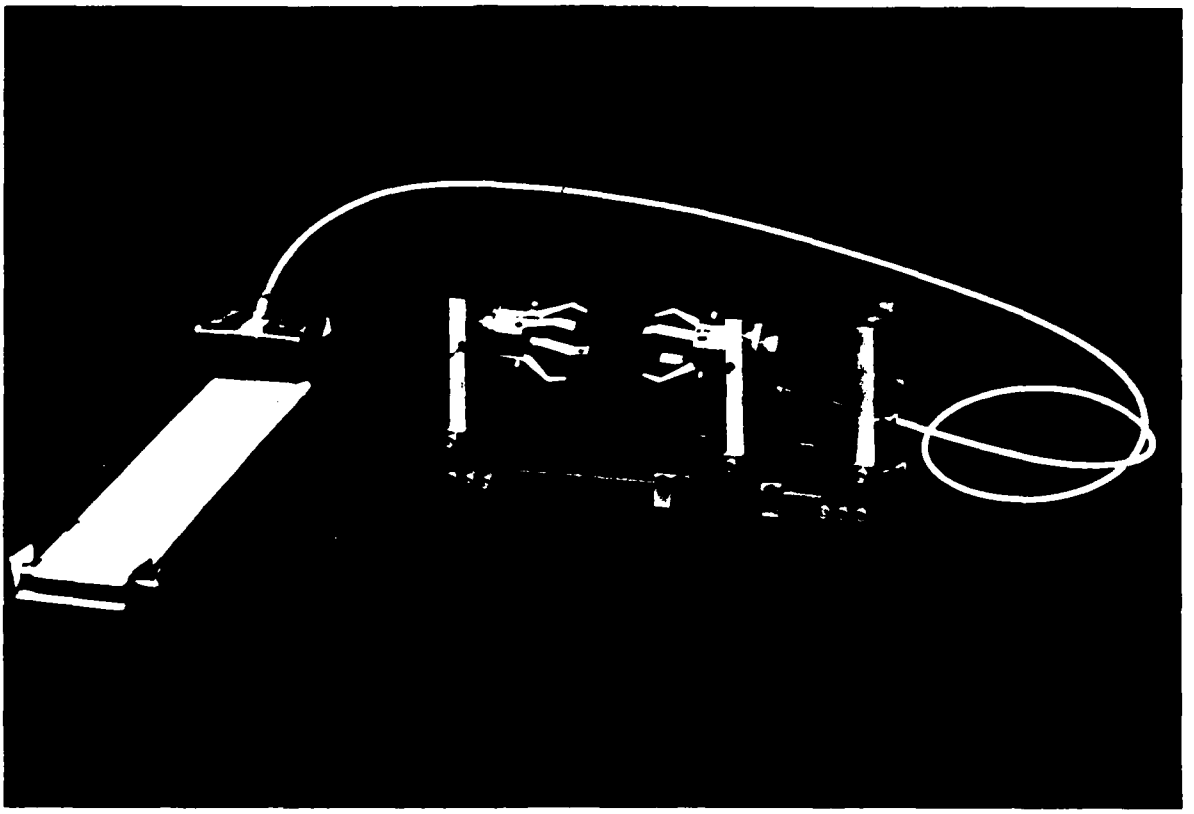

FIGURE 13 Fixture for Holding and Sectioning Discs

cut. It gives an indication of the relatively clear separation between laminae. In figure 15 we show a tensile specimen (under zero load) cut in the circumferential manner without an attempt at clearly excising a single lamina, exposing the distinct cross lamination at about $\pm$ 30°. With great care and patience single laminae can be excised. For example Figure 16(a) shows a single lamina specimen of the 90° variety, a magnified view of which is shown in figure 16(b).

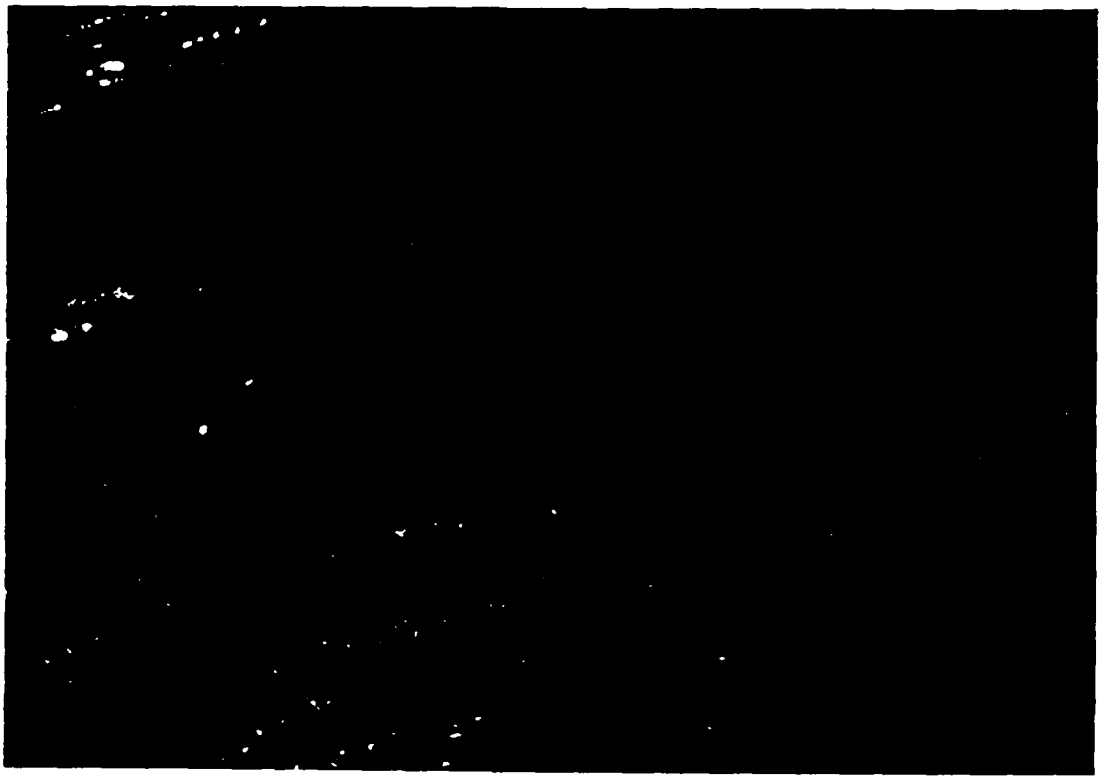

FIGURE 14 Sagittal Section Through Annulus Fibrosus

From figure 16 is is clear that the width and length determination poses no great difficulty; although the boundary is far from uniform the specimen width poses a much smaller problem than the specimen thickness. Accordingly we proceeded to determine the average thickness from the length and width measurements made with the aid of a microscope and a knowledge of the density. Because exposure of the material to differing wet environments affects the dimensions and thus the

FIGURE 15 Tensile Specimen (Multiple Laminae) Cut Circumferentially from Disc (Scale in mm)

swelling and density, all these measurements need to be made at different water concentrations.

Holding the specimen in clamps for relaxation testing proved one of the greatest problems for data repeatability. Because variations in clamping pressure with its resulting protrusion of the specimen as well as location of the specimen in the clamps was subject to sizeable variations, it became

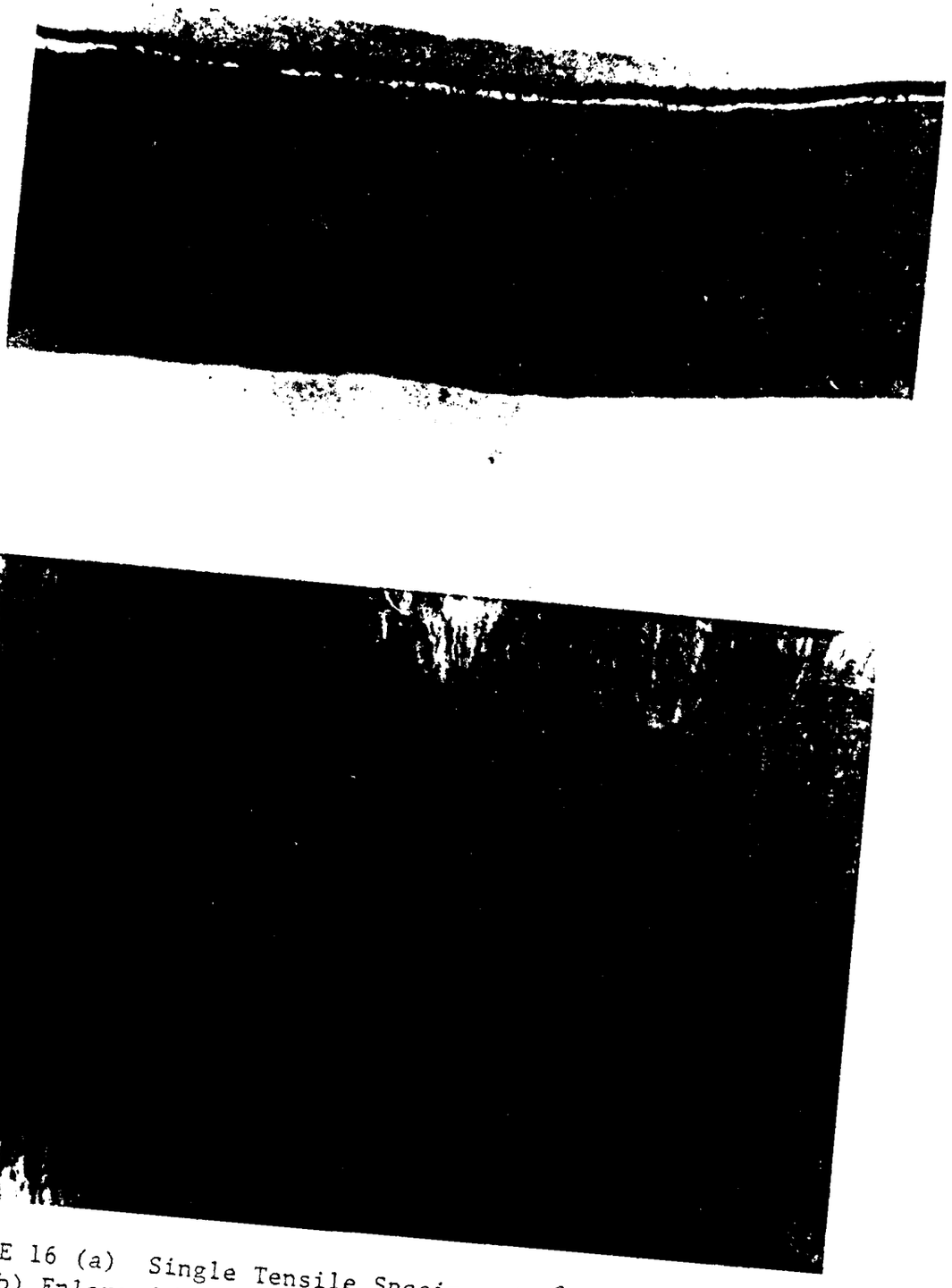

FIGURE 16 (a) Single Tensile Specimen (90^{o}, ~8 mm wide) and (b) Enlarged View (round objects are air bubbles)

necessary to normalize that problem. This was accomplished by "squashing" small brass rings out the ends of the specimens as shown in Figure 17. This needed to be done with enough pressure to ensure that slippage would not occur on the one hand, but not so much that the ring would cut the specimen; deburring of the ring was absolutely necessary. Specimen length was defined as the length between nearest edges of the end rings. Conditioning of the specimens was effected with these end rings in place. But before describing that conditioning and the test procedures for relaxation measurements we present first the essential pieces of equipment used.

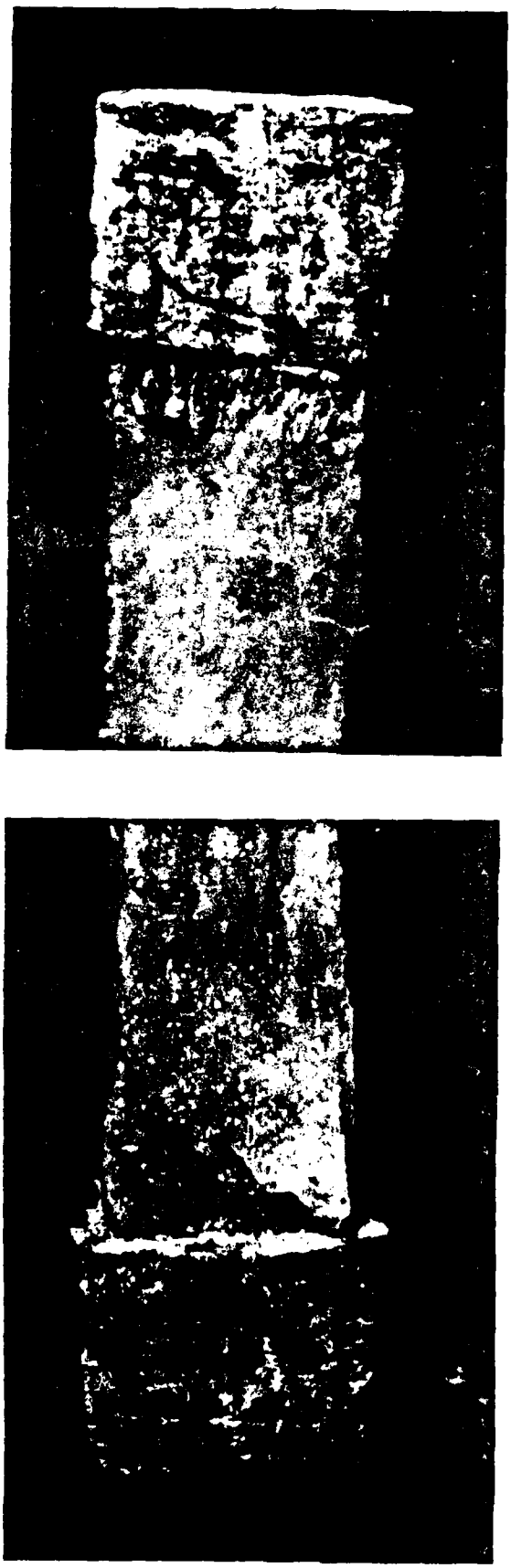

FIGURE 17 Brass Clamps at Ends of Multiple Layer Specimen

6. EQUIPMENT

During the initial phases of this work relaxation testing was accomplished with an Instron tester. Basically an engineering testing machine laid out for testing up to 12,000 lb. loads the machine was slower than desirable by about one order of magnitude. The Instron machine accepted a (BEMCO) temperature enclosure (loaned) which was mounted on the cross head of the Instron but the conditioned air had to be adducted from a separate power unit (Tenney chamber) which supplied air of a predetermined temperature and humidity. Our initial tests were conducted in moist air (see Appendix I).

It soon became apparent, however, that both the limited test speed of the Instron as well as the (moist) air environment posed significant limitation for our investigations.

Therefore a combined relaxometer-conditioner (Figure 18) was constructed along with a moisture cell which allowed testing in appropriate saline solution. The latter, shown in figure 19 is mounted inside the relaxometer-conditioner. Its sides are made of flat plexiglass pieces instead of a round tube to avoid optical distortion when viewing (photographing) the specimen through the parts of the relaxometer-conditioner. Thermally conditioned air enters from the Tenney unit; the relative humidity need not be controlled because the specimen is submerged in saline solution during testing.

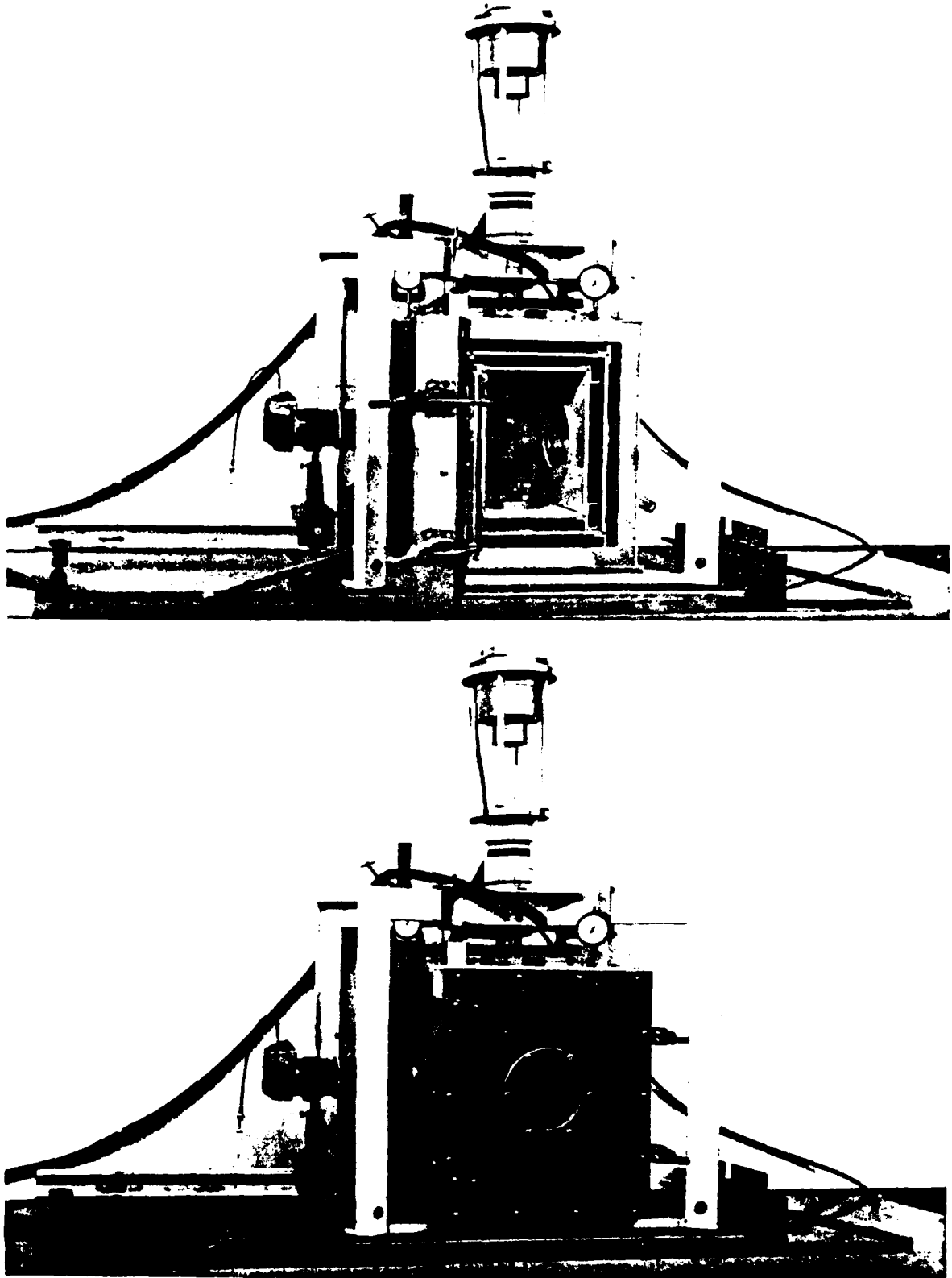

FIGURE 18 Relaxometer-Conditioner

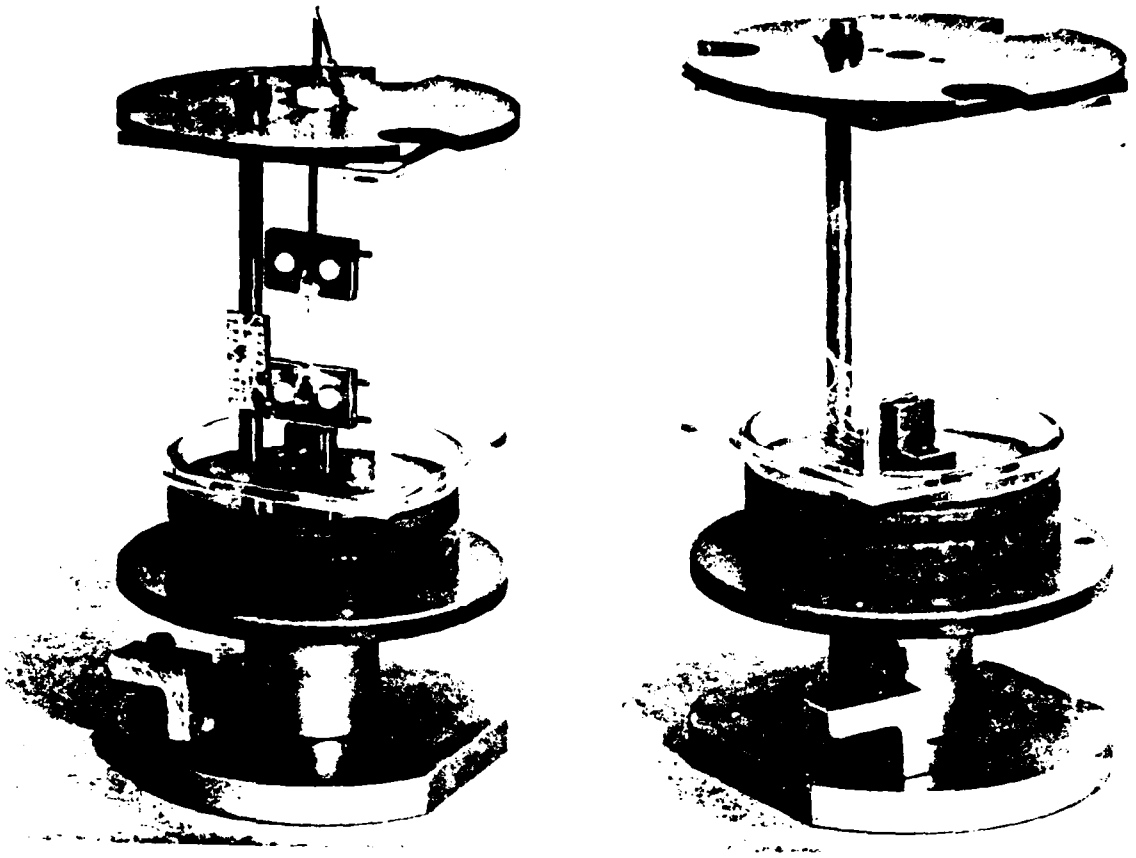

FIGURE 19 Moisture Cell Mounted Inside of Relaxometer-Conditioner - With and Without Specimen

The chamber acts as the straining load. One side of the specimen is attached to the chamber which is raised a small amount from its support plate, while the other end is fixed against the load cell (see Figure 19) which in turn is mounted on the stationary frame. The chamber is held suspended by a vacuum pad. At the start of the test, the vacuum is eliminated allowing the test chamber to drop a predetermined amount, thus elongating the specimen. The drop motion is damped by a suitable

parallel arrangement of two plates. The sides of the chamber have windows to allow continuous observation of the specimen, as required for example, to photograph the specimen in order to determine the strain. The need for determining the strain precisely for each test results from the fact that due to dust, and some friction, the cabinet will not drop precisely by the preset amount, but instead may vary by up to $\pm$ 0.005.

The load cell was mounted high and far from the chamber in order to aviod its recording of air pressure which jetted out through the aperature in the chamber through which the specimen was connected to the load cell.

It is, in general very difficult to mount a specimen in this apparatus in such a way that without load application the specimen is just ready to be stretched (zero strain). In order to arrange that the specimen be strained whenever the cabinet-load is applied the distance between the load cell and the chamber could be adjusted via a very fine thread seating screw. Thus for every new specimen mounted in the fixture this adjustment was made by trial and error so that prior to testing a marginally small or zero load acted on the specimen.

7. STRESS FREE RESPONSE TO WATER ENVIRONMENT

A dominant variation in these experiments is the water concentration in the material. It was our intention to study the material response under equilibrium conditions, i.e., such that the water concentration would not change with time. It was necessary, therefore, to determine the characteristic diffusion time for specimens of the type used. We note here peripherally that for the anisotropic laminae a simple diffusion coefficient is not very informative, and not more informative for specimens consisting of multiple layers. Instead of measuring appropriate diffusion coefficients we dealt with geometries similar to those used in the relaxation experiments.

In order to control the water concentration in the material specimens we experimented with several environments of saline solutions. Although we finally settled on solutions of NaCl, we investigated mixtures of a) methanol-water, b) lithium-perchlorate solution and c) chondroitin sulfate solution. Methanol-water swelled the specimens by unreasonably large amounts and the test temperatures were too high to prevent rapid vaporization. Lithium perchlorate seemed to irreversibly damage the material leaving the material distinctly brown and somewhat hardened. The chondroitin sulfate solution turned out to be very viscous and it seemed that equilibrium of water absorption was not achievable within several days.

Absorption History

In order to determine the time to reach water equilibrium specimens were placed in solutions of NaCl in different strengths. The weakest solution represented in these measurements was 15% because at 10% there appeared clear signs of damage. Pure water had the effect of causing gradual disintegration of the samples by forcing fissures to be separated from them.

In Figure 20 we show the water absorbed by single laminae as a fraction of the final weight. (W ≡ wet weight, D ≡ dry weight). We note that for all solutions equilibrium is achieved within 4 hours, but the final concentration equilibrium depends on the environment. The time to reach equilibrium seems to increase with saline concentration, but that effect is not very strong. In Figure 21 we show a cross plot of Figure 20, in which the curve for 352 min ($\doteq \infty$ time) is taken as representing the equilibrium concentration as a function of saline environment.

In Figure 22 we show the dimensional changes resulting from different saline environments, which by virtue of Figure 21 can also be interpreted as a function of equilibrium water concentration. The dimensional changes are recorded with the use of a microscope; although the data scatter is not small due to the small size of the specimens the anisotropy of the lamina material is clearly evident: The measurements were taken on 0^{o} and 90^{o} single lamina specimens parallel and perpendicular to the fibers; the swelling perpendicular to the

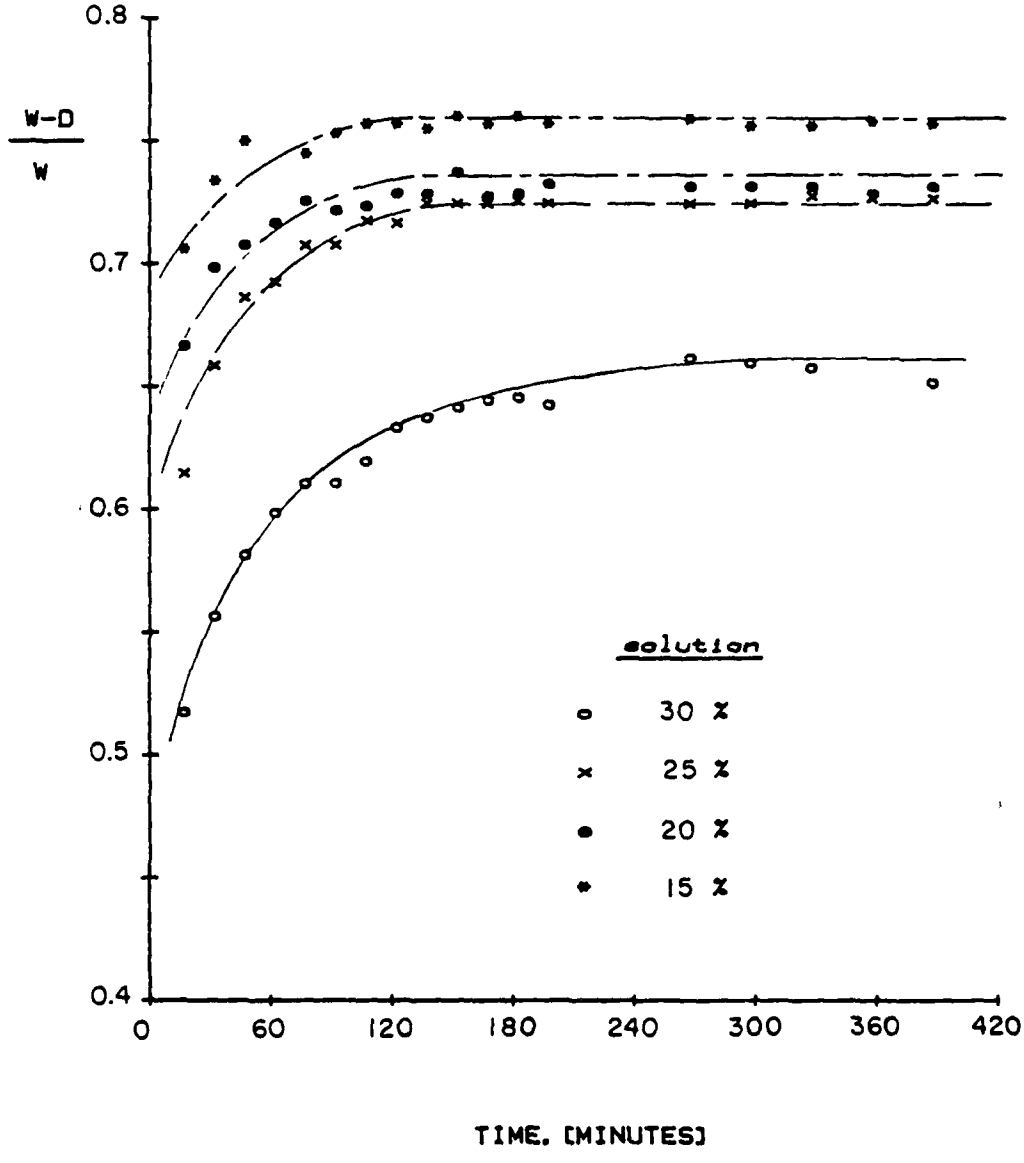

FIG. 20 FRACTION OF WATER ABSORBED BY SINGLE LAMINA AS A FUNCTION OF TIME IN DIFFERENT SALINE SOLUTIONS

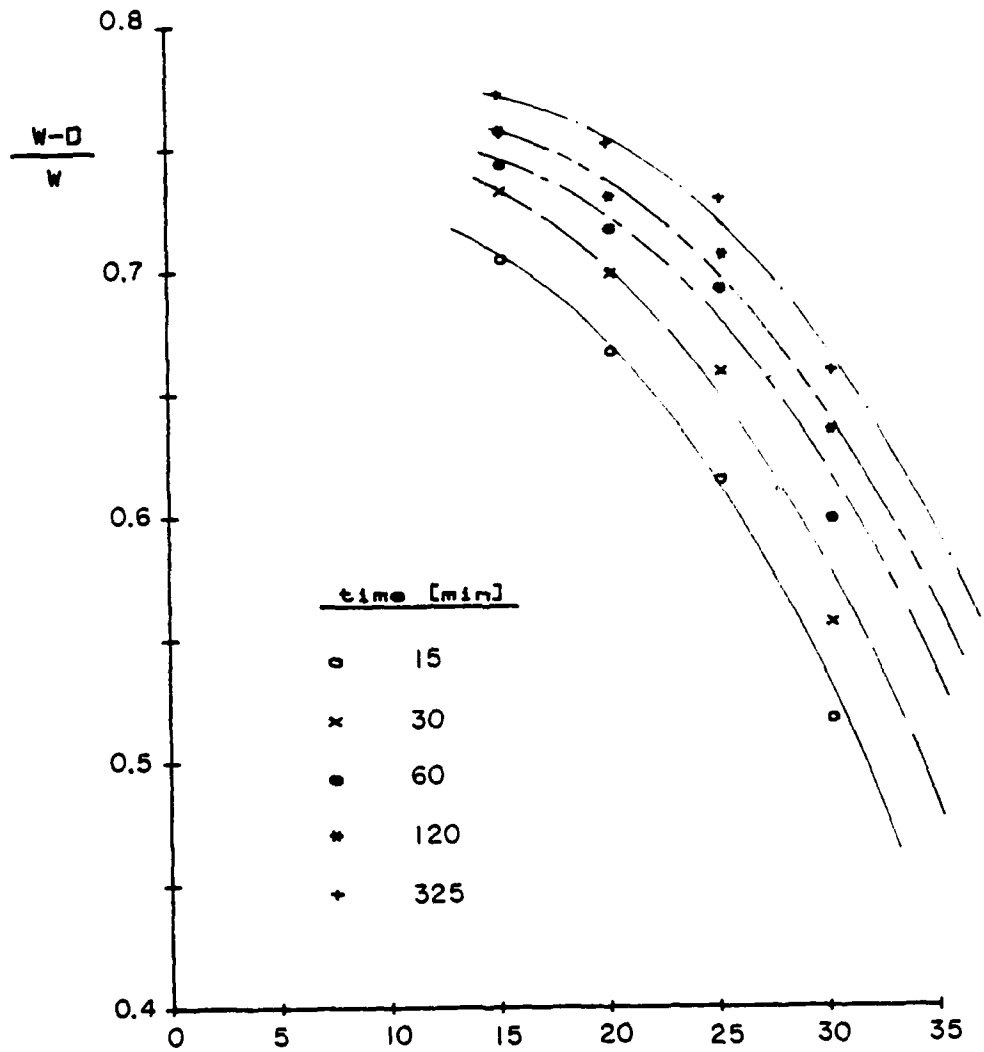

FIG. 21 EQUILIBRIUM CONCENTRATIONS OF WATER IN SINGLE LAMINA AS A FUNCTION OF SALINE CONCENTRATIONS

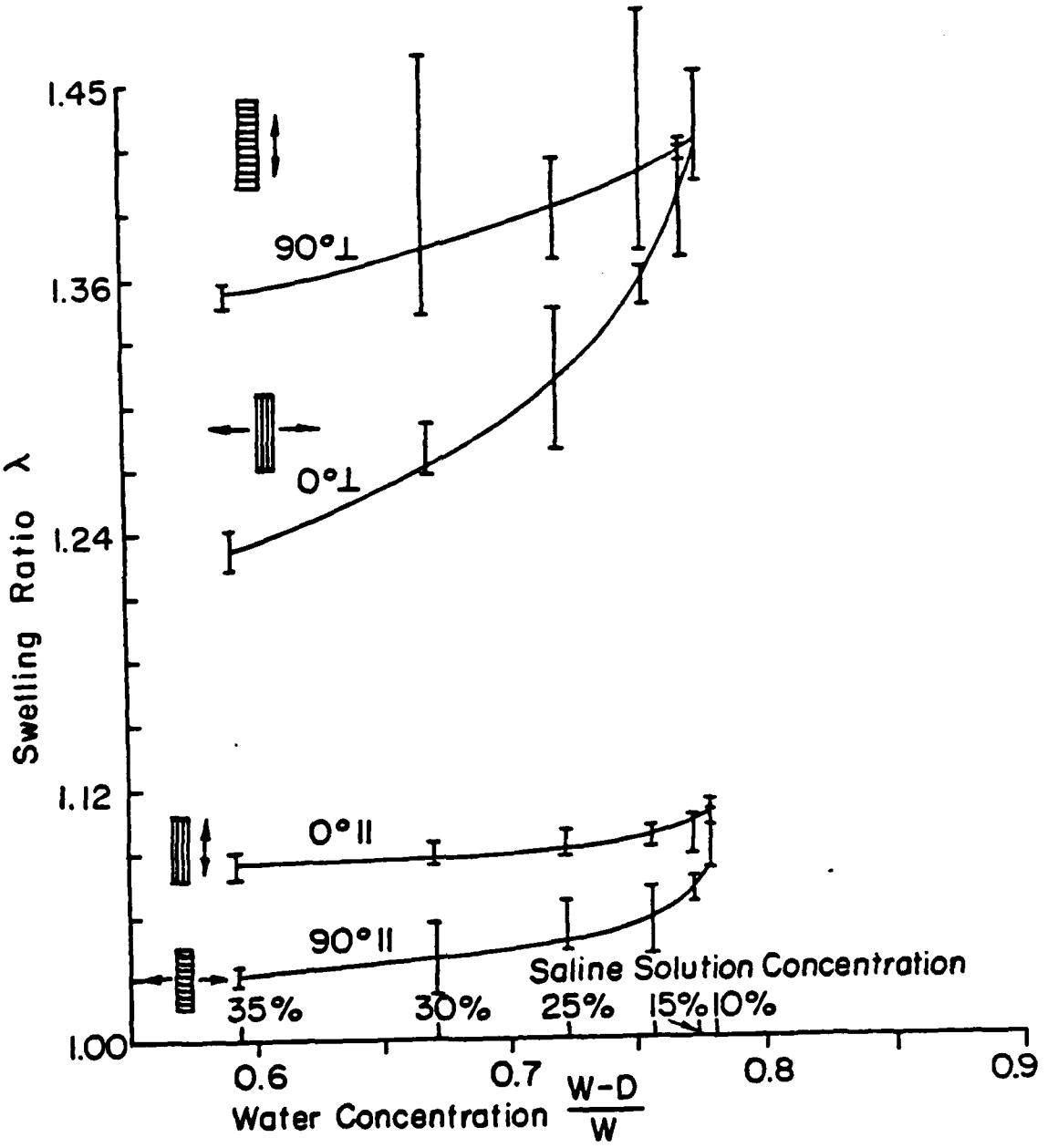

FIG. 22 SWELLING RATIO OF SINGLE LAMINAR SPECIMENS

fibers is on the order of four times that in the fiber-parallel direction.

We now turn to the behavior of specimens composed of several laminae. In Figure 23 we show the relative weight gain as a function of time. We first note that different saline solutions lead to different water diffusion rates and to only slightly differing equilibrium values. It appears that the initial diffusion rates are clearly a function of the saline environment. To examine that point we plot the data in Figure 23(a) against log time as in Figure 24. If we write, F denoting some function,

$$\frac{W - D}{W} = F(t \cdot \phi_c)$$

where ϕ_c is a factor depending on the saline concentration in the environment, then the data in Figure 24 should collapse into a single curve upon shifting them along the log t axis. This has been done in Figure 25 where the curve for 30% has been held fixed ($\phi_c(30\%) = 1$) and the other curves have been shifted by amounts log ϕ_c given by the inset graph. The long time equilibrium comcentrations of water in the specimens resulting from different environments is given by the uppermost curve of Figure 26 which corresponds to 4½ hours; note that the variation of the concentration is considerably less here than for the specimens of a single lamina being on the order of (W-D)/W = 0.6 - 0.63. By contrast the single lamellae yielded (W-D)/W = 0.6 to 0.78 over the same range of saline concentrations; on the average the latter are noticibly higher than the former.

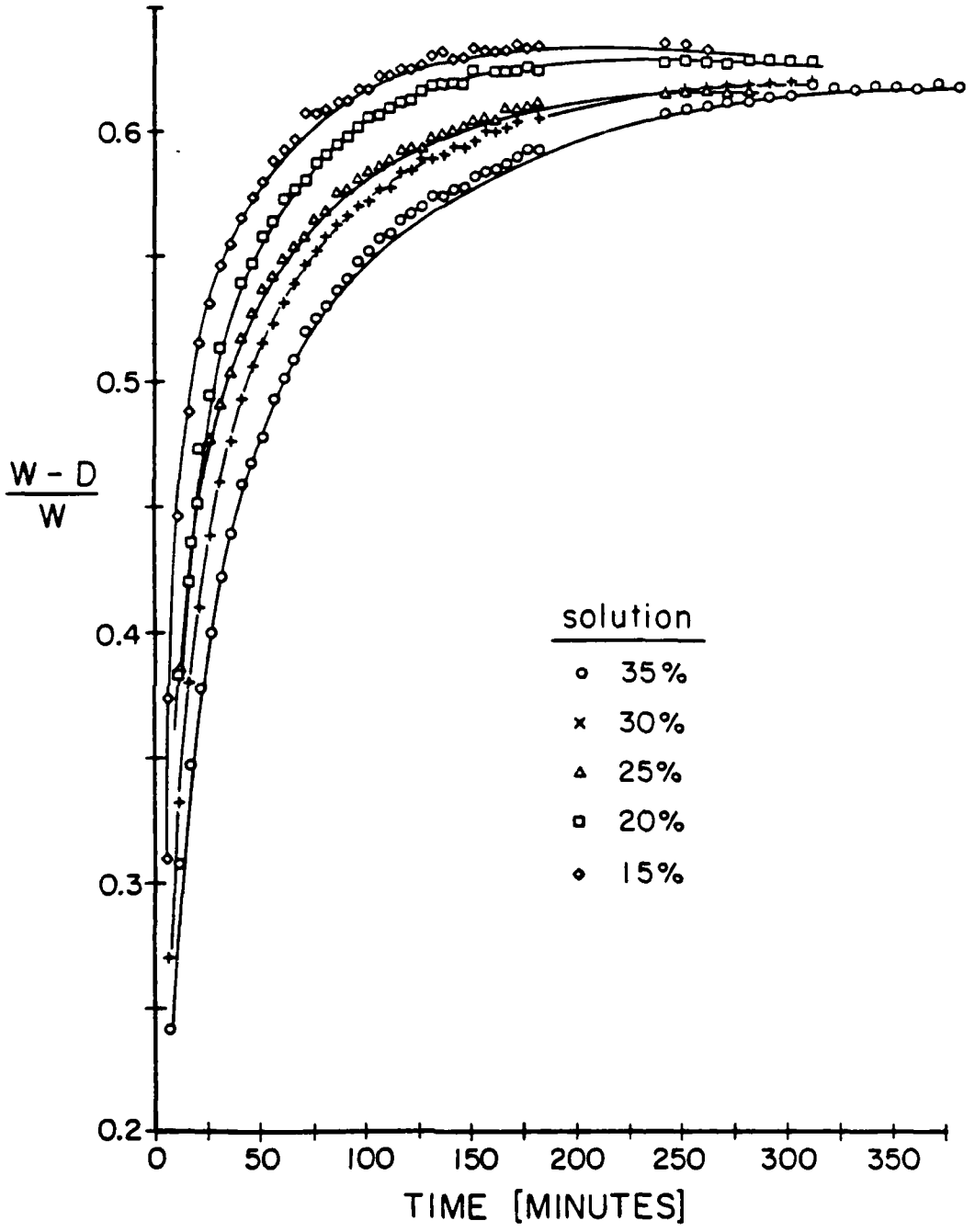

FIG. 23a FRACTION OF WATER ABSORBED BY MULTIPLE LAMINA SPECIMENS AS A FUNCTION OF TIME IN DIFFERENT SALINE SOLUTIONS

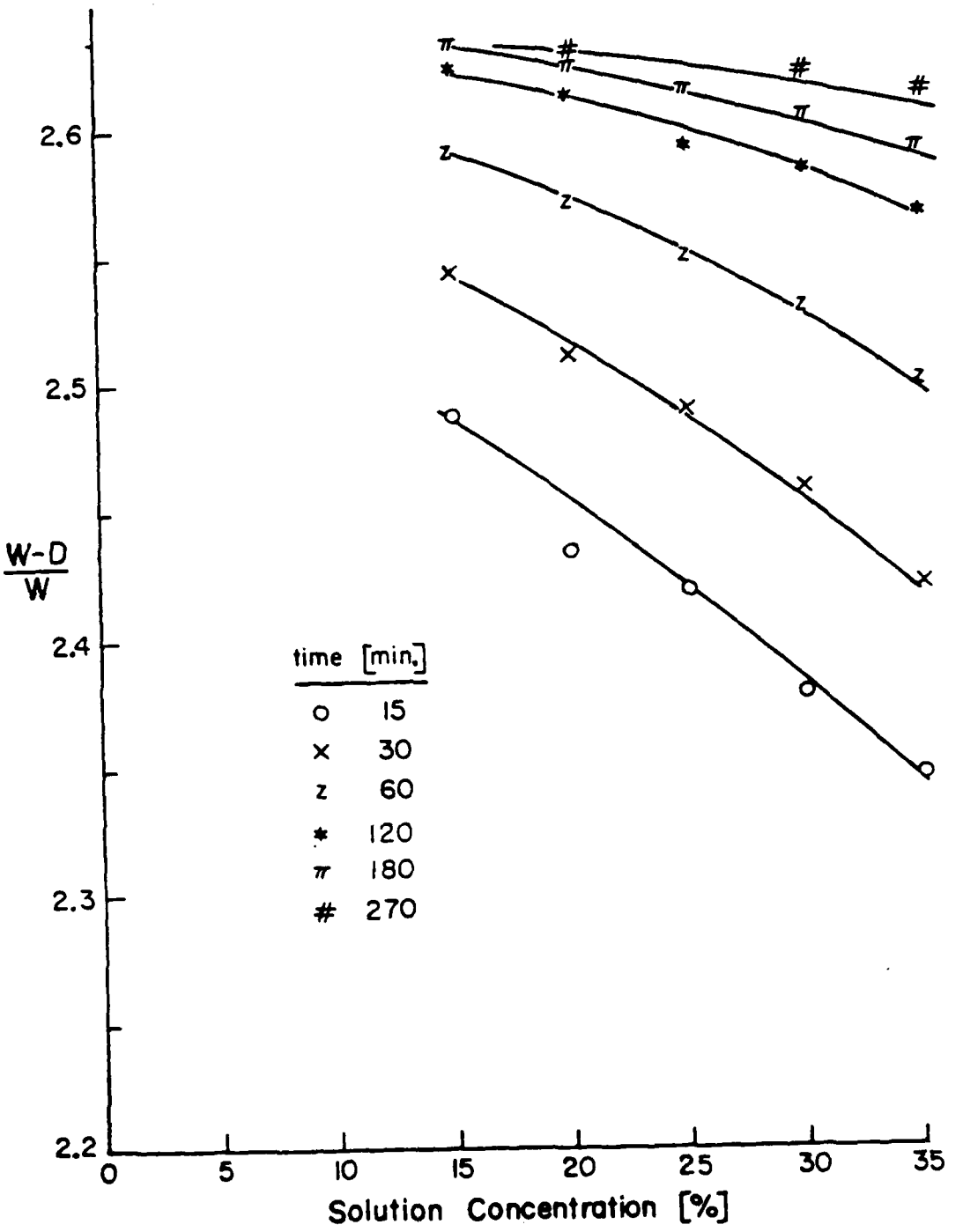

FIG. 23b Equilibrium absorption of water in multiple lamina specimens

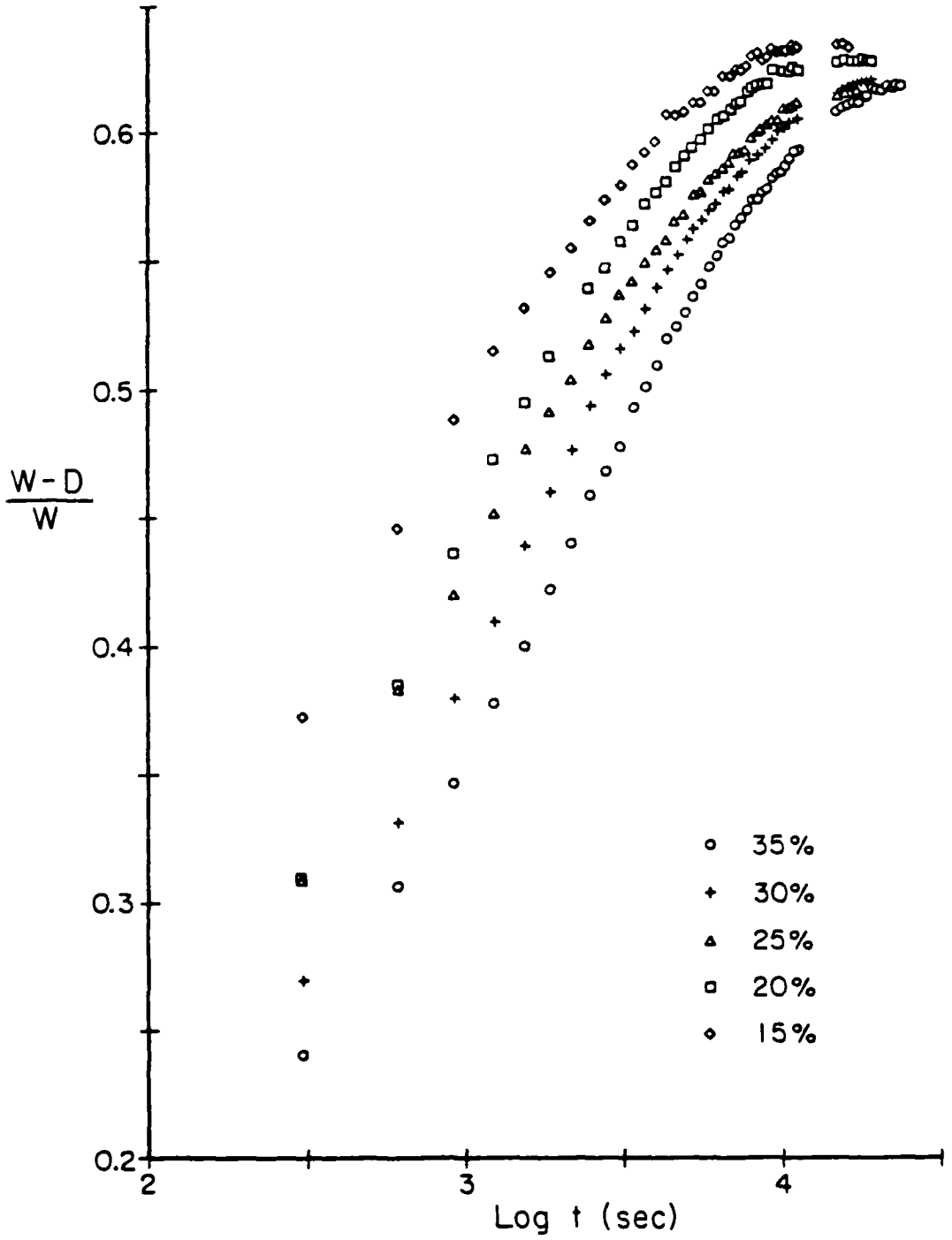

FIG. 24 WATER ABSORPTION OF FIGURE 23a PLOTTED AGAINST LOG-TIME

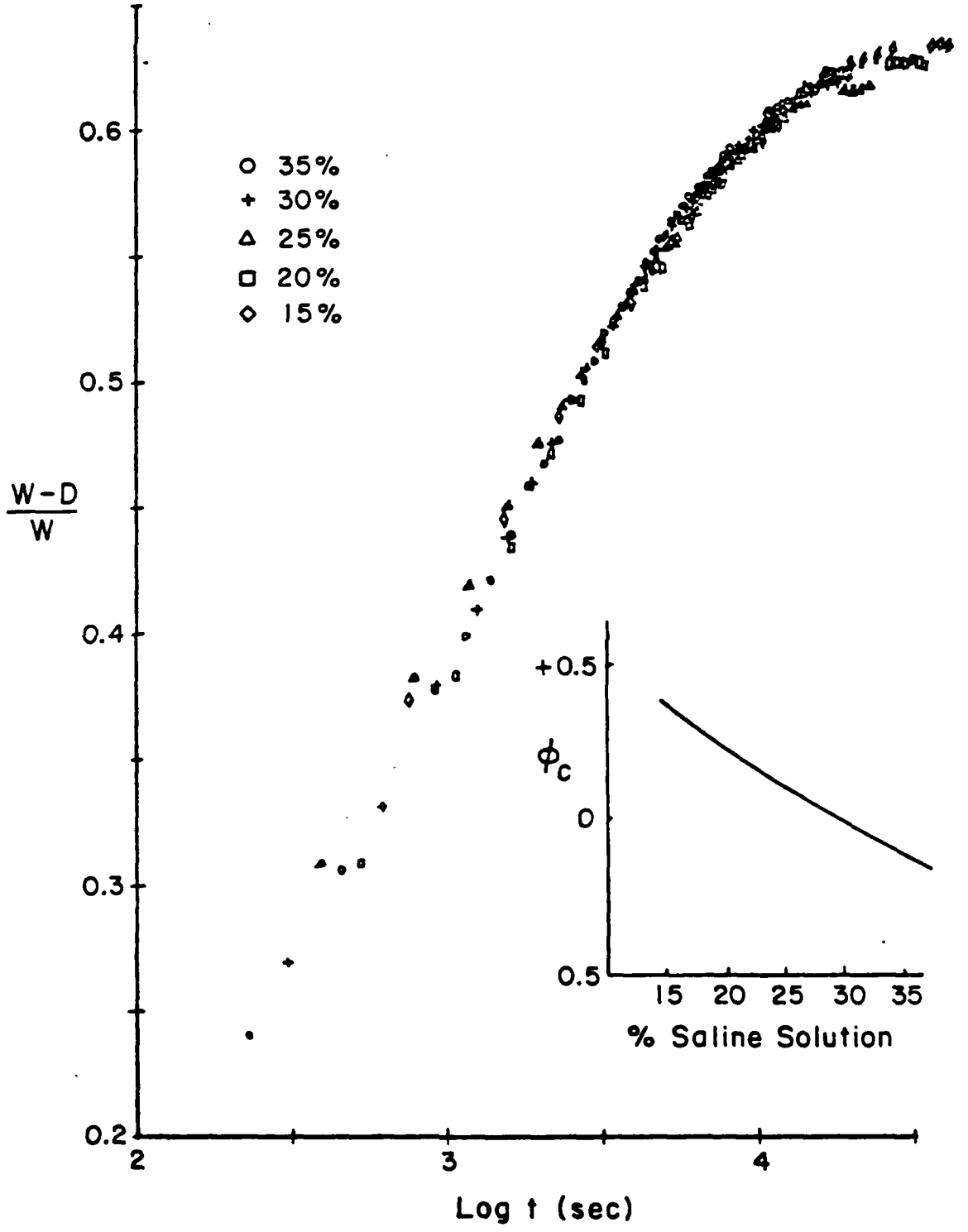

FIG. 25 MASTER WATER ABSORPTION CURVES
(see text for explanation)

The reason for this is, in all likelihood the stress and/or strain interaction with the swelling process. It is probably true that the collagen fibers swell less than the mucopolysaccharide matrix: swelling of single lamina specimens is pronounced by a factor of about 4 normal to the fiber direction when compared with that parallel to the fiber. Thus one deduces that the fiber will constrain swelling in multilamina specimens. That effect will constrain the amount of water taken up by multi-layer material leading to lower water absorption by the latter when compared with single laminae.

It was desirable to prepare multi-lamina specimens the thickness of which was small compared to their lateral dimensions, while being of uniform quality. That preparation was extremely difficult and we were only successful to generate small tensile specimens with reasonably uniform appearance. If a large specimen could have been obtained the swelling in the circumferential and vertical directions could have been measured. As it was that determination could only be made on slender specimens excised in the horizontal and in the vertical directions. Because the fiber constraint in these two types of specimens is different, the dimensional changes in these two types should be different too. For example, the swelling in the vertical direction (direction of spinal axis) as determined from vertical and horizontal specimens (c.f. Figure 12) is shown in Figure 26 while the corresponding data for swelling in the horizontal (circumferential) direction is shown in

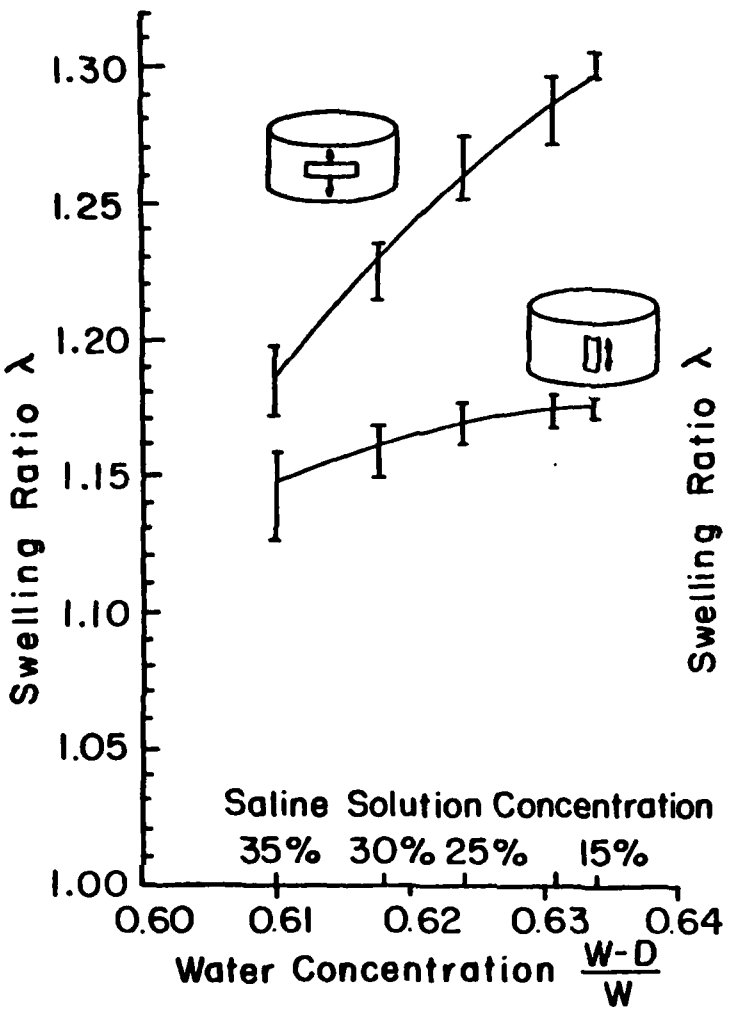

FIG. 26 SWELLING RATIO OF MULTI-LAMINAR SPECIMENS IN VERTICAL DIRECTION

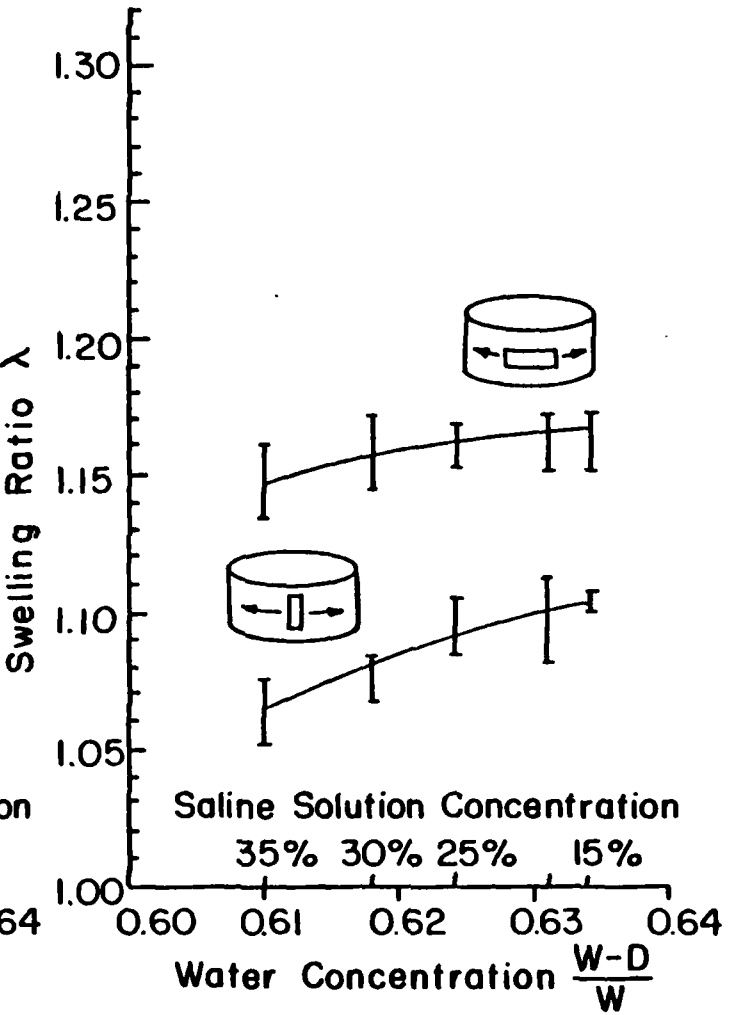

FIG. 27 SWELLING RATIO OF MULTI-LAMINAR SPECIMENS IN LONGITUDINAL DIRECTION

Figure 27. While the data from the two types of specimens are different, as expected, one sees that on the whole the disc material swells in the direction of the spinal axis about twice as much as in the circumferential direction.

We note here for later reference that the swelling behavior is important in the determination of the relaxation behavior of the material. While we have reduced all stresses and thus the relaxation modulus to properties corresponding to 30% saline solution the specimen dimensions change with changing water concentration and this change needs to be accounted for in the computation of the material stiffness. In fact, if A_{30} is the cross sectional area at 30% saline solution and A the area for any other saline environment, then the moduli reported later must be multiplied by the factor A_{30}/A; note that $A = A_{30}\lambda^2/\lambda_{30}^2$ where the λ's are the appropriate swelling ratios for the geometry used so that $A_{30}/A = (\lambda_{30}/\lambda)^2$.

8. MEASUREMENT OF THE POISSON CONTRACTION

One property often used in engineering analyses of orthotropic or isotropic materials is the Poisson contraction. If ε_1 is the axial strain on a slender rod specimen, and ε_2 is the transverse strain, then Poisson's ratio ν, defined as

$$\nu = - \frac{\varepsilon_2}{\varepsilon_1}$$

is one of several (two in the case of isotropic material) material parameters.

The difficulty with measuring this quantity is basically the small specimen size and the somewhat irregular boundaries of the specimen. Two methods were explored to perform this measurement, namely photographic recording with subsequent image scan processing and the obscurator method.

Photographic Recording and Image-Scan Processing: In this method the specimen is photographed on a high resolution photographic plate. The negative is scanned with a precision densitometer (scan resolution about 1 μm) and the densitometer output is computer processed. Figure 28 shows a scan plot across the width of a sample (rubber) specimen. The center portion of the plot represents the specimen; the drop-off in density values signals the edge of the specimen. In order to define the specimen edge, it was necessary to define a density gradient (say the maximum) as representing the edge. Motion of that edge resulting from dimensional changes due to time variations in Poisson's ratio would then be gauged by the motion of

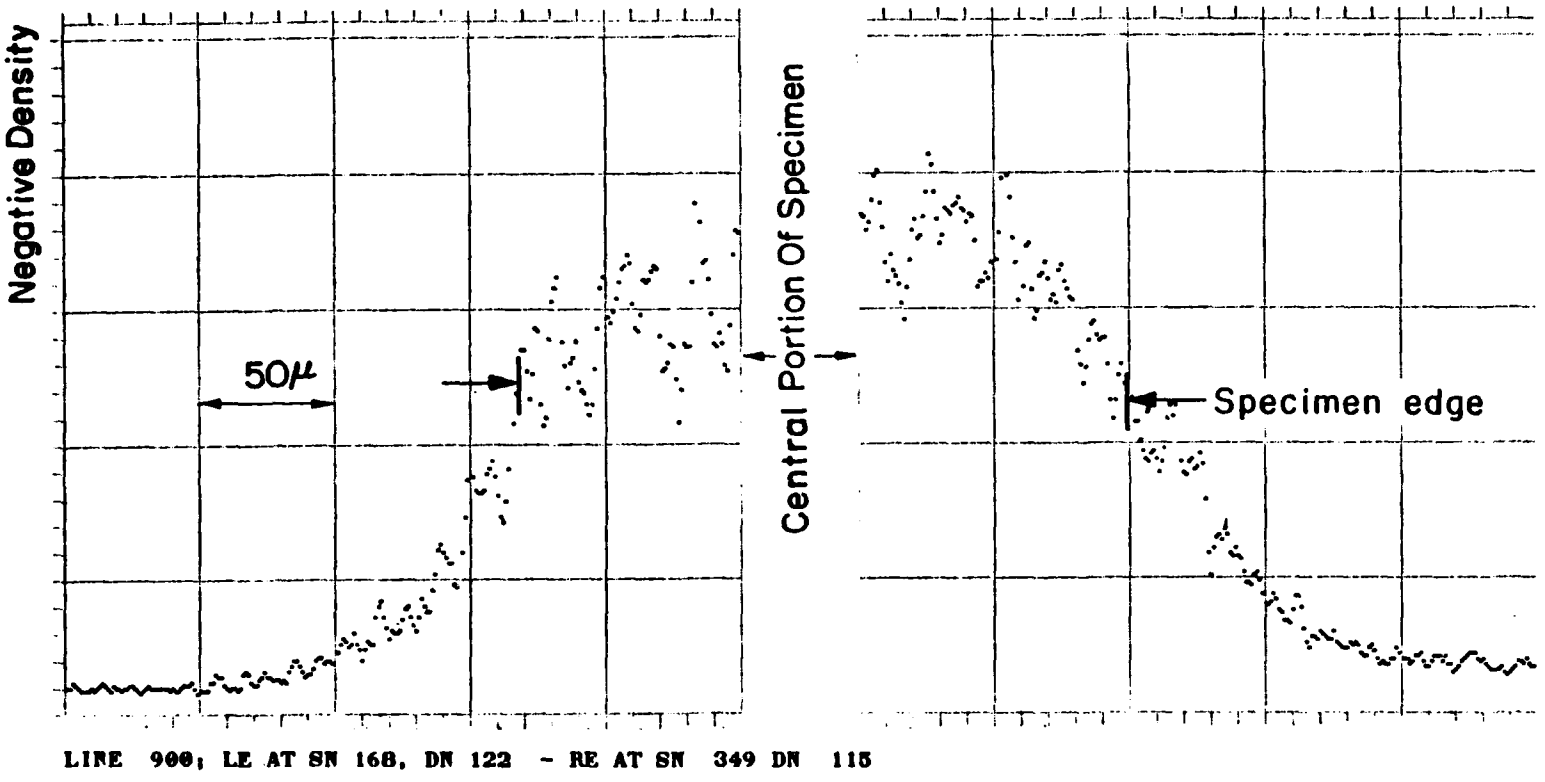

FIG. 28 DENSITOMETER EVALUATION OF SPECIMEN EDGES PHOTOGRAPHED ON HIGH RESOLUTION FILM

the highest gradient of the density profile.

Initially it was believed that the resolution of this recording technique was on the order of 1-2 microns. This estimate was derived from the use of high resolution film (plates for astronomic work) and the stated 1 micron accuracy of the scanner. However, analysis of actual measurements showed the resolution to be on the order of 10-20 microns. This resolution was judged inadequate for our purposes.

Obscuration Method: This is an optical technique in which dimensional changes in the specimen change the in- and out-put of a photo multiplier tube. Its function and operation are described in Appendix II. The result of that investigation was that it also was not sufficiently accurate for determining changes in Poisson contraction with time. However, because it is a relatively straight forward method it has useful applications in other areas of biomechanics where specimen size limitations are not quite so severe.

9. STRESS RELAXATION OF DISC LAMINAR MATERIAL

Because of equipment limitations our earliest work was performed in a moist air environment. Typical values of the relative humidity of the air ranged from 20% to 98% with associated water concentrations ranging between 10% and 68%. Also, specimen preparation was still a more "painful" operation than during the later phases of work and therefore only single laminar specimens excised in a circumferential direction (30-40^{o} fiber orientation with respect to tension axis) were tested. The results of that study were reported in the paper attached here as Appendix I . The net result of that study was to point out the great sensitivity of the mechanical properties to water concentration.

The research performed since then in different saline environments amplifies on this water sensitivity, and possibly some revision of the earlier results are in order. We note, however, that the earlier work dealt with a significantly different environment and with distinctly drier specimens than in the more recent work. The latter is a bit more appropriate to in vivo conditions than the former in that the moisture content naturally present in a disc is on the order of 67% and the data acquisition range is about 60% to 78% for single laminae and 62% to 64% for multiple specimens.

Many relaxation tests were performed because the fragility of the specimens often caused premature failures. In order

to avoid the gradual mechanical deterioration of the specimens under repeated loading it was necessary to reduce the strain to levels on the order of 1% which makes accurate strain determination difficult. As the strain was reduced the effect of swelling changes on the original specimen lengths became more important so that the screw attachment described in section 6 needed to be devised; in the absence of this adjustment unreasonably large changes seemed to occur in the relaxation behavior.

The same specimen was always used for several measurements without taking it out of the measurement apparatus. That ensured that data scatter due to positioning of the specimen ends was virtually eliminated.

One would naturally ask for evidence that repeated specimen use does not lead to damage accumulation with a consequent reduction in specimen rigidity. Accordingly the following test sequence was initiated: Relaxation measurements were conducted at 35, 30, 25, 20, and 15% salt concentrations. This was the normal test sequence. After completion of that sequence some duplication testing was performed at 25% and 20% saline concentration and virtually no change outside of the normal experimental variations was apparent. Figure 29 shows the repeat tests; for a discussion on the divergence at longer times, see below.

We are, therefore, reasonably confident that material degradation during testing was not a significant factor in our measurements.

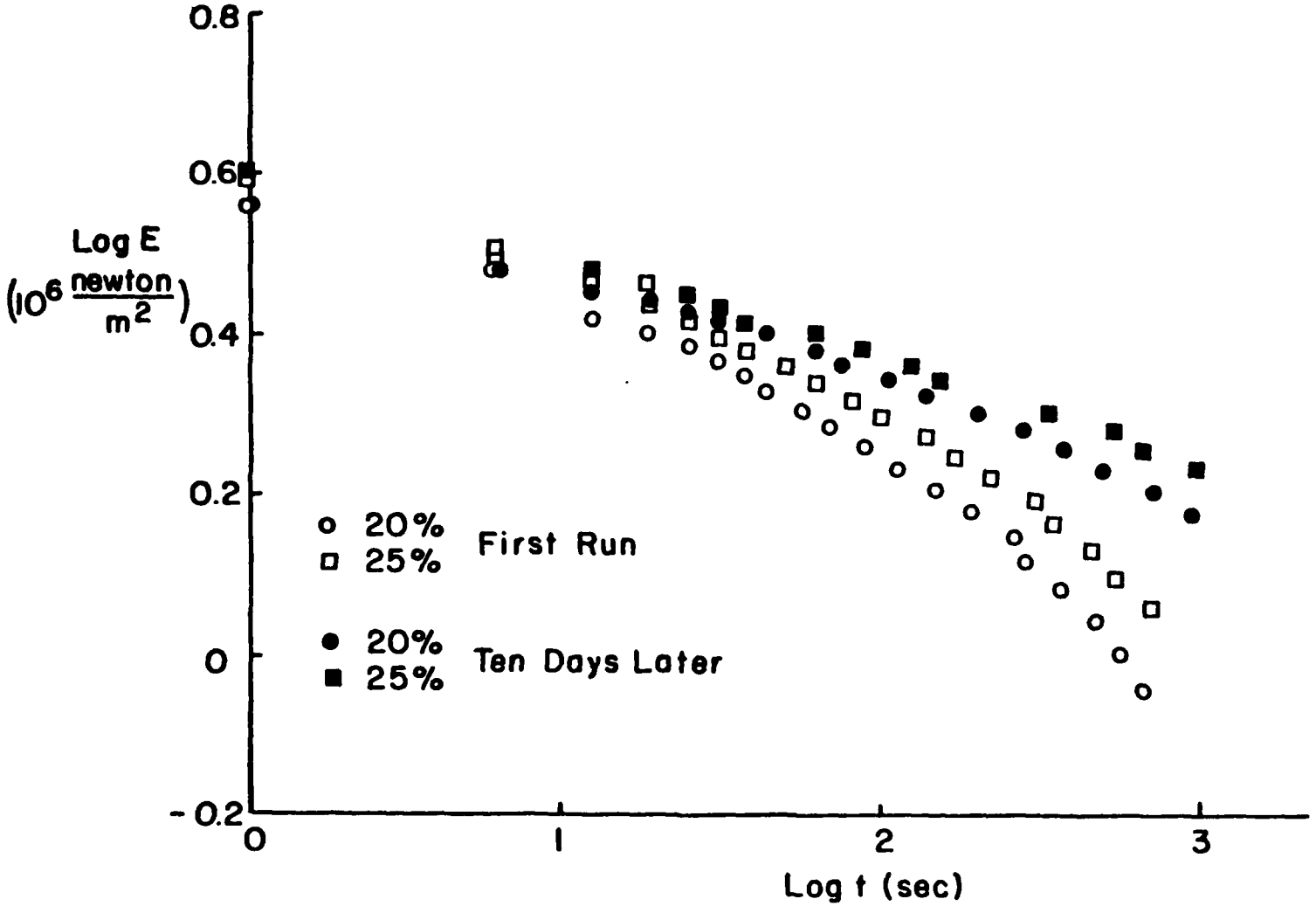

FIG. 29 REPEAT TESTS ON THE SAME SPECIMEN AFTER A COMPLETE TEST SEQUENCE IN 35%, 30%, 25%, 20% AND 15% SALINE SOLUTIONS

Relaxation was measured on single lamina specimens in which collagen fibers run in the tensile direction and on others in which these fibers ran transverse to the tensile axis. In addition specimens with several layers were tested which were excised from a disc in the horizontal and in the vertical directions as defined in Figure 12.

It was the intention to examine whether the data procured from single lamellae could be used to synthesize the response of the multilaminar specimens. This was not possible for two reasons that became apparent during the course of the work: first, the moisture absorption of the multilayer specimens is significantly different from that for single layer specimens; that gives rise to different material behaviors leaving one with some uncertainty as to the precise interrelation. That uncertainty seemed to be on the same order of magnitude as experimental variations, so that comparison of such computations with experimental results is not necessarily meaningful. Second, it turned out to be more difficult than anticipated to excize multilayer specimens of precisely known layer make-up. While the separation of laminae is "fairly" distinct it was uncertain from an edge count how many layers the specimen contained and how thick each layer thickness should be assigned.

In view of these uncertainties we point out that the relative magnitude of the relaxation moduli are of the correct relative magnitude, as an examination of Figures 30-33 will verify. These figures show the relaxation behavior of the

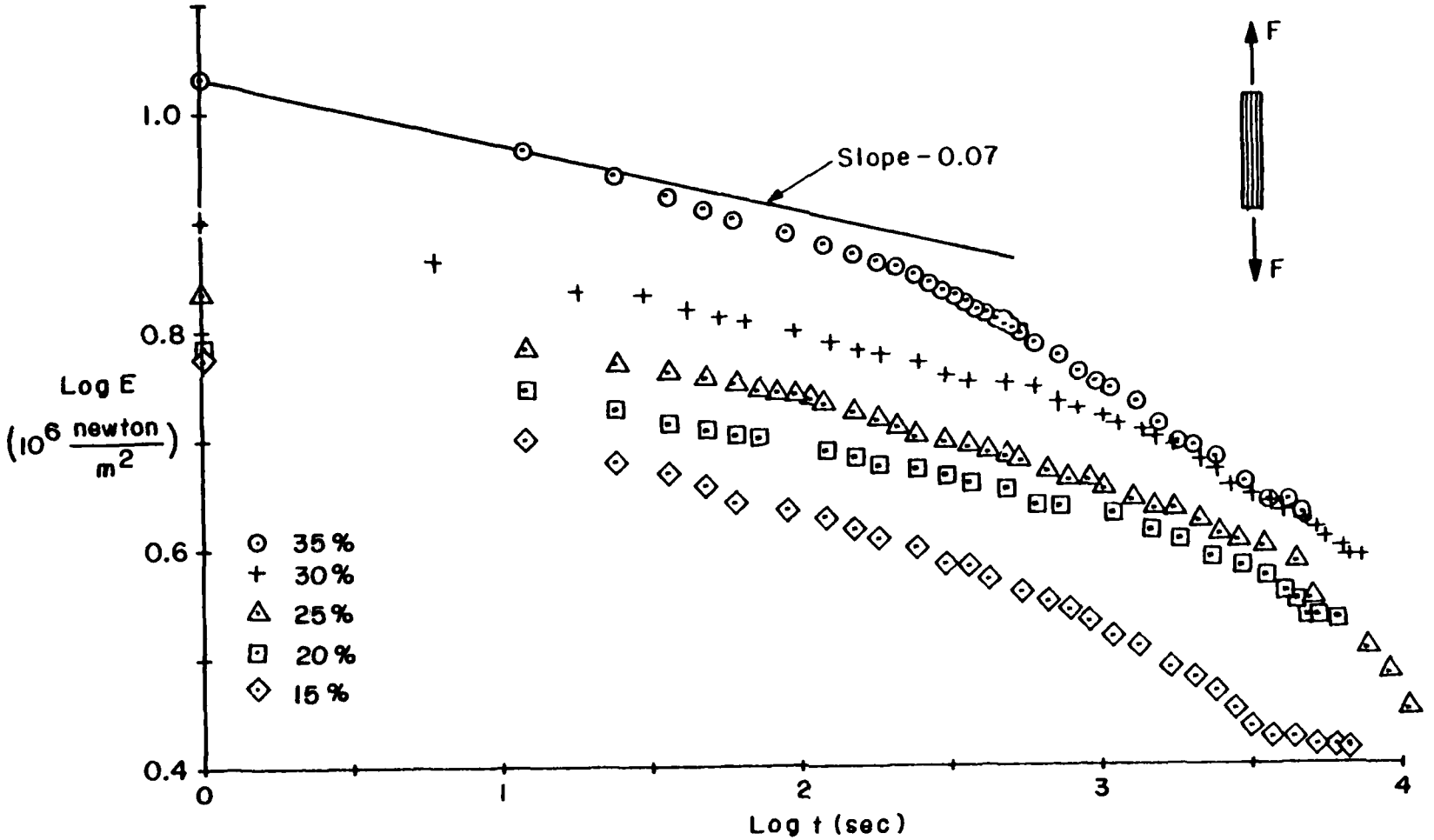

FIG. 30 RELAXATION MODULUS OF 0° SINGLE LAMINA BASED ON CROSS SECTIONED AREA AT 30% SALINE SOLUTION

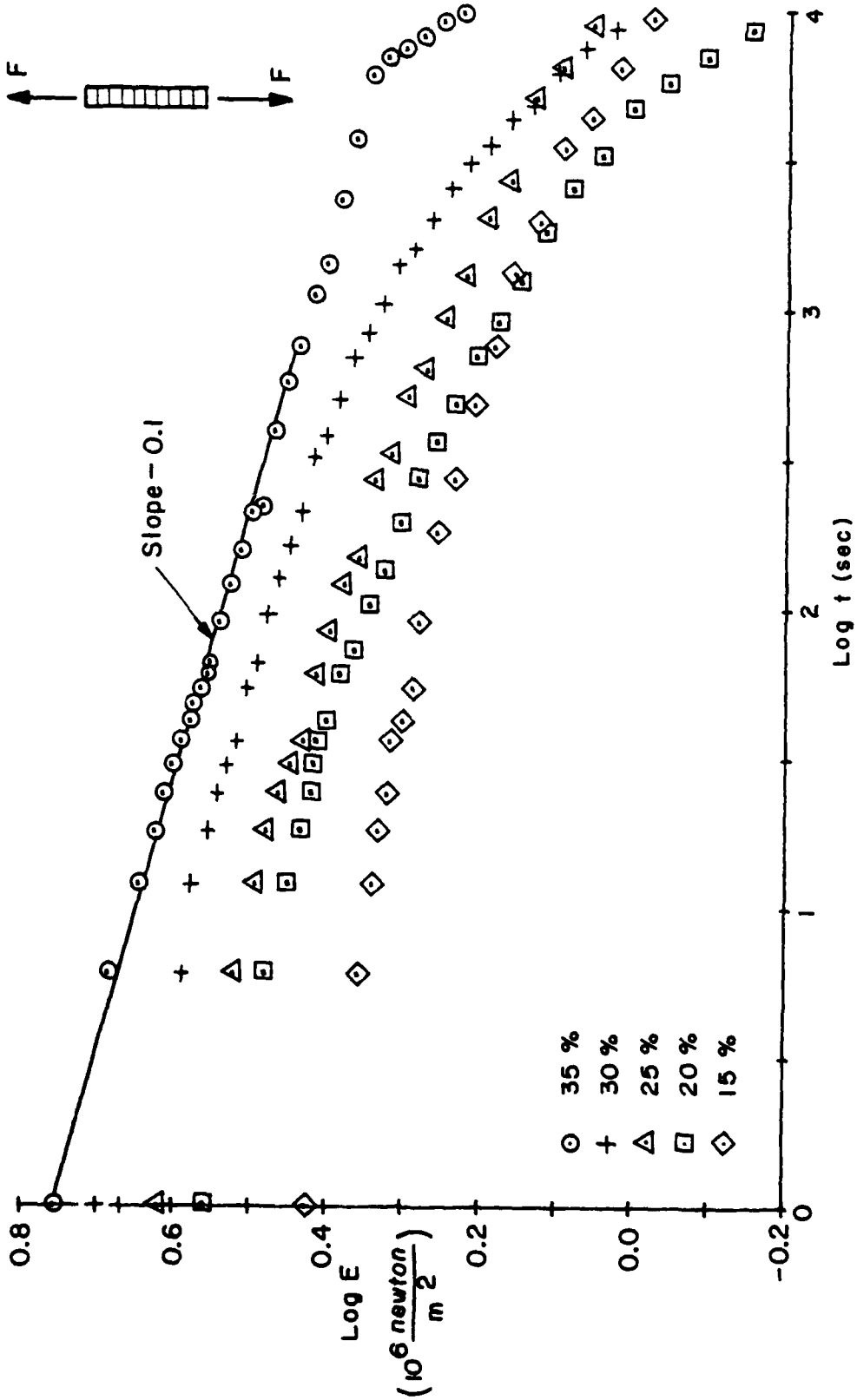

FIG. 31 RELAXATION MODULUS OF 90° SINGLE LAMINA BASED ON CROSS SECTIONED AREA AT 30% SALINE SOLUTION

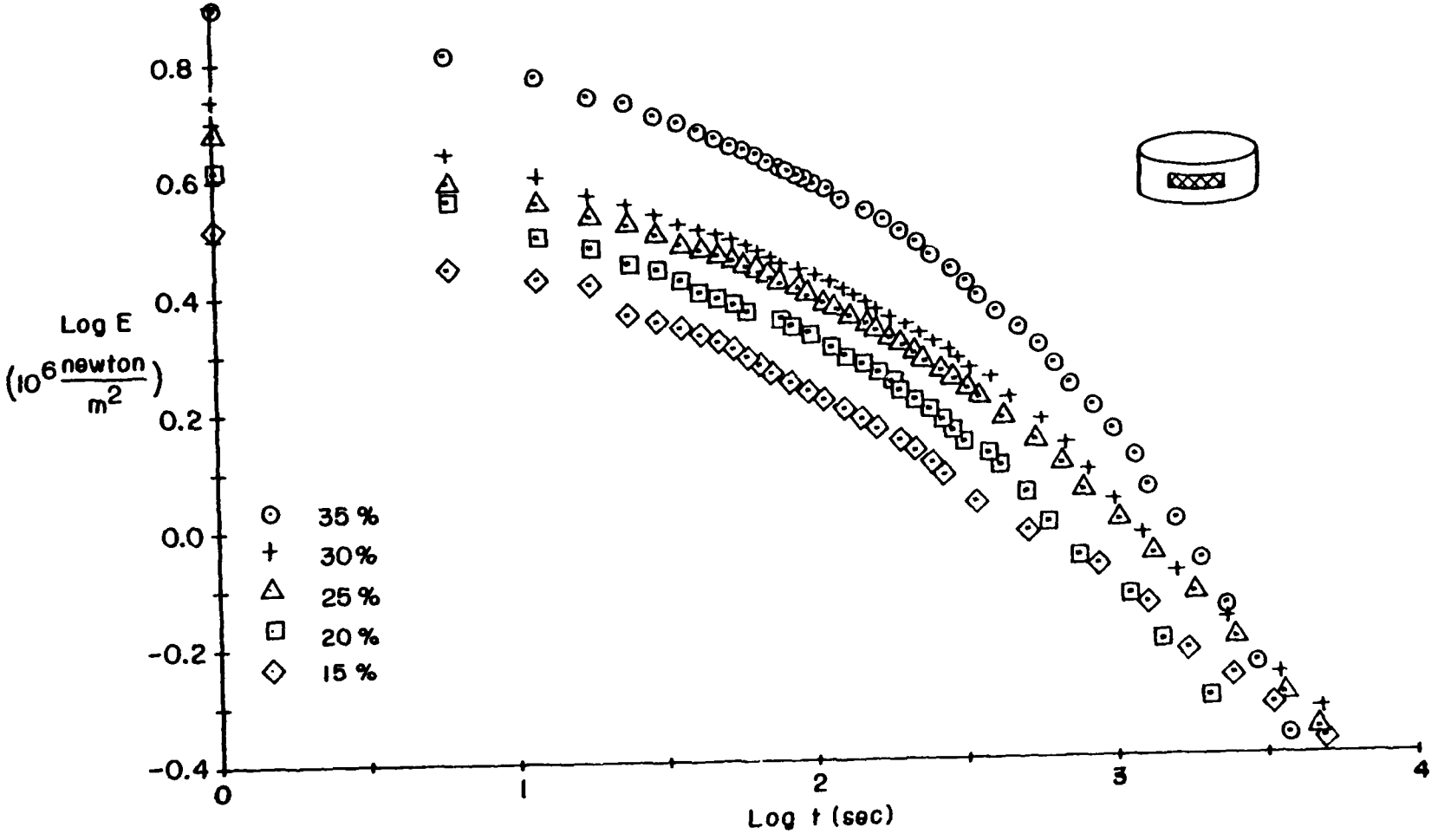

FIG. 32 RELAXATION MODULUS OF MULTIPLE LAMINA DISC MATERIAL; HORIZONTAL EXCISION; BASED ON CROSS SECTIONED AREA AT 30% SALINE SOLUTION

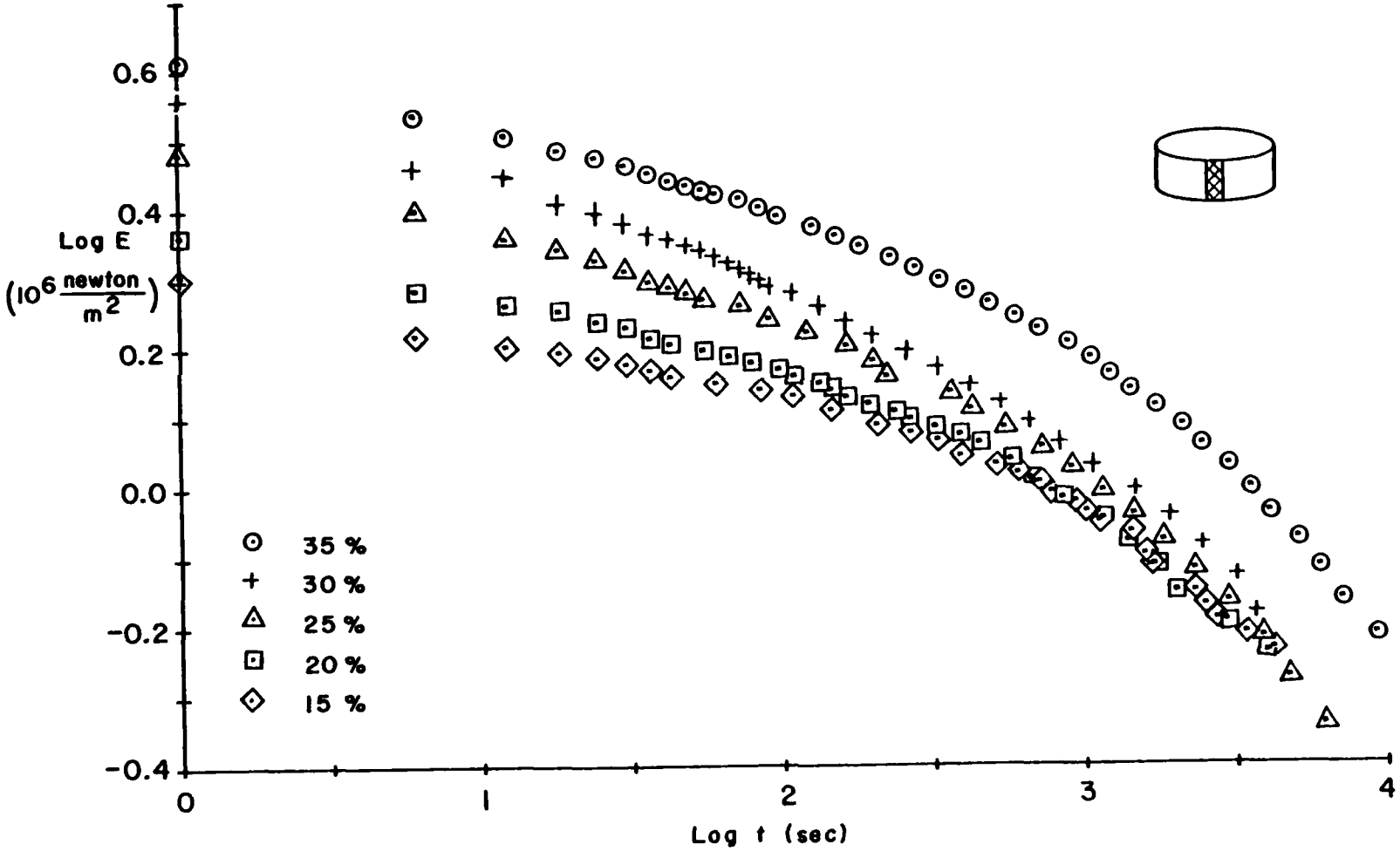

FIG. 33 RELAXATION MODULUS OF MULTIPLE LAMINA DISC MATERIAL; VERTICAL EXCISION; BASED ON CROSS SECTIONED AREA AT 30% SALINE SOLUTION

the four types of specimens mentioned just above. We now point out the important and typical characteristics:

a) The relaxation modulus of the zero-degree laminae is the highest.

b) The 90^{o} lamina has a modulus which is lower by only a factor on the order of 3.

c) While it is not immediately apparent from those figures because of differences in the vertical scale it is of interest to note that the relaxation of the 90^{o} laminae is on the order of 10 times faster than that of the 0^{o} specimens.

d) Excepting the tests on multi-layer vertical specimens involving high water content, the multi-layer specimens have relaxation data intermediate to the 0^{o} and 90^{o} relaxation moduli, as they should.

e) The relaxation moduli for the horizontal and vertical specimens are surprisingly close, the one for the vertical specimen tending to be lower, but hardly by a significant amount in view of the data scatter. This observation leads one to believe that in spite of the obvious appearance of anisotropy a nearly isotropic behavior of the disc material in the cylindrical surfaces may be a tolerable approximation. This implies nothing of course about linear or non-linear deformation characteristics.*

---

*Observations of non-linear deformation characteristics have been discussed in Appendix I. We assume that for the present work the same, or similar behavior exists and dispense, therefore with strain as an additional parameter.

f) The rate of relaxation appears to be on the correct order of magnitude when compared with the earlier data in Appendix I. Specifically in Appendix I, Figure 9, one estimates the log-log slope of the relaxation modulus for the highest water concentration (58% for 86% relative humidity air) to be about -0.07; for the present data one estimates for the 0^{o} 60% water content a slope of -0.07 and a value of -0.1 for the 90^{o} specimen with 60% water content.

Let us now discuss in more detail the effect of water on relaxation behavior, particularly in light of the earlier results for single lamina excised horizontally as delineated in Appendix I.

Superficial examination of figures 30-33 indicates that the effect of water in the range of concentrations studied here is not merely to influence the relaxation time; for if that were so each set of data should be reducible to a single master curve by translating the data from different concentrations horizontally along the log time axis: Even allowing for liberal experimental uncertainties will not effect a credible superposition of the data.

We therefore discuss two possibilities, to explain these circumstances, namely Stress Induced Changes in Water Content and Inter-Molecular Forces Occasioned by Water Infusion. We turn our attention first to the possibility of Stress Induced Water Absorption.

We note first that the log-log slopes of the relaxation curves show relatively little change during the first 15 minutes, i.e., the log-log relaxation slope is fairly constant; thereafter relaxation becomes more pronounced. That time range is roughly on the same order as the diffusion time scale exemplified by Figure 20: within 10 minutes approximately half the equilibrium value for water content has been achieved.

Assume now that when a load is applied additional water may diffuse into the material (open system) and suppose the diffusion rate is not affected by the stress. Then one might expect that the additional water absorbed accelerates the relaxation process much as a temperature rise or solvent take-up changes the relaxation behavior of non-biological polymers: the increased rate of relaxation manifests itself in a steepening of the log-log plot of the relaxation modulus. If one were to follow that argument one would conclude that the initial portions of the relaxation modulus having - within experimental variations - a nearly constant slope on the log-log plots should provide the (initial) equilibrium behavior. Accordingly we show in Figures 34 and 35 the composite master curves of the single lamellae based on the short time data.

If the "accelerated" relaxation beyond 1000 sec is induced by additional water absorption then one would expect that higher strain, with the accompanying higher stresses would produce an enhanced acceleration or, what is equivalent, push the acceleration due to water infusion towards shorter times. An important consequence of this possibility is that if various

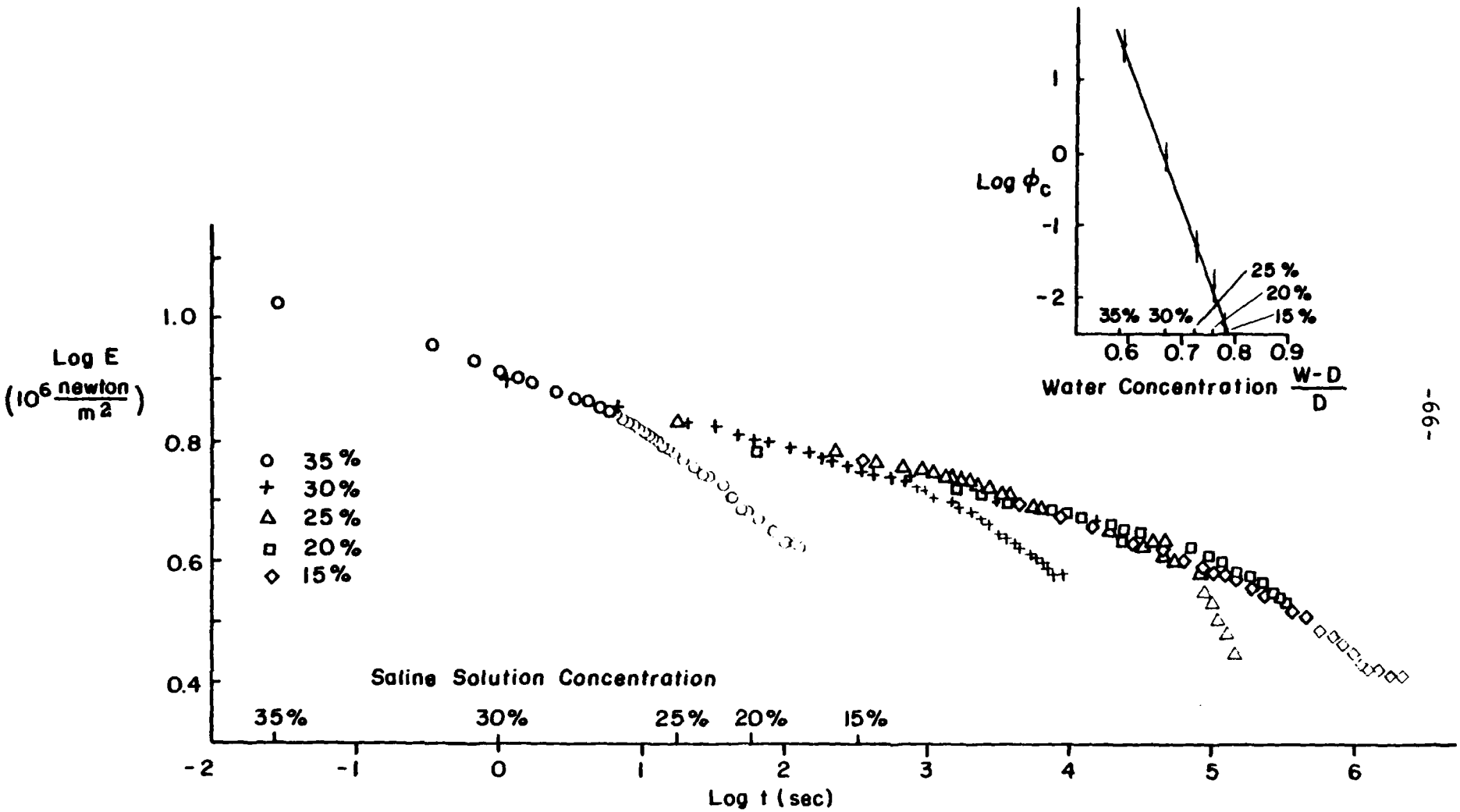

FIG. 34 MASTER RELAXATION CURVE FOR 0° SINGLE LAMINA USING SHORT TIME RESPONSE FOR MASTER CONSTRUCTION

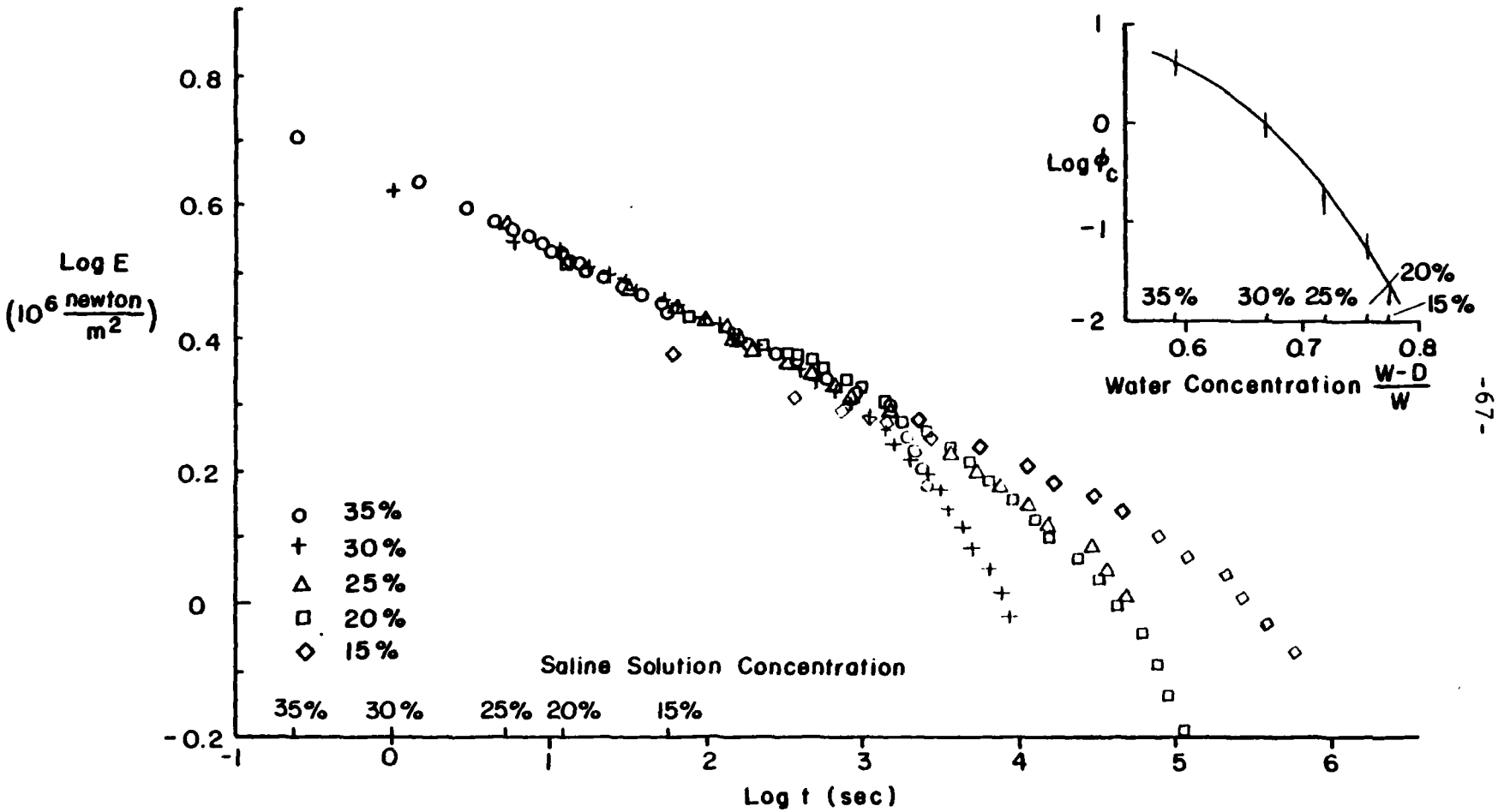

FIG. 35 MASTER RELAXATION CURVE FOR 90° SINGLE LAMINA USING SHORT TIME RESPONSE FOR MASTER CONSTRUCTION

amounts of prestrain are applied to a specimen then the acceleration phase would set in earlier for the higher prestrains. Alternately, if the prestrain connot be controlled very well then the acceleration phase would become noticeable at different times after the test has started. This observation is corroborated by two results: first we notice a significant variation in the longtime relaxation which may result from our inability to control the prestrain on a specimen to better than about ½% strain, i.e., about 50% of the strain amplitude used to measure the relaxation behavior; that prestrain may well be responsible for the observed variation.* Second we observe that for the multilayer specimens which required a higher preload for straightening than the flimsy single lamellae the "relaxation accelaration" occurred earlier than in the latter.

While this prestrain is probably responsible for the lack of superposition in the samples we must be aware of another possibility. Recall that the specimens are clamped with small brass rings at the ends which rings have been "squashed" to provide the clamping force. For multi-layered specimens we must assume that the force transfer from the outer specimen surface to the fibers belonging to the inner layer is perfect, so that the latter appear also clamped. In fact, if that transfer is not perfect than the mucopolysaccharide matrix

---

*It is unfortunate that at the inception of the program there was no estimate available on the magnitude of this possible effect to design the equipment appropriately. It appears that our care for adjustment procedures on the specimen were simply not fine enough to take care of this unexpected sensitivity.

holding the various layers together can undergo shear deformation (creep) index load which would also lead to force relaxation on the specimen. We assume that this is not the case because we would then expect that upon repeated use (6-10 times) of a specimen the end clampings should perhaps have given way; this was not observed, in fact no systematic changes on successive and repeated measurements were observed.

While all our observations thus point toward delayed abnormal relaxation behavior due to stress induced water absorption we cannot close our minds to possible alternate explanations. That brings us to the second possible reason for failure of a simple time-moisture superposability, namely,

Intermolecular Force Variations due to Water.

In non-biological elastomers the material stiffness is affected by temperature in two ways, once via the change in free volume which manifests itself in the time-temperature trade-off and secondly by entropic effects on chain configuration. The latter effect is not believed to affect the relaxation process and makes the long-time modulus proportional to the absolute temperature. Suppose that water has a like effect on modifying the intermolecular cohesion forces beyond the modification of the relaxation process. If that were so one might argue that possibly all the affect of water is reflected in a multiplicative function of water concentration on the modulus. Accordingly all relaxation curves should be superposable by shifting them along the vertical axis. This

attempt is shown in Figures 36(a)-(d) with a quite reasonable result, though not uniformly so.

However, we note two facts: first, the discrepancies at longer times of relaxation are not removed and, second, the initial portions of the relaxation curves all have essentially the same slope so that vertical shifting should apply well to that portion of the curves. In fact the initial straight line portions of the curves represent the same power law, and without a curvature in those segments no unique combination of vertical and horizontal shifting is possible.

We conclude this section with the affirmation that certainly additional work is needed to clarify these questions. However, in view of all our past knowledge of solvent action in polymers and in view of how this solvation behavior explains at least qualitatively the observed phenomena, whenever quantitative statements connot be made we feel at this time that the effect of water is primarily found in affecting the time dependence of relaxation or creep.

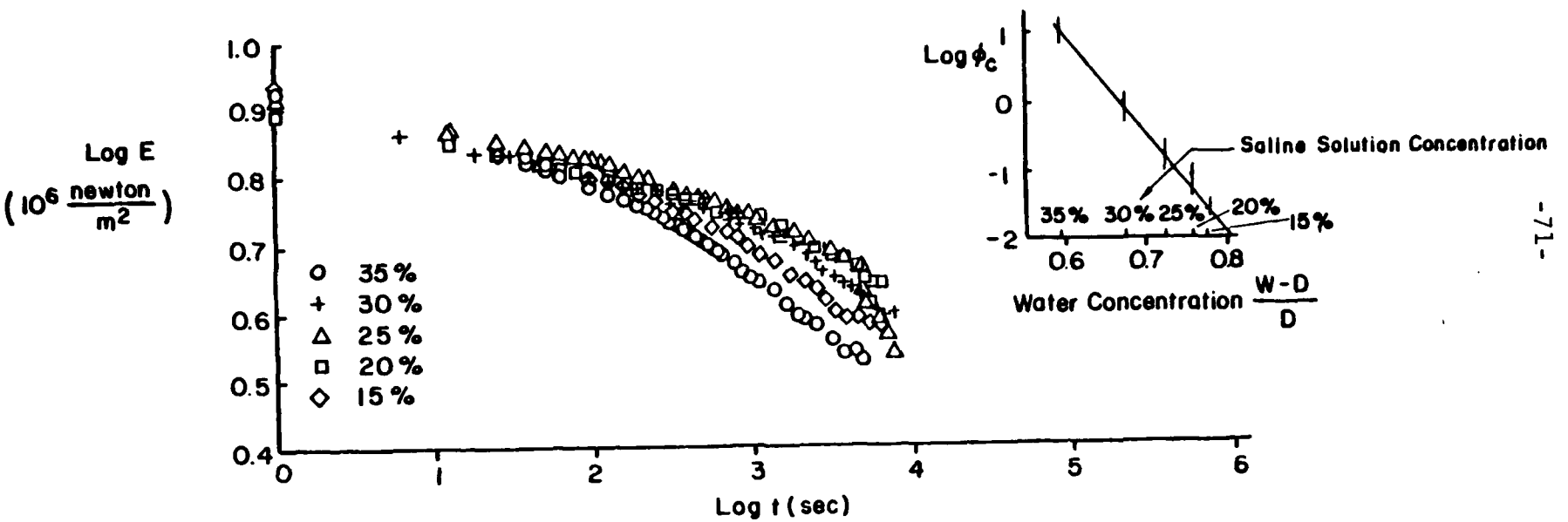

FIG. 36a MASTER CURVE OF 0° SINGLE LAMINA SPECIMENS ASSUMING WATER CONTENT AFFECTS ONLY MAGNITUDE OF RELAXATION MODULUS NOT RELAXATION BEHAVIOUR

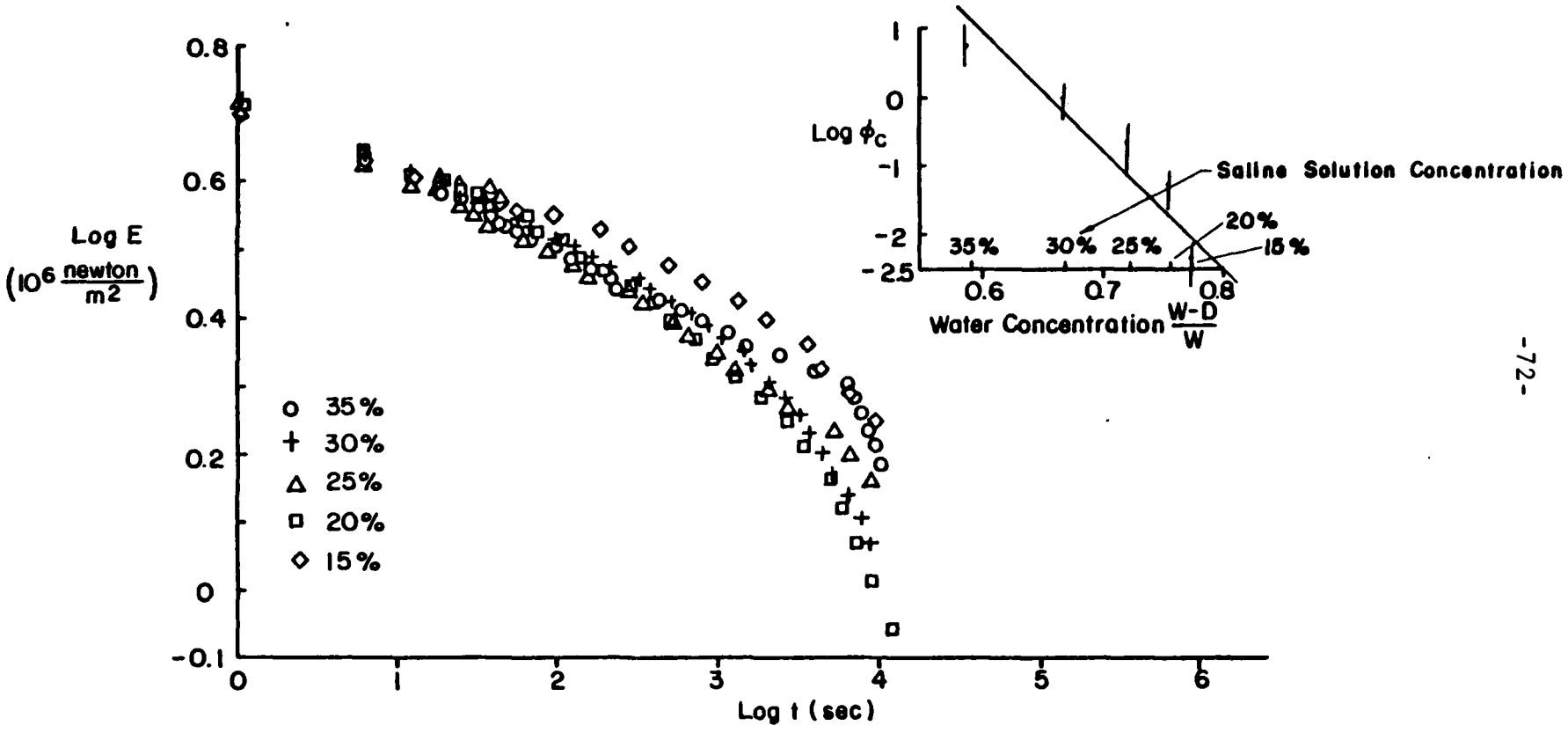

FIG. 36 b MASTER CURVE OF 90° SINGLE LAMINA SPECIMENS ASSUMING WATER CONTENT AFFECTS ONLY MAGNITUDE OF RELAXATION MODULUS NOT RELAXATION BEHAVIOUR

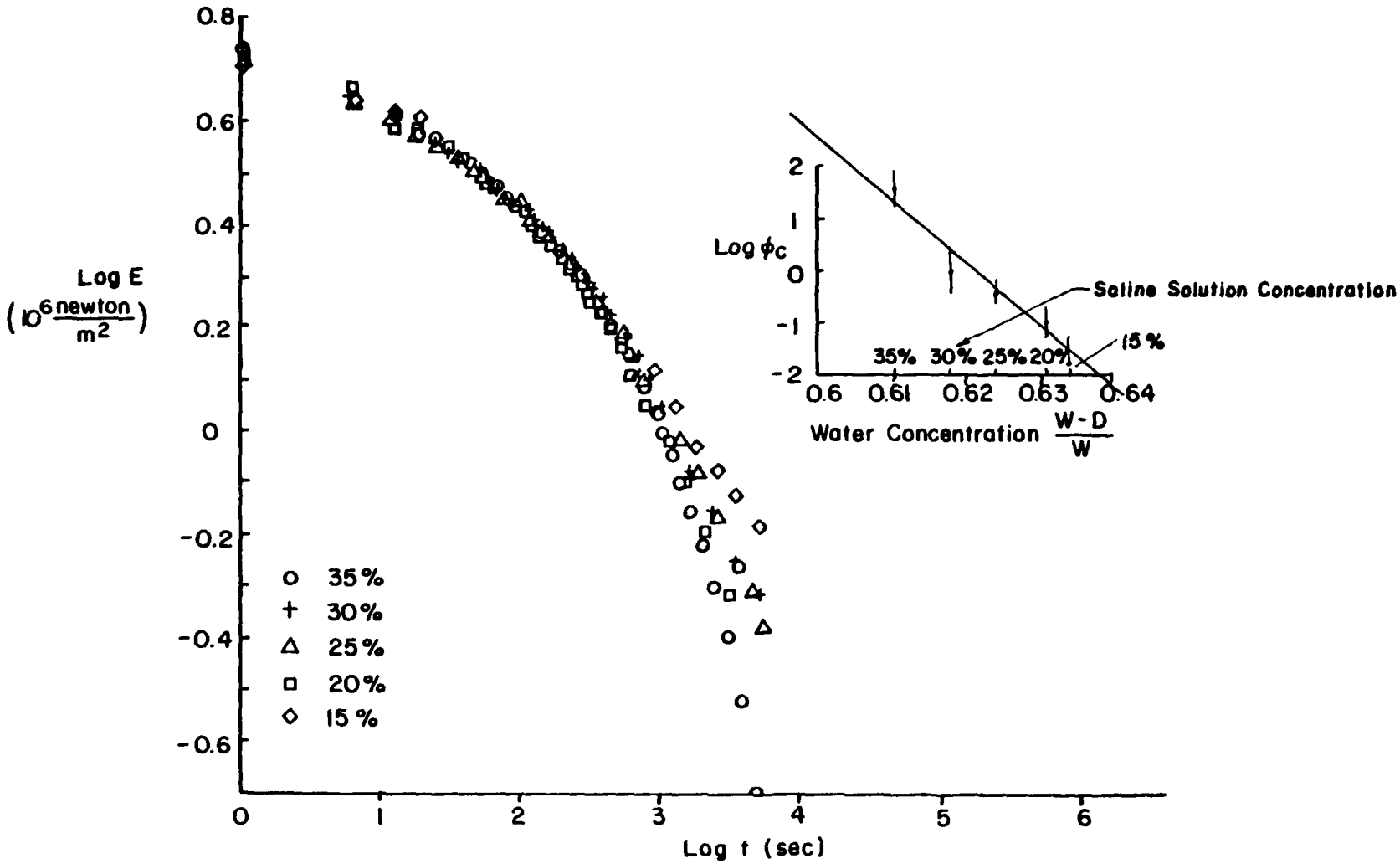

FIG. 36c MASTER CURVE OF HORIZONTAL MULTIPLE LAMINA SPECIMENS ASSUMING WATER CONTENT AFFECTS ONLY MAGNITUDE OF RELAXATION MODULUS NOT RELAXATION BEHAVIOUR

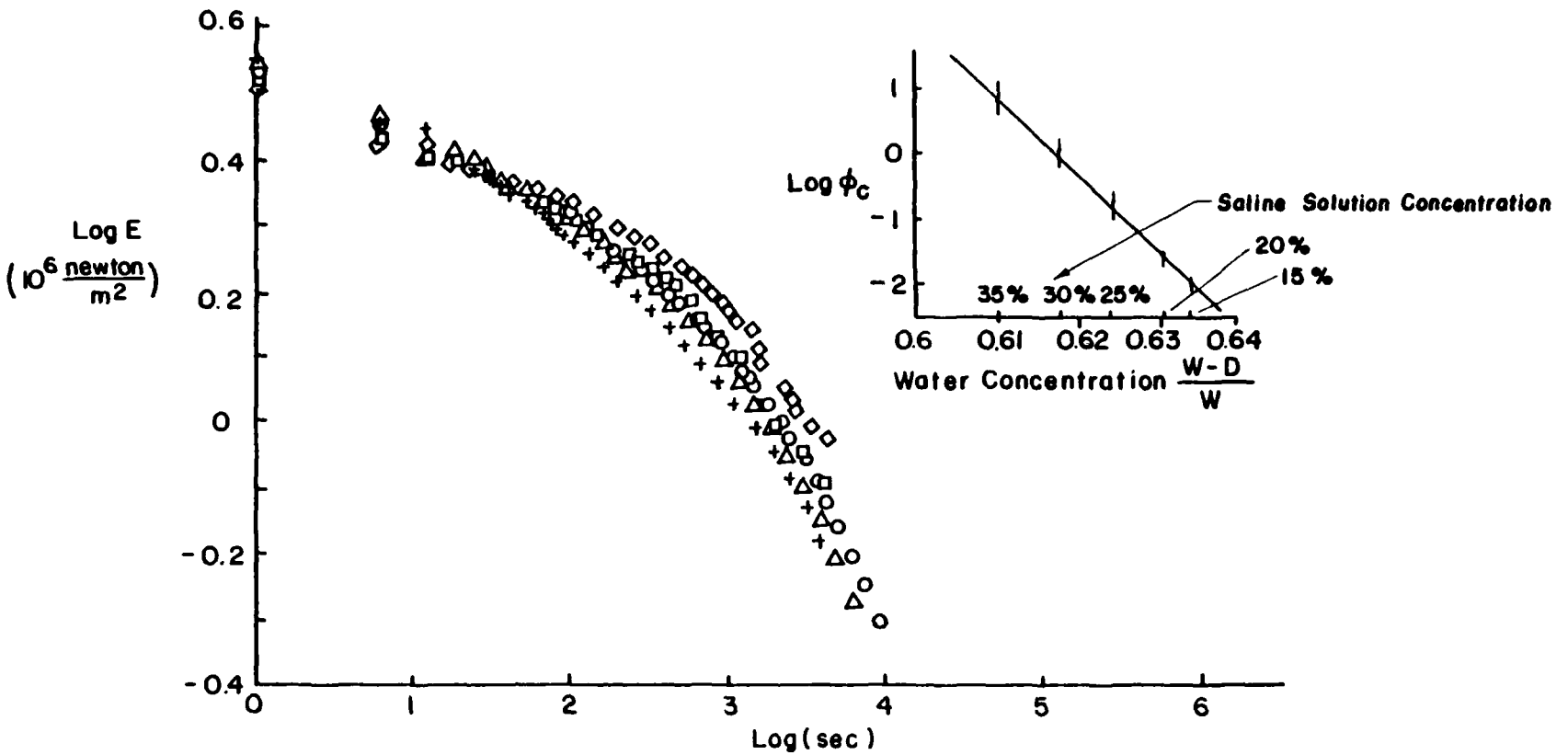

FIG. 36d MASTER CURVE OF VERTICAL MULTIPLE LAMINA SPECIMENS ASSUMING WATER CONTENT AFFECTS ONLY MAGNITUDE OF RELAXATION MODULUS NOT RELAXATION BEHAVIOUR

10. PERIPHERAL STRESS ANALYSIS EFFORT

One of the recurring pieces of information required in disc response is the intra-discal pressure when the spine is loaded axially. This information is important to estimate the load carrying ability of the disc, especially with regard to failure; but it is also important to know this internal pressure for a deformation analysis of the disc if diagnostics related deformations are carried out.

While powerful numerical codes are available to compute solutions to virtually any boundary value problem provided the appropriate constitutive behavior of the material(s) is known and provided sufficient money is available for its execution, simpler solutions may be obtained to generate stress and deformation related information. We delineate here an approximate solution for an annular disc with circular plan form. Because of the surprisingly close viscoelastic stiffness of the disc material in the horizontal and vertical direction as outlined in the last section we shall treat this problem as one involving linearly elastic behavior. We shall first solve the problem for a compressible solid and then particularize the solution to incompressibility.

Problem Formulation: We consider a right circular annulus attached to rigid (vertebral) bodies as an analogue to the disc; this choice eliminates parametric variation of the disc plan-form shape characterized by Farfan (Ref. 16) in terms of

posterior outline. Referring to Figure 37 we represent the annulus fibrosus by an annular ring of inner and outer radius "a" and "b" respectively; the disc thickness is 2h. The nuclear material is considered to be incompressible, but the annulus possesses a shear and bulk modulus μ and K, while the shear modulus for the nucleus vanishes. The deformation of the annulus under axial compression is governed by the constraints that the nuclear cavity retains constant volume and that the tractions vanish on the outer surface while the annulus remains attached to the rigid endplates.

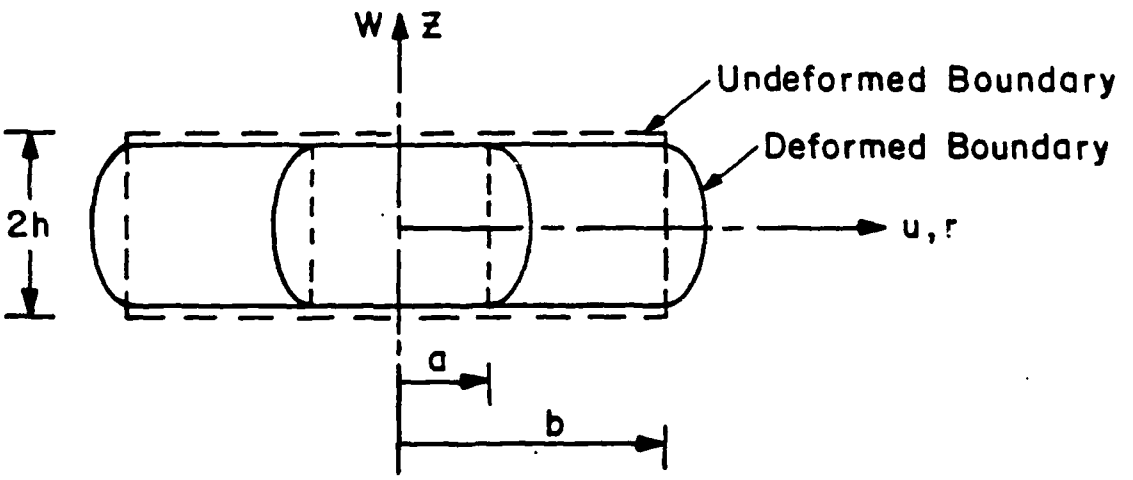

FIG. 37 CIRCULAR DISC ANALOGUE WITH RADIUS a OF LIQUID FILLED CAVITY

With reference to Figure 37, we choose displacements in the z, r and θ directions respectively as

$$w = \varepsilon_o z$$
$$u = \frac{1}{h^2}(h^2-z^2)g(r) \tag{1}$$

where g(r) is a function to be determined from equilibrium and the boundary conditions as spelled out below. The displacement functions (1) cannot satisfy point-by-point equilibrium; therefore the z-averaged equilibrium will be enforced, i.e., the non-vanishing equilibrium equations will be averaged over the thickness 2h of the disc.

We use the constitutive law

$$\tau_{ij} = \lambda\varepsilon_{KK}\delta_{ij} + 2_\mu\ \varepsilon_{ij} \tag{2}$$

with μ the shear modulus and λ the Lamé constant, in terms of Poisson's ratio ν and μ or Youngs' modulus E:

$$\lambda = \frac{2\nu\mu}{1-2\nu} = \frac{E\nu}{(1-\nu)(1-2\nu)} \tag{3}$$

The strain displacement relations render, in view of (1)

$$\varepsilon_z = \frac{\partial w}{\partial z} = \varepsilon_o$$
$$\varepsilon_r = \frac{\partial u}{\partial r} = \frac{1}{h^2}(h^2-z^2)\frac{dg(r)}{dr}$$
$$\varepsilon_\theta = \frac{u}{r} = \frac{1}{h^2}(h^2-z^2)\frac{g(r)}{r} \tag{4}$$
$$\varepsilon_{rz} = \frac{1}{2}\frac{\partial u}{\partial z} = -\frac{z}{h^2}\,g(r)$$
$$\varepsilon_{r\theta} = \varepsilon_{\theta z} = 0$$

so that the stress components become, primes denoting differentiation with respect to r,

$$\begin{aligned}
\sigma_z &= \frac{1}{h^2}(h^2-z^2)\lambda\left[\frac{g(r)}{r} + g'(r)\right] + (2\mu+\lambda)\varepsilon_o \\
\sigma_r &= \frac{1}{h^2}(h^2-z^2)\left[(2\mu+\lambda)g'(r) + \lambda\frac{g(r)}{r}\right] + \lambda\varepsilon_o \\
\sigma_\theta &= \frac{1}{h^2}(h^2-z^2)\left[\lambda g'(r) + (\lambda+2\mu)\frac{g(r)}{r}\right] + \lambda\varepsilon_o \\
\tau_{rz} &= -2\mu\frac{z}{h^2}g(r) \\
\tau_{r\theta} &= \tau_{\theta z} = 0
\end{aligned} \tag{5}$$

The equilibrium equation in the radial direction after being averaged over the disc height 2h becomes then

$$\begin{aligned}
&r\,g''(r) + rg'(r) - \left[\left(\frac{r}{H}\right)^2 + 1\right] g(r) = 0 \\
&\text{with } H^2 \equiv \left[(\lambda+2\mu)/3\mu\right]h^2
\end{aligned} \tag{6}$$

The solution to this Bessel equation is

$$g(r) = AI_1\left(\frac{r}{H}\right) + BK_1\left(\frac{r}{H}\right) \tag{7}$$

where I_1 and K_1 are modified Bessel Functions of the first and second kind and of order one; the constants of integration A and B need to be determined from the average boundary conditions at r=a and r=b. On the outside surface we have

$$\bar{\sigma}_r = \frac{1}{2h}\int_{-h}^{h}\sigma_r\,dz = 0 \quad \text{at } r=b \tag{8a}$$

while on the inside an unknown pressure P acts so that

$$\bar{\sigma}_r = - P \tag{8b}$$

This pressure is determined by the constraint that the nucleus pulposis, being liquid like, is incompressible and that therefore the cavity maintains constant volume during deformation. That condition is expressed by

$$2h\pi a^2 = \int_{-h(1+\varepsilon_o)}^{h(1+\varepsilon_o)} \pi U^2(a,z)\, dz \tag{9}$$

which renders, after some algebra

$$g(a) = - \frac{3}{4} a\varepsilon_o \tag{10}$$

Suppose we satisfy the boundary conditions (8a) and (8b) then the magnitude of the pressure needs to be adjusted such that (10) is satisfied.

Use the following notation

$$I_1' = \frac{d}{dr} I_1\left(\frac{r}{H}\right); \quad K_1' = \frac{d}{dr} K_1\left(\frac{r}{H}\right)$$

$$X(r) = \frac{2}{3}\left\{ 2\, I_1' + \lambda\left[I_1' + \frac{1}{r} I_1 - \frac{2}{a} I_1(a)\right]\right\} \tag{11}$$

$$Y(r) = \frac{2}{3}\left\{ 2\mu K_1' + \lambda\left[K_1' + \frac{1}{r} K_1 - \frac{2}{a} K_1(a)\right]\right\}$$

Then

$$\bar{\sigma}_r = A\, X(r) + B\, Y(r) \tag{12}$$

and the constants A and B are determined from the boundary conditions (8)

$$\begin{bmatrix} X(a) & Y(a) \\ X(b) & Y(b) \end{bmatrix} \begin{Bmatrix} A \\ B \end{Bmatrix} = \begin{Bmatrix} -P \\ 0 \end{Bmatrix}$$

as
$$A = -\frac{P\,Y(b)}{\Delta} \qquad (13)$$
$$B = \frac{P\,X(b)}{\Delta}$$

with
$$\Delta = X(a)Y(b) - X(b)Y(a) \qquad (14)$$

Use of (10) results in

$$P = \frac{3}{4}\varepsilon_o a \left\{ \frac{Y(b)}{\Delta} I_1\left(\frac{a}{H}\right) - \frac{X(b)}{\Delta} K_1\left(\frac{a}{H}\right) \right\} \qquad (15)$$

so that
$$A = -\frac{3a\varepsilon_o}{4} \frac{Y(b)}{Y(b)I_1 \frac{a}{H} - X(b)K_1 \frac{a}{H}}$$

$$B = \frac{3a\varepsilon_o}{4} \frac{X(b)}{Y(b)I_1\left(\frac{a}{H}\right) - X(b)K_1\left(\frac{a}{H}\right)} \qquad (16)$$

Having determined the constants of integration one may evaluate the average stresses, in particular the axial stress $\bar{\sigma}_z$. Then the total axial load L carried by the disc is

$$L = \pi a^2 P + 2\pi \int_a^b \sigma_z(r,h)\, r\,dr \qquad (17)$$

where the pressure P is given by (15); accordingly that portion of the load carried by the nucleus L_n is

$$L_n = \frac{\pi a^2 P}{L}$$

$$= \frac{1}{1 + 2\int_a^b \frac{\sigma_z(r,h)}{P} \frac{r}{a} \frac{dr}{a}}$$

and the portion carried by the annulus L_a is

$$L_a = 1 - L_n$$

First Check of the Solution: For a thin <u>solid</u> disc the solution is available in reference 17; for incompressible solids that solution simplifies considerably. However, the present solution is more complicated because it accounts for the nucleus with singular Bessel functions and we found the expansion for incompressible solids laborious. Therefore the present solution was compared with the simpler reference for $\nu = 0.49995$ and the solutions are equal within plotting accuracy, as shown in Figure 38. In Figure 39 are shown examples of stress distributions for flat discs when the nucleus radius is non-zero. Alternate geometries are readily treated.

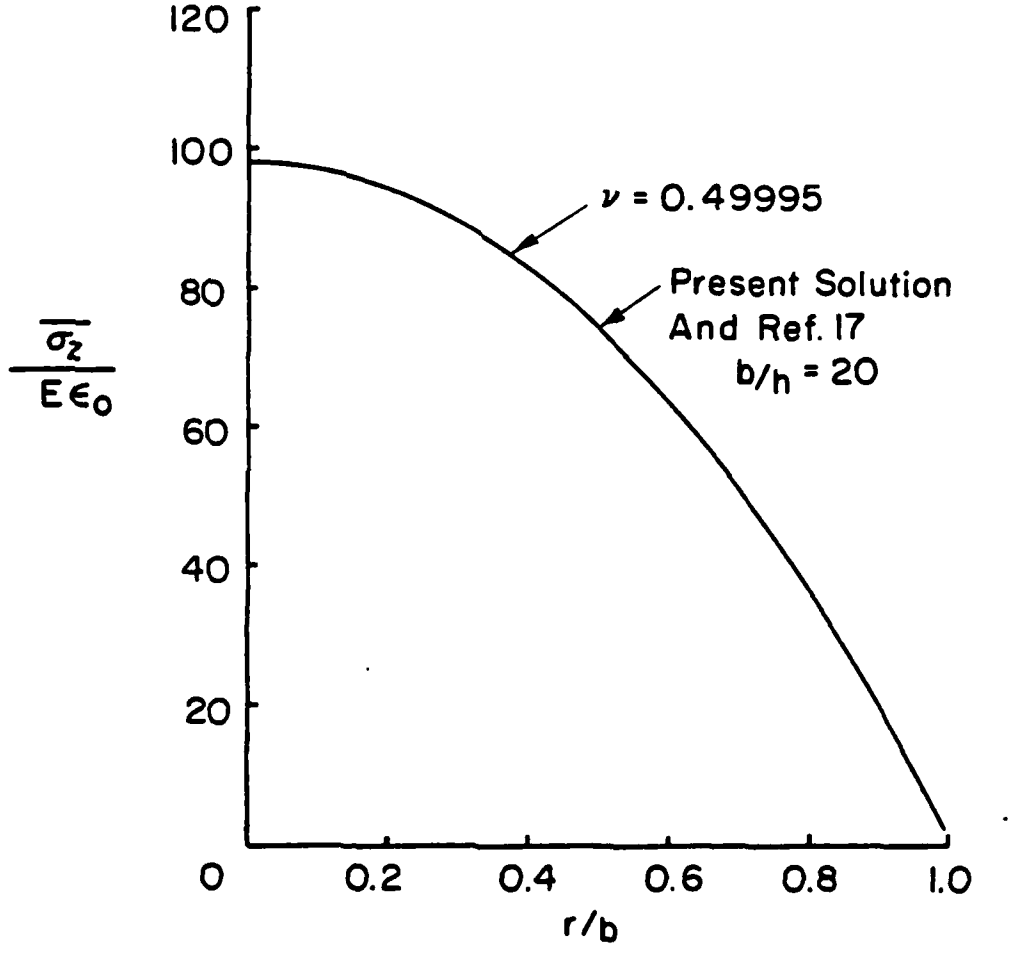

FIG. 38 PRESSURE DISTRIBUTION IN A SOLID DISC – COMPARISON WITH RESULTS OF REF. 17

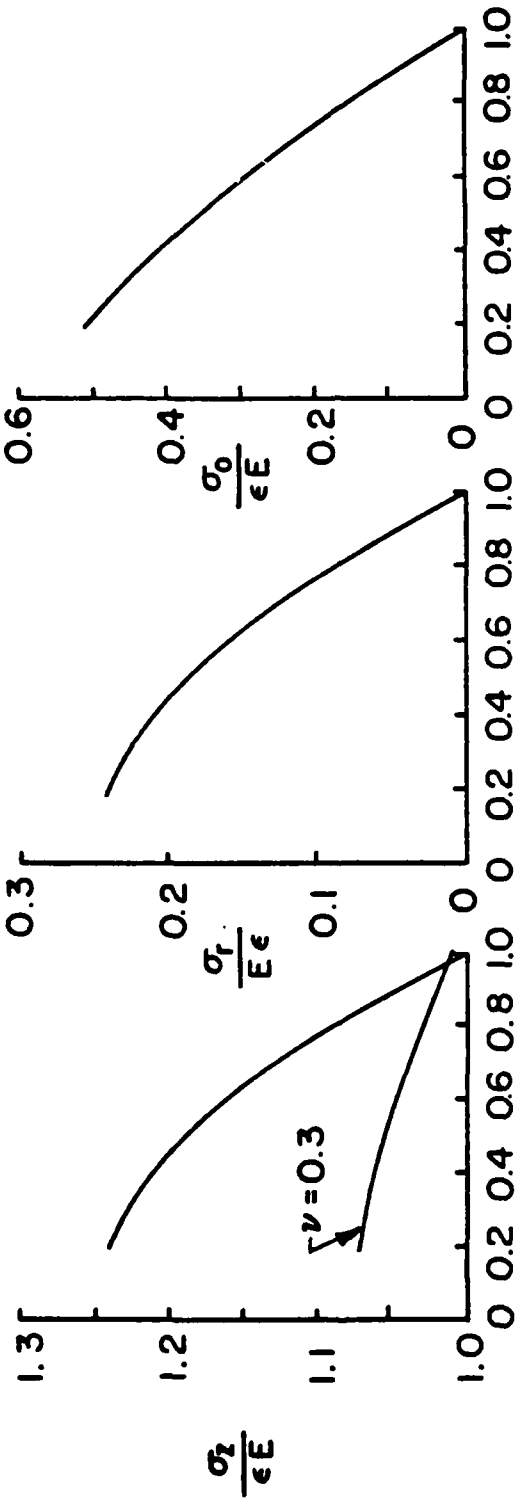

FIG. 39 STRESS DISTRIBUTION IN ANNULUS, b/a = 5, NEARLY INCOMPRESSIBLE SOLID (EXCEPT ONE EXAMPLE WITH ν=0.3)

11. REFERENCES

1. Time, coverstory: That Aching Back; July 14, 1980.
2. Schultz, A. B.; Mechanics of the Human Spine; Appl. Mech. Reviews; 1974.
3. Schultz, A. B.; Belytschko, T. B.; Biomechanics Research and Education at UICC, American Society of Engineering Education, Annual Conference, RPI; Troy, N.Y.
4. Galante, J. O.; Tensile Properties of the Human Lumbar Annulus Fibrosus; Acta Orthop. Scand. Suppl. 100; 1967.
5. Virgin, W. J.; Experimental Investigations into the Physical Properties of the Intervertebral Disc; J. Bone Jt. Surg.; Bol. 33B, No. 4, 607-611; 1951
6. Kazarian, L.; Creep Characteristics of the Human Spinal Column; The Orthopedic Clinics of North America, Vol. 6, No. 1; 1975
7. Dickson, I. R.; Naylor, A., et al.; Variations in Protein Components of Human Intervertebral Disc with Age; Nature, Vol. 215; 1967.
8. Naylor, A.; Intervertebral Disc Prolapse and Degeneration: The Biochemical and Biophysical Approach; Spine, Vol. 1, No. 2, 108-114; 1976.
9. Lyons, H., Jones, E., Quinn, F. K., and Sprunt, D. H.; Changes in the Protein-Polysaccharide Fractions of Nucleus Pulposus from Human Intervertebral Disc with Age and Disc Herniation; J. Lab. Clin. Med.; 68:930; 1966.

10. Püschel, J.; Der Wassergehalt Normaler und degenerieter Zwischenwirtelscheiben; Beitr. path. Anat. 84, 123; 1930.

11. De Pukey, P.; The Physiological Oscillation of the Length of the Body; Acta. Orthop. Scand. 6:338; 1935.

12. Panagiotacopulos, N. D., Knauss, W. G., Bloch, R.; On the Mechanical Properties of Human Intervertebral Disc Material; Third International Congress of Biorheology; Biorheology Vol. 16; 317-330; 1979

13. Charnley, J.; The Imbibition of Fluid as a Cause of Herniation of the Nucleus Pulposus; Lancet Vol. 1, 124-127; 1952.

14. Naylor, A., Smare, D. L.; Fluid Content of the Nucleus Pulposus as a Factor in the Disk Syndrome - A Preliminary Report; Br. Med. J. Vol 2; 975-976; 1953.

15. Bush, H. D., Horton, W. G., Smare, D. L., Naylor, A.; Fluid Content of the Nucleus Pulposus as a Factor in the Disk Syndrome - Further Observations; Br. Med. J. Vol 2; 81-83; 1956.

16. Farfan, H. F.; Mechanical Disorders of the Low Back; Lea & Febiger, Philadelphia; 1973.

17. Lindsey, G. H., et al.; The Triaxial Tension Failure of Viscoelastic Materials; Aerospace Research Laboratories Report ARL 63-152; September 1963.

12. ACKNOWLEDGEMENTS

The writer wishes to thank all those who participated in this work. In particular he wishes to thank Nicolas Panagiotacopulos who initiated the interest in this work, Prof. P. Harvey and M. Patzakis who sustained the work with advice and action. Last, but not least, many thanks are due to Dr. L. Kazarian whose forsight and interest in this problem provided the fertile ground in which this work could grow.

13. APPENDICES

BIORHEOLOGY Vol. 16, pp. 317-330
Pergamon Press Ltd. 1979. Printed in Great Britain

THIRD INTERNATIONAL CONGRESS OF BIORHEOLOGY

ON THE MECHANICAL PROPERTIES OF HUMAN INTERVERTEBRAL DISC MATERIAL

N. D. Panagiotacopulos
W. G. Knauss
R. Bloch

California Institute of Technology, Pasadena, California

(Received 1.3.1979; in revised form 30.4.1979.
Accepted by Editor Y.C.B. Fung)

ABSTRACT

The viscoelastic response of human intervertebral disc material is studied. It is shown that the water concentration in the material has a dominant effect on the relaxation behavior. The studies are performed on small specimens cut from laminae which are excised from the anterior portion of an L4-L5 disc. Some consequences of this water sensitivity for laboratory testing and in-vivo response are discussed.

INTRODUCTION

The human spine consists of a series of vertebrae which are separated from each other by discs and surrounded by ligaments and muscles. The main mechanical function of the spine is to support the upper body and transmit the weight/force to the legs. The discs, which contribute approximately one-third of the overall length of the spine, allow deformations of the spine, and may act as energy or shock absorbers. The low back region of the spine, known as the lumbar region, is subjected to most of the loads experienced by the body and thus that spinal part is most prone to disc damage.

A frequent problem is that of the "herniated disc" which is defined as the extrusion of the jelly-like material from the center of a disc (nucleus pulposus) through the disc wall (annulus fibrosus). While the proclivity to herniation with age depends in part on the biochemical changes that occur in the material of the disc during its maturation process it is also true that disc herniation is a mechanical problem of failure. It seems, therefore, that its treatment, as well as its possible prevention, would be aided by an improved understanding of the mechanical behavior of the disc material under various modes of deformation. In fact, determination of the mechanical properties is a necessary precursor to understanding the rate dependent failure behavior of discs.

Upon reviewing the work in this field, one finds that by far most of the experimental work on the human intervertebral discs has been carried out on autopsy specimens, such as segments of the spine consisting of two vertebral bodies with their intervening disc, or with sizeable sections of the annulus fibrosus (Refs. 1 - 5). Most of these experiments were intended to obtain average mechanical properties of the total disc, while assuming at the same time, that the disc material exhibits elastic behavior. However, to the best of our knowledge, only a few experiments (Ref. 6) recognize the viscoelastic character of the disc material. In this paper, we report a study which is concerned with the viscoelastic behavior of the components of the disc structure.

For orientation purposes, it is first necessary to briefly discuss the structure of the disc. It is a highly inhomogeneous element of the spine which connects to the vertebrae via cartilaginous end plates (as shown in Fig. 1a). The central volume is occupied by the nucleus pulposus, a jelly-like substance containing short fibers of mucopolysaccharide. This nucleus is contained in the annulus fibrosus, a system of fiber reinforced layers having roughly kidney-shaped cross sections (as shown in Fig. 1b). The fibers consist of collagen and are bound together by a matrix of mucopolysaccharide. In each layer these fibers alternately form angles of $\pm 50^{\circ}$ with the spinal axis. Although the layers, and thus the fiber orientation are rather distinct, there are some fibrous interconnections between individual layers, but on the whole they are fairly separate, especially in the anterior portion of the annulus and in the case of young, healthy discs. It has been reported that there are approximately 12 - 14 layers, but our experience indicates a considerably larger number. The thickness of individual layers tends to

KEY WORDS: collagen, intervertebral disc, biosolids

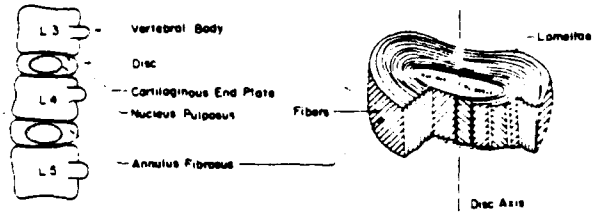

FIG. 1

Disc Geometry

increase towards the nucleus pulposus.

Early in our studies of the mechanical behavior of disc material, we discovered that water has a dominant effect on the viscoelastic response of disc material. In order to document that effect, we present here studies conducted in a moisture controlled air environment. Accordingly, we discuss in section 2 some molecular aspects of the effect of solvents on the mechanical behavior of polymers as a model for our own hydroviscoelastic studies.

We next document in sections 3 and 4 problems of specimen preparation and physical measurements. Tests results and data analysis are presented in section 5, followed by a brief analysis of the consequences of these results in connection with both laboratory testing of spinal disc material as well as in vivo changes due to aging.

MOLECULAR ASPECTS

The materials of the annulus fibrosus are natural polymers and share with synthetic ones certain macroscopic physical properties such as creep and relaxation. For reasons of brevity, we shall not discuss here the relation of these properties to the microstructure, but assume the reader to be familiar with that knowledge (Refs. 7 - 9). Primarily for the purpose of nomenclature we recall that short time behavior (glassy response) and long time behavior (rubbery plateau*) bound the transition region in time. In many engineering problems involving polymers, the temperature has a profound effect on the rate with which molecular deformation or molecular rearrangement processes occur. Increased temperature heightens the degree of freedom available to the molecule or its segments by enlarging what is often referred to as the free volume (Refs. 7 - 9). In a similar way, the introduction of solvent molecules decreases the intermolecular forces mutually acting on chain segments and increases thus the freedom with which chain segments can move relative to each other. The net result is that the rate of molecular deformation processes is increased as the temperature is raised and/or solvent (including water) is introduced. This change in the rate of deformation or relaxation can manifest itself as a multiplicative factor to the time, which factor depends on the temperature (Refs. 7 - 10) and/or on the amount of solvent present (Refs. 11 and 12). Since viscoelastic data is recorded typically on a logarithmic time basis, the multiplicative function of temperature or moisture appears as an additive (or subtractive) function along the logarithmic time axis. Thus relaxation or creep curves tend to "shift" along the (horizontal) log-time axis to shorter times if the temperature and/or solvent content increases, and conversely. Whether such "hydrothermal shifting" of mechanical response data is valid for any particular polymer can be ascertained only through adequate experimental inquiry. In our subsequent work other experimental problems associated primarily with the small size of specimens overshadow this uncertainty, and we therefore assume that such a moisture-time trade-off relationship exists.

*There is no need in this work to be concerned with the possibility of unbounded flow for extremely long times.

AD-A094 791 CALIFORNIA INST OF TECH PASADENA GRADUATE AERONAUTIC--ETC F/G 6/16
HYGROVISCOELASTICITY OF THE HUMAN INTERVERTEBRAL DISC.(U)
JUL 80 W G KNAUSS AFOSR-77-3139
UNCLASSIFIED GALCIT-SM-80-18 AFOSR-TR-81-0084 NL

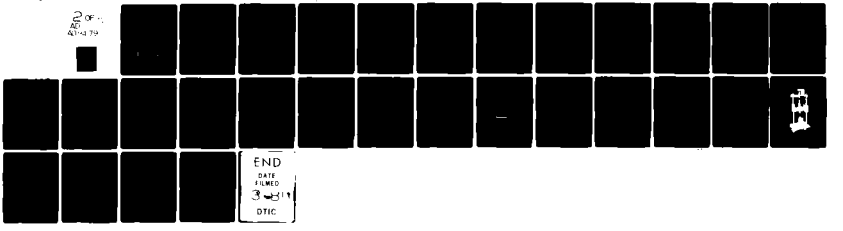

END
DATE FILMED
3-81
DTIC

Because the disc material is subjected to different environments during preparation and testing, the question of chemical changes arises. To date, we have gauged such chemical changes by two simultaneous requirements, namely that 1) no observable discoloration occur and 2) that upon returning a specimen to an initial reference environment, no clear change in the desired mechanical properties will be produced. For example, heating the disc material to 42° C results in a brown hue, probably as a result of oxidation, while immersion in lithium perchloride (LiClO4)* caused slight discoloration and embrittlement. We found that drying and moisturizing specimens would not change the mechanical properties, except that after 6 to 10 such cycles of drying and moisturizing, it appeared that the material becomes less hydrophylic when exposed to a humid environment.

SPECIMEN PREPARATION

Perhaps the most difficult procedure in this investigation sequence is the specimen preparation; it sets the pace of the work reported here. Lumbar sections are obtained from unclaimed human bodies approximately 24-28 hours after death. These bodies were not embalmed but refrigerated. The excised spinal sections were immediately placed in plastic bags and embedded in dry ice. We assumed that the resulting freezing and thawing did not affect the mechanical properties.

Specimens of approximately a single lamella are separated carefully from the anterior portion of the disc as described in Reference 13. Figure 2 shows a transmission micrograph of a single lamella specimen. It is clear from the fiber-reinforced structure of

FIG. 2

Transmission Micrograph of Single Lamina Showing Nearly Unidirectional Fiber Orientation.

the lamella that orthotropic properties are characteristic for this laminar material. However, in this initial investigation we did not study the anisotropic aspects of the material, but concentrated only on its viscoelastic behavior; therefore strip specimens were cut with a special jig from laminae so as to yield test specimens as large as possible. We

*Observed during our search for salt solutions to control the moisture environment for the specimens.

thus used specimens for which the fiber direction was about 30° with respect to the tensile axis. Typical specimen dimensions were 10-15 mm by 2-3 mm and .01 mm thick.

EXPERIMENTAL TECHNIQUE

An Instron tester, equipped with a load cell (maximum load 500 gm*) was used to perform the relaxation measurements. A Bemco-conditioning chamber was attached to the crossbar of the Instron tester into which the atmosphere was pressure fed from a Tenney environmental chamber. The maximal relative humidity used was 86% (at 37° C). At higher relative humidities, small temperature changes caused precipitation of water droplets on the specimen which resulted in large changes in the relaxation force. Although we have succeeded in some cases to produce environments of higher relative humidity, these uncertainties in environmental control were a continuous source of concern.

In order to determine the time to achieve equilibrium of the moisture content, dried specimens were suspended on a wire mesh from a Mettler electronic balance into a control chamber. Figure 3 shows the rate of weight gain, indicating that one-half hour of

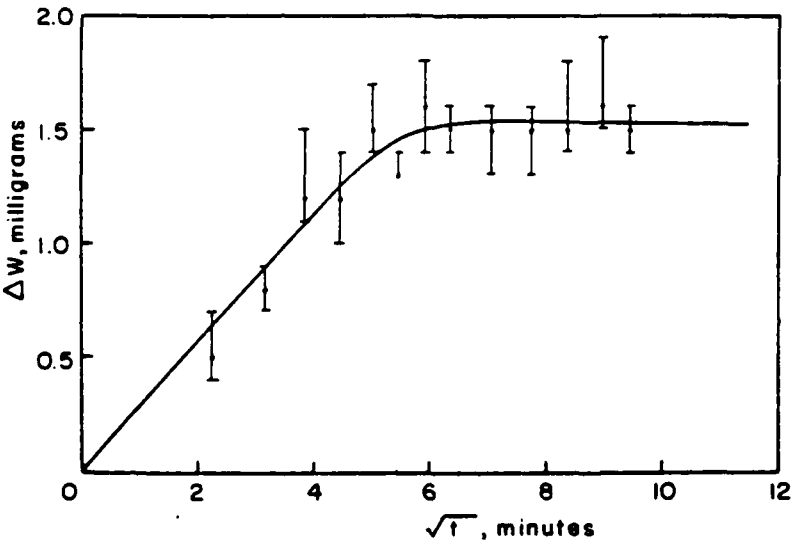

FIG. 3

Specimen Gain of Water in Air at 32% RH, Dry Bulb Temperature = 32° C.

moisture conditioning prior to measurements was adequate. In the same manner, the amount of equilibrium water absorption was measured as a function of the environmental humidity. The specimen was dried overnight in a vacuum before a sequence of 4-6 measurements were performed per day.

We define the (percent) water content or water concentration as the ratio of the weight of the water absorbed to the total weight of the (wet) specimen. The results are shown

*Since the load in the present tests ranged between 25 and 100 mg, great care needed to be exercised to eliminate friction of the wire connecting the specimen to the load cell. Also, since the pressure-fed moist air could escape from the conditioning cabinet along the wire, the load cell had to be removed far enough in order not to respond to the impinging air.

in Figure 4. The solid line represents the least square fit of a straight line to the data and the dashed line, a linear regression analysis.

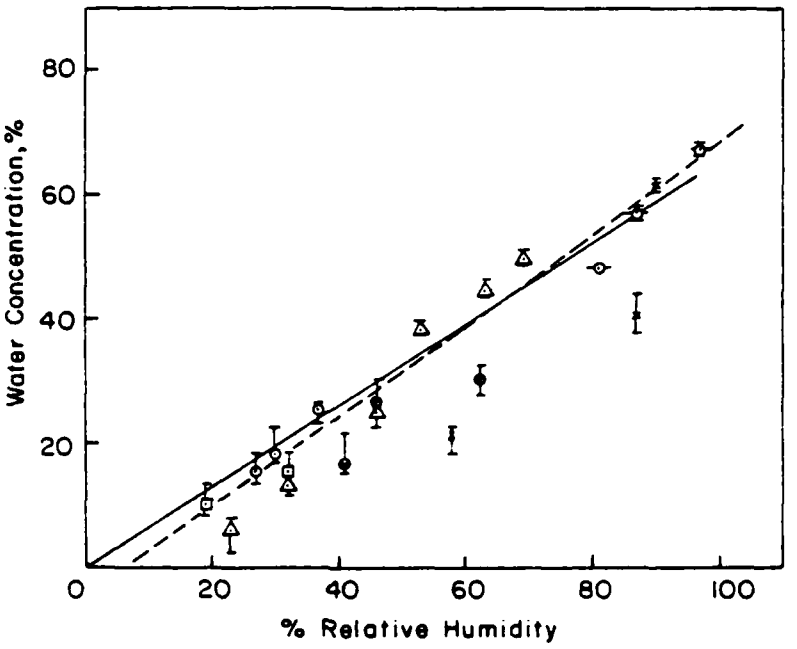

FIG. 4

Water Concentration (Water Absorbed/Wet Weight) in Disc Lamella as a Function of Environmental Relative Humidity. Each Point is the Average of 15 Measurements —— Least Squares Fit-----Linear Regression. Symbols Represent Measurements on Different Days on Same Specimen Starting with Specimen Dried in Vacuum.
⊡ 11-16-78 ⊛ 11-17-78 ⊙ 11-22-78 △ 11-28 and 29-78
x 1-10-79.

Although Figure 4 shows water contents as high as 69% at nearly 95% RH, it was very difficult with our equipment to maintain the RH control such as to avoid condensation. Therefore, in our measurements of material relaxation, the maximum water content achieved in moist air was only 56%. This is low compared to the 70% moisture content estimated or expected in disc material of mature adults. In a following publication we deal with environmental test conditions which are closer to those appropriate for in vivo conditions. As we shall see below, the present test conditions lead to material response that is associated with very short duration or high frequency loading of disc material with realistic moisture content. Thus the results presented here are still meaningful in spite of the relatively low water content.

It is pertinent to mention here that, in general, the amount of solvent absorbed by a polymer depends on the magnitude and state of stress. Therefore, a specimen under strain in a relaxation test may change its water content during the duration of the test. In fact, it is possible that a substantial amount of stress relaxation is induced by take-up of additional water rather than by molecular rearrangement. In the present study, we ignored the possible flow of water into the stressed specimen; later studies confirmed our belief that this neglect did not lead to any significant error.

Specimens were held in specially manufactured grips made partially of plexiglass so that the specimen could be viewed during clamping for careful alignment. In these initial tests, the separation of these grips was used to determine the uniaxial strain, but it was difficult to determine clearly the condition of simultaneous zero-load and zero-strain. This uncertainty was magnified if a specimen was removed from the grips and reclamped. For this reason, we conducted test sequences whenever possible, without regripping the

specimen.

The biggest problem encountered in the present study was the uncertainty in the strain achieved. Later studies concentrated, therefore, on the elimination of that problem which could result in variation of measured relaxation modulus.

The specimen dimensions were determined under a low power microscope, its thickness with a micrometer when the specimen was placed between two glass plates of known thickness.* Because we had (and have) difficulty of producing specimens of highly uniform thickness, this thickness variation produced inhomogeneous stress and strain regions in the specimen; but this error was unavoidable.

The Instron force measuring unit (load cell, amplifier, and pen recorder) allowed a resolution of 5 mg and a drift during a typical test during 4 hours of less than 2%.

The humidity was monitored and controlled via copper-constantan thermocouples according to pre-set dry ($\pm$ 0.2° C) and wet ($\pm$ 0.5° C) bulb temperatures.

Whenever a single specimen was used without regripping for a sequence of tests, a sufficient time period was allowed between tests equalling never less than five times the duration of the previous test (see Ref. 13). When the same specimen was used in a test sequence, the possibility existed that mechanical damage resulted in a progressive change of the relaxation behavior. We found that by conducting tests on any specimen below 6% strain, no mechanical damage became apparent. Only final tests were conducted at higher strain values but always less than 10%. Not all of the results of these tests are reported here.

TEST RESULTS

Specimens of approximately a single lamella from an anterior circumferential section of the annulus fibrosus were used. The specimens were first dried and weighed, then placed in the conditioning chamber until the water content achieved equilibrium with the moist air environment. The dimensions and weight were determined just prior to start of the relaxation tests. For reasons of brevity in presentation, we dispense here with details of the data reduction and refer the interested reader to Reference 13 which contains additional information on the sensitivity of the relaxation process to water content. Suffice it to state here again that because of the uncertainty in the (cross sectional) dimensions of the specimen, the magnitude of the relaxation modulus is similarly uncertain. But when the same specimen was used, the same uncertainty adheres to all measurements performed on it.

If Figures 5 and 6, we present the relaxation stress (relaxation force per unit undeformed cross sectional area) for 58% water content. We note first that the rate of relaxation is reasonably independent of the strain ε. This observation admits the factoring of the stress into the functions $E(t)$ and $\varepsilon \cdot g(\varepsilon)$ which depend, respectively, on time and strain only. We write, thus, for the engineering stress

$$\sigma = \varepsilon \cdot g(\varepsilon) \cdot E(t) \qquad (1)$$

where the function $g(\varepsilon)$ obeys $\lim_{\varepsilon \to 0} g(\varepsilon) = 1$.

If we let t = constant in (1) (isochronal points), we can determine $g(\varepsilon)$ from a cross plot of the data in Figure 5. Allowing that for $0 \leq \varepsilon \leq 1\%$ $g \doteq 1$, the resultant function is shown in Figure 7. Assuming that the same function applies at different water contents, we plot in Figure 8 the isochronal stress-strain curves for two additional water contents drawing on the corresponding relaxation data depicted in Figure 6. We extract thus from Figures 5, 6 and 7 the (small strain) relaxation modulus $E(t)$ in the range of a few seconds to 3 hours as shown in Figure 9 (only three of the five curves in Figure 5 are represented here to avoid unnecessary cluttering of data points).

We note that different water contents produce distinctly different rates of relaxation. In view of the uncertainty of the cross sectional area, the magnitude of the relaxation modulus is equally uncertain. Moreover, because the specimens were regripped for tests

*Later work relies on weight and density measurements to estimate an average specimen cross section.

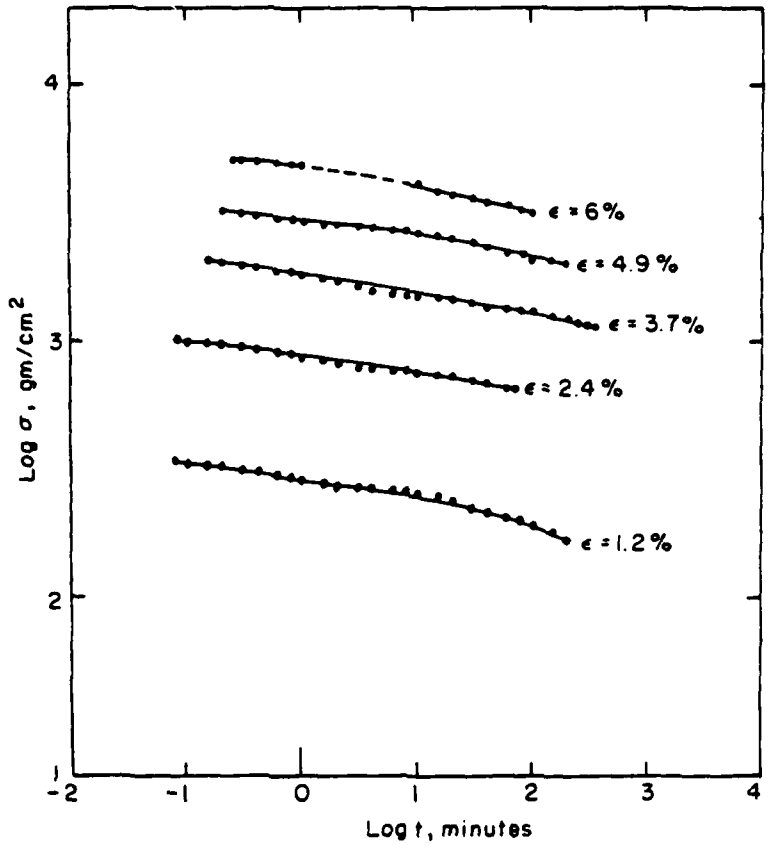

FIG. 5

Relaxation Stress at 58% Water Concentration under Different Strains; Single Lamella Specimens (L4 - L5).

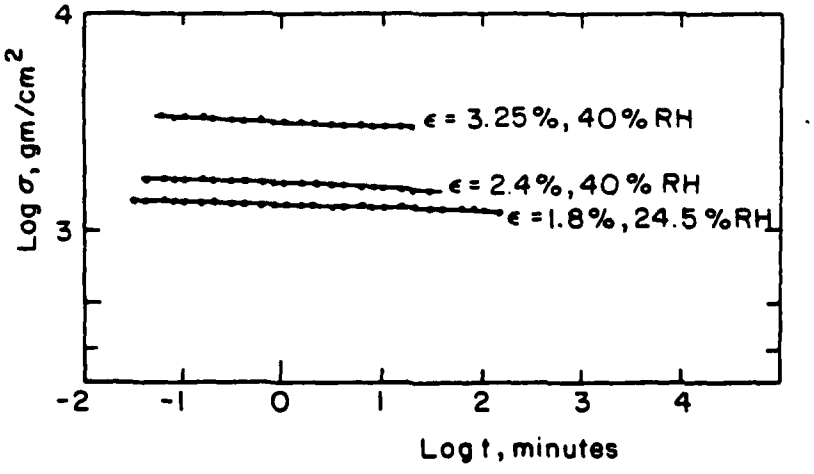

FIG. 6

Relaxation Stress at Two Water Concentrations and Different Strains (L4-L5). Cross Sectional Area Based on Conditions of 58% Water Concentration.

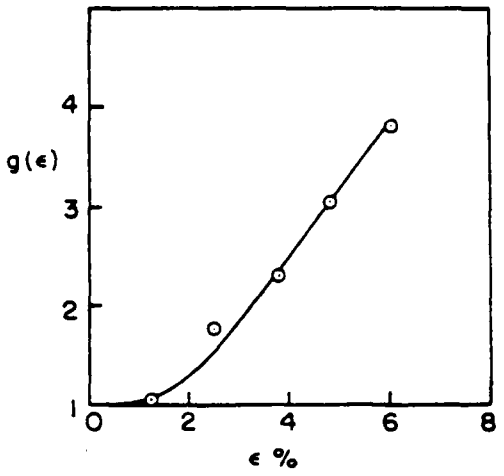

FIG. 7

Non-Linear Strain Function g(ε) Used in Normalizing Relaxation Behavior of Lamellar Disc Specimens.

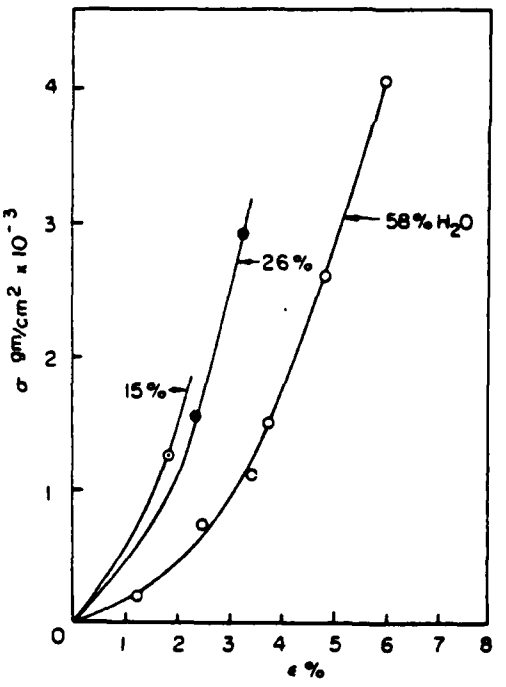

FIG. 8

Isochronal (10 Minute) Stress-Strain Relations Derived from Figures 5 and 6 for Different Water Concentrations.

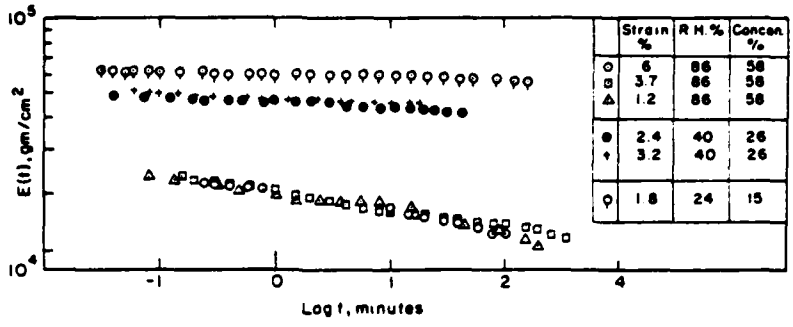

FIG. 9

Small Strain Relaxation Modulus E(t) for Different Water Concentrations. (Specimen Dimensions Correspond to Water Concentration of 58%.

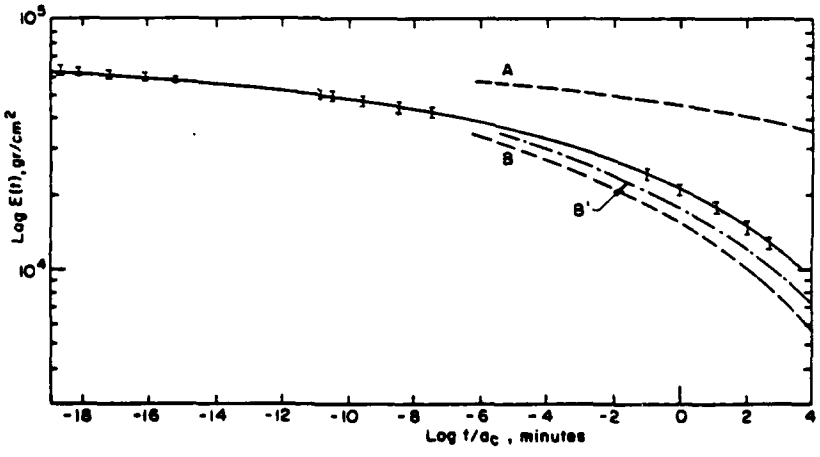

FIG. 10

Composite Master Relaxation Curve of Spinal Disc Material in Tension I-Bars Represent the Range of Data at the Three Water Concentrations of Figure 9. Water Concentrations—58%; – – – A-26%; – – – B-70%; – · – B'-65%. See Text for Explanation of B and B'.

at the three different humidities, additional uncertainty arises as to the relative magnitude of the modulus at these three water contents.

Although the data are sparse, and no additional data can be obtained from the samples cut from the same disc, it is instructive to attempt constructing a "mastercurve" from them. We do this in the belief that the principles underlying synthetic polymers are valid for natural ones, and that the infusion of moisture into the spinal material affects the time scale (relaxation rate) by a multiplicative factor a_c which depends on the specimen's moisture content. This is done in Figure 10 to produce a smooth curve from the three segments separated by gaps. The corresponding concentration shift factor a_c is shown in Figure 11. In view of the earlier discussion on the accuracy of the size of the relax-

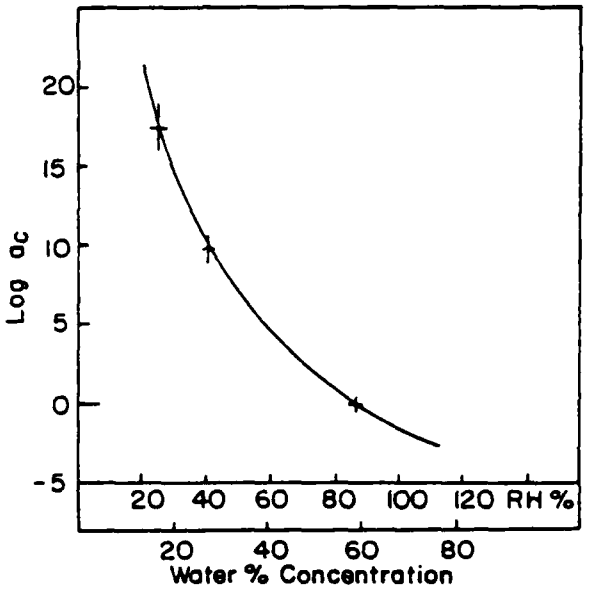

FIG. 11

Shift Factor for Time-Water Trade-Off in Relaxation.

ation modulus, it needs to be mentioned that the shift procedure, and in particular, the shift factor, is subject to that accuracy.

IMPLICATIONS OF THE SENSITIVITY OF THE RELAXATION BEHAVIOR TO WATER CONCENTRATION

It will be noticed that the time scale of the composite solid curve in Figure 10 extends to times of fractions of nano-seconds. This extended range is barely of physical significance since mechanically macroscopic events, especially in the human body, occur over a time range of milli-seconds. Nevertheless, if more data could have been obtained at relative humidities intermediate to those reported here, in particular at, say 75%, 65%, 55%, the gaps in the master curve between the 86% RH corresponding to the micro-second time range would have been available. As the data stands, the solid line in Figure 10 represents a best estimate for the material behavior in that time range.

The fact that lower than in-vivo moisture content leads to remarkably slower relaxation behavior has important implications in testing for material properties if provisions for maintaining the moisture concentration are not provided. Let us illustrate the possible error incurred in measuring the tensile properties of disc material in a drying atmosphere by an estimate for a circular rod. For reasons of simplicity, consider a surface layer of thickness D (refer to Fig. 12) to be more dried out than the interior. In reality there would, of course, be a continuous gradient of moisture rather than a distinct layer and the attendant analysis would be a bit more involved. Nevertheless, let us compute the

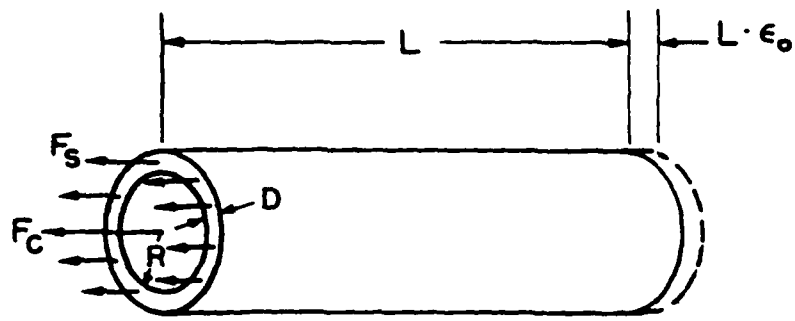

FIG. 12

Concentric Cylinders Modelling Different Rates of Relaxation in Core and (Drier) Surface Layer.

average relaxation stress assuming that the core of the cylinder relaxes at a rate commensurate with 70% water concentration, while the surface layer has dried in an atmosphere of 40% RH. Since the axial strain ϵ_o is the same* in the two concentric cylinder portions, we have for the force in the core

$$F_c = \pi R^2 \cdot g(\epsilon_o) \cdot E_c(t) \cdot \epsilon_o \tag{2}$$

where the subscript "c" denotes relaxation behavior commensurate with 70% water concentration. The force in the surface layer is for $D \ll R$

$$F_s = 2\pi RD\, g(\epsilon_o)\, E_s(t) \cdot \epsilon_o \tag{3}$$

with E_s denoting relaxation behavior at 40% RH (26% water concentration). The total force is $F_c + F_s$ and the average stress $\bar{\sigma}$ is

$$\bar{\sigma} = \frac{F_c + F_s}{\pi(R^2 + 2RD)} \tag{4}$$

or

$$\frac{\bar{\sigma}}{\epsilon_o}\, g(\epsilon_o) = E_c(t)\left\{1 + \frac{2D}{R}\left(\frac{E_s(t)}{E_c(t)} - 1\right)\right\}. \tag{5}$$

The second term in brackets constitutes the error of neglecting that the outside layer is drier than the core. Figure 13 shows this term for $D/R = 0.05$ and indicates that even for such a relatively thin layer, sizeable errors may result because of the different rate of relaxation in the (drier) surface material and the core material.

*Actually, the strain in the outside layer would have to account for shrinkage due to drying. We ignore this fact here, but note that its inclusion in the calculation would make the calculated effect still larger.

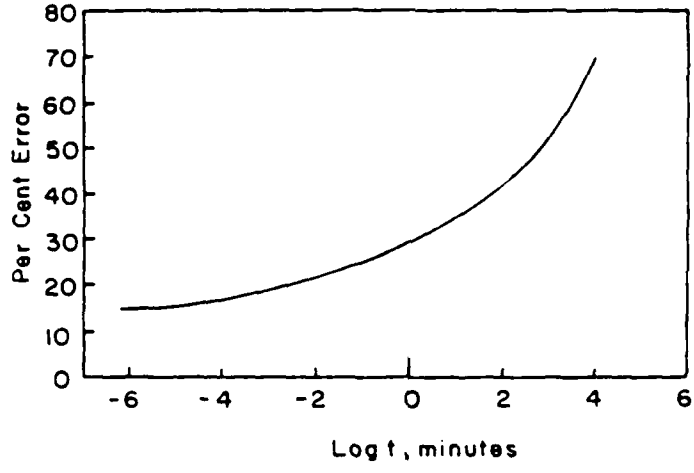

FIG. 13

Error in Measuring Relaxation Modulus at 70% Water Concentration (~ Body Conditions) Due to a 5% Thick Surface Layer of Material at 26% Water Concentration (40% RH).

Finally, we consider a consequence of these preliminary findings which relates to the material behavior in the human body. As man ages, the water content of the body, including the disc, changes. We do not know how much that change is, nor whether it is larger than the variations from one individual to another. However, the results shown here allow us to estimate how much the mechanical properties of the disc material change as a result of alterations in water concentration in the disc material. Suppose that a 5% decrease in water concentration occurs from a nominal value of 70%. From Figure 11 we deduce that this corresponds to a lengthening of the relaxation time by a factor of about 10. This corresponds to shifting the relaxation curve B in Figure 10 to the right by one decade to generate curve B'. Recall that curve B is the estimated response of disc material under "normal" body conditions (70% water content). Then curve B' for the drier disc material results in a relaxation modulus that is about 25% larger (stiffer) at comparable times. Thus a relatively small change in water content induces a very significant change in the mechanical properties of the disc material.

While we do not yet know how the strength characteristics of disc material change with water content, it would not be surprising to find them affected in a similarly sensitive manner. In fact, on the basis of our knowledge relating to synthetic polymers, we would expect a like sensitivity to water concentration for the failure behaviors of disc material.

Although it may be yet a little premature to conjecture on possible failure behavior it is, perhaps, permissible to do so in the interest of stimulating further interest in and understanding of the failure of spinal discs.

If for illustrative purposes we confine attention to uniaxial tension data we note that the failure stress in non-biological polymers is a monotonically increasing function of the strain rate R (in tests employing constant rates of specimen extension); however, the strain at failure does not change monotonically with the strain rate (14) as indicated qualitatively in Figure 14. High rates in this plot correspond to short times in relaxation measurements of Figure 10 and conversely for low rates. In our present work we are not yet sure of whether the time scale in Figure 10 corresponds to rates to the right ($R > R_*$) or to the left ($R < R_*$) of the failure strain maximum. We believe that the portion of the relaxation behavior shown in Figure 10 may be similar to the near-glassy behavior of synthetic polymers in the primary transition. If that were so then the comparative rate range in Figure 14 would correspond to $R > R_*$. Under this assumption, let us now ask for the effect of lowering the moisture content in the material. By virtue of Figure 11 we deduce that a lowering of the water content would shift the failure curves to the left as indicated by the dashed curves in Figure 14. We conclude then that, upon holding the deformation rate constant the failure stress sustained by the drier material increases while the strain capability decreases. However, if the drier material is deformed more slowly than the "normal" material the same strain capability may be achieved as for the wetter material.

If these conjectures turn out to be in the right direction they would be indicative of a remarkable way in which nature optimizes this biological structure: as the water con-

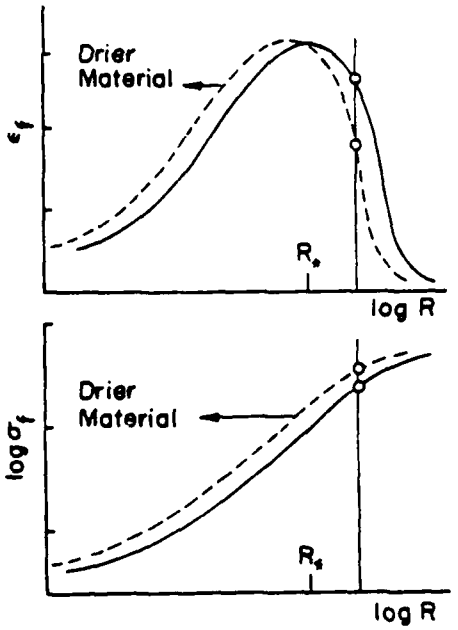

FIG. 14

Qualitative Plot of Failure (Rupture) Strain ϵ_f and Stress σ_f in Uniaxial Tension as a Function of Constant Strain Rate R in Synthetic Polymer.

centration in the disc material drops with age a potential loss in deformability of the material is compensated by the slower deformation speeds associated with receding youth. While this trade-off in water-content and speed-of-motion would not necessarily be one-to-one at every age it would not be unreasonable that this behavior prevails as a trend over a period of years or decades.

ACKNOWLEDGMENTS

The authors are indebted to Professors P. Harvey and M. Patzakis of the Orthopedics Department at USC County Medical School for continued guidance and discussions. This work was supported by the directorate of Life Sciences of the Air Force Office of Scientific Research under Lt. Col. D. Maio and parallels work done under Dr. L. Kazarian of the Biodynamics and Bioengineering Division of the Wright-Patterson Air Force Base.

REFERENCES

1. Virgin, W.J., "Experimental Investigations into the Physical Properties of the Intervertebral Disc", J.Bone Jt.Surg., Vol. 33B, No. 4 (1951), pp. 607-611.

2. Brown, T., Hansen, R.J., and Yorra, A.J., "Some Mechanical Tests on the Lumbosacral Spine with Particular Reference to the Intervertebral Disc", J.Bone Jt. Surg., 39A, (1957), pp. 1135-1164.

3. Galante, J.O., "Tensile Properties of the Human Lumbar Annulus Fibrosus". Acta Orthop. Scand. Suppl. 100, (1967).

4. Yamada, H., "Strength of Biological Materials". Wihliams and Wilkins, Baltimore, (1970).

5. Wu, Yao, "Mechanical Behavior of the Human Annulus Fibrosus", J.Biomechanics; Vol. 9, (1976), pp. 1-7.

6. Kazarian, L., "Creep Characteristics of the Human Spinal Column". The Orthopedic Clinics of North America, Vol. 6, No. 1, (1975).

7. Tobolsky, A.V., Properties and Structure of Polymers, John Wiley & Sons, Inc., New York, (1960).

8. Ferry, J.D., Viscoelastic Properties of Polymers, John Wiley & Sons, Inc., New York, (1961).

9. Bueche, F., Physical Properties of Polymers, Interscience Publishers, Dayton, Ohio, (1962).

10. Williams, M.L., Landel, R.F., and Ferry, J.D., "The Temperature Dependence of Relaxation Mechanisms in Amorphous Polymers and other Glassforming Liquids", J. Am. Chem. Soc., Vol. 77, (1955), pp. 3701-3707.

11. Jenckel, E., and Heusch, R., "Die Erniedrigung der Einfriertemperatur organischer Gläser durch Lösungsmittel". Kolloid Zeitschrift, Vol. 130, No. 2, (1953), pp. 89-105.

12. Kelley, F.N. and Bueche, F., Journal of Polymer Science, "Viscosity and Glass Temperature Relations for Polymer-Diluent Systems". Vol. L, (1961), pp. 549-556.

13. Panagiotacopulos, N.D., Bloch, R., Knauss, W.G., Harvey, P., and Patzakis, M., "On the Mechanical Properties of the Human Intervertebral Disc". California Institute of Technology, Pasadena, CA 91125. GALCIT SM #78-13, (1978), AFOSR-TR-78-0054.

14. Smith, T.L., "Strength and Extensibility of Elastomers", Rheology, Vol. V, F.R. Eirich (ed.), Academic Press, (1969), pp. 127-221.

A TECHNIQUE TO MEASURE POISSON CONTRACTION IN SMALL BIOLOGICAL SPECIMENS

by

W. G. KNAUSS

and

V. H. KENNER

California Institute of Technology

Pasadena, California

Abstract - The task of characterizing the mechanical properties of fibers from intervertebral discs has led to a simple non-contact method for measuring Poisson contraction in such specimens. Experiments to evaluate the method are described. Utilizing the results of these tests, resolution levels and practical limitations for the method are discussed.

Introduction

The mechanical characterization of even isotropic materials requires the determination of two (elastic) constants or (viscoelastic) time-dependent functions. For materials which are sufficiently stiff and permit suitable specimen size, a uniaxial test in which both longitudinal and transverse (electrical or mechanical) strain gages are used provides both Young's modulus and Poisson's ratio for elastic materials, or corresponding time-dependent functions otherwise. However, for more compliant materials and, in particular, materials where the specimen size is intrinsically small, the determination of a second material parameter is more difficult.

The work presently reported was motivated by the desire to characterize the time-dependent behavior of intervertebral disc material. Such specimens, which are approximately 10 mm long with an average cross-section of 2 mm by 0.5 mm are amenable to uniaxial relaxation experiments, which were successfully conducted to acquire one material parameter. This report describes an apparatus developed and experiments conducted to measure the lateral contraction of small, soft material samples exemplified by the spinal disc material.

The use of a non-contact type of measurement is practically required for the situation of interest. However, specimen surface irregularity and corresponding difficulties in modifying

such surfaces to be reflective, or diffuse, or ruled mitigate against the use of interferometric or moiré techniques. Direct distance measurement at high magnification is possible. However such measurements are typically time consuming, yield information at no more than several axial positions along a specimen that may be both property-wise and geometry-wise nonuniform, and are not suited to monitoring time-dependent dimensional change. The shadowgraphic method described below does not require any special surface properties for the specimen, although it does require opacity. It permits an averaging measurement over an appreciable portion of the specimen length which is advantageous for specimens whose dimensional tolerances are not precisely controlled. Further, time-dependent monitoring is easily accomplished. The method is reminiscent of that reported by Saylak[1] but differs in permitting averaging over specimen length and in its lower level of complexity.

Experiment

The basic concept of the experimental method is to cast the shadow of a portion of an opaque specimen on an otherwise uniformly (both spatially and temporally) illuminated photodetector field (c.f. fig. 1) so that a change in specimen width corresponds to a change in the total light incident on the detector. A schematic diagram of the apparatus used to accomplish this is shown in fig. 2. The beam from a 5 mw ruby laser (Spectra Physics Stabilite Model 120/249) is first spatially

filtered and then collimated to produce a spatially uniform circular beam of approximately 50 mm diameter. The specimen, held in a straining frame (cf fig 3), is interposed into this beam, casting a vertical shadow. The rectangular light field incident on the photodetector is determined by a system of knife edges located between the specimen and the photodetector. Two horizontal edges are vertically adjustable and define the top and bottom of the field. Two vertical edges attached to micrometer heads are horizontally adjustable and both define the vertical edges of the field and allow for calibration. The output of the photodetector is recorded on a strip recorder.

In order to explore the limitations of this apparatus, we measured the lateral contraction in rubber specimens (SBR) approximately 25 mm long with widths ranging from roughly 2 to 4 mm. A specimen was mounted in the straining frame under sufficient tension to keep it taut. The top and bottom knife edges were then adjusted so that the shadow of approximately the middle third of the specimen was passed to the photodetector. Both vertical knife edges were then closed down until all light was blocked and then singly advanced in .025 mm steps throughout the operating range. This produced a strip chart record of output vs. knife-edge locations for each side of the specimen which, upon replotting, are typified by the calibration curves shown in fig. 4a. As discussed below, it became desirable during the course of the experiments to modify the apparatus by eliminating the spatial

filter. A calibration for the configuration without the spatial filter is presented in fig. 4b. After setting each knife edge so that the operating point was in the linear portion of the respective calibration curve, the specimen was extended known amounts through a 0.787 thread per mm loading screw. The maximum extension applied was 7.62 mm, corresponding to a specimen elongation of approximately 30%. After testing and while still in the loading frame, the dimensions of the specimen were measured in the initial state using an optical comparator.

Results

The data were reduced by taking the average of the two calibration curve slopes at the operating points (fig. 4) and applying the reciprocal of this number (mm of opening per unit of chart deflection) to the output resulting from stretching the specimen. Typical plots of transverse (contraction) strain $\Delta w/w_o$ vs. longitudinal strain $\Delta \ell/\ell_o$ are presented in figs. 5 and 6 for the four specimens labeled 1 through 4, respectively. Figure 5 represents results obtained with the spatial filter in place while fig. 6 shows results in the absence of the spatial filter. The solid curves in these figures represent the equation

$$\frac{\Delta w}{w_o} = \frac{1}{\sqrt{\frac{\Delta \ell}{\ell_o} + 1}} - 1 , \qquad (1)$$

which expresses incompressibility.

The vertical extent of the error rectangles shown in figs. 5 and 6 represents the predominant experimental error, namely, jumps or long-time drift in the laser output. The horizontal dimension of the error rectangles indicates the worst uncertainty in inferring specimen elongation from turns of the loading screw, and was ascertained experimentally by measuring actual elongations with an optical comparator. The points denoted by the symbol "x" in figs. 5 and 6 represent measurements made using the optical comparator, which has a least count of 2.5×10^{-3} mm. The error band associated with this measurement (fig. 6) was found experimentally by repeating the measurements three times.

Discussion

It was found that after a warm-up period of several hours the laser output was quite stable, with power variations of approximately 1% over a duration up to about 9 hours. However, when the spatial filter was included the variations in output could at best be reduced to approximately 2%. Furthermore, the variation in this case consisted in sharp (several seconds) discontinuities evidently associated with laser instability arising from reflection at the aperture back into the laser cavity. Thus some tests were conducted without the spatial filter in place. As can be seen from the two different calibration slopes of fig. 4, this configuration sacrificed spatial

uniformity, although the linearity of the individual curves is improved relative to the calibration shown in fig 4a. Since data reduction was based on an average slope obtained from the two curves it is implicitly assumed that specimen contraction is the same on either side. The smaller error limits and corresponding decrease in data scatter with multiple loadings for fig. 6 as compared to fig. 5 is due to removal of the spatial filter.

The vertical error bar of fig. 6 for specimen 4 corresponds to a change of specimen thickness of 6 μm. This value, which is taken as the resolution limit of the present apparatus, places a lower limit on specimen width for a prescribed value of experimental error. If, for illustrative purposes, a material is assumed to be imcompressible, then the sample thickness w_o necessary to give a specified error in the measurement of Δw is easily determined as given in fig. 7 for several values of acceptable error.

Several error sources are associated with specimen geometry. First, the gauge length is effectively shortened by the constraint to lateral motion at the gripped ends. This is of course minimized by maximizing specimen length. Second, variations in specimen width and thickness will affect the results as sections of variable dimensions enter or leave the field of view during stretching of the specimen. This consideration is particularly important when large axial strains

are applied. Third, width and/or thickness changes give rise to nonuniform strain along the length of the specimen. If width variations are small and regular enough so that the approximation of one-dimensional strain is reasonable, the statement of a stress-strain law (taken as linear here) permits determination of the actual changes in illuminated field area ΔA. For a specimen of constant thickness and varying width whose average value is w_{avg}, the ratio of actual area change to that expected if the width were constant is

$$\frac{\Delta A}{\Delta A_{expected}} = \frac{\ell / w_{avg}}{\int_0^{\ell} \frac{ds}{w}} , \tag{2}$$

where ℓ is the length which w is averaged over and s is the position along the specimen. Evaluation of eq. (2) for sinusoidal thickness variation between a minimum thickness t_1 and a maximum thickness t_2 produces

$$\frac{\Delta A}{\Delta A_{expected}} = \frac{2\sqrt{w_1/w_2}}{(1 + \frac{w_1}{w_2})} . \tag{3}$$

Calculations from eq. (3) show that the experiment is insensitive to modest variations in specimen thickness; for 10% and 50% variations of this parameter the errors will be only 0.1% and 5.7%, respectively.

The transverse contractions of specimen 1 and 3 (figs. 5 and 6) were found to be well below the anticipated incompressible values. For this reason, the results of the shadow

experiment were checked independently by measurements made in an optical comparator. For specimen 3 (fig. 6) agreement was well within the measurement error. For specimen 1 (fig. 5) the comparator measured value was even lower. In this case it was found, by examination under 50X magnification, that extensive edge cracks existed which resulted in highly nonuniform strain, and this nonuniformity was taken as an explanation of the less than anticipated lateral contraction. The results for both specimens 2 and 4 differed from incompressible behavior by less than the respective experimental errors.

Acknowledgment

The authors wish to express their appreciation to Mr. Bob Calvet for his contributions to the development of the apparatus. The work was funded by the Air Force Office of Scientific Research, [redacted].

AFOSR-77-3139

Reference

1. Saylak, D., "True Stress-Strain Properties for Filled and Unfilled Polymers and Elastomers as Functions of Strain Rate and Temperature," Applied Polymer Symposia, No. 1, 247-260 (1965).

Nomenclature

ΔA, $\Delta A_{expected}$	change in illuminated field area for nonuniform and uniform specimens, respectively
ℓ, ℓ_o, $\Delta\ell$	specimen length, initial length and change in length, respectively
r	resolution
s	position
w, w_o, Δw, w_{avg}	specimen width, initial width, change in width and average width, respectively

Captions for Figures

Fig. 1 Light field (a x b) and shadow cast by specimen before (w_o) and after (w) stretching parallel to the dimension b.

Fig. 2 Top view of the experimental apparatus.

Fig. 3 Straining Frame.

Fig. 4 Calibration records for a) the spatial filter in place, and b) the spatial filter removed. The arrows denote the operating points for the subsequent experiments.

Fig. 5 Transverse vs. longitudinal strain for two runs with the spatial filter.

Fig. 6 Transverse vs. longitudinal strain for two runs without the spatial filter.

Fig. 7 Minimum specimen width for several error levels vs. longitudinal strain. Here r represents the resolution (taken as 6μm) and the error $E = r/\Delta w$.

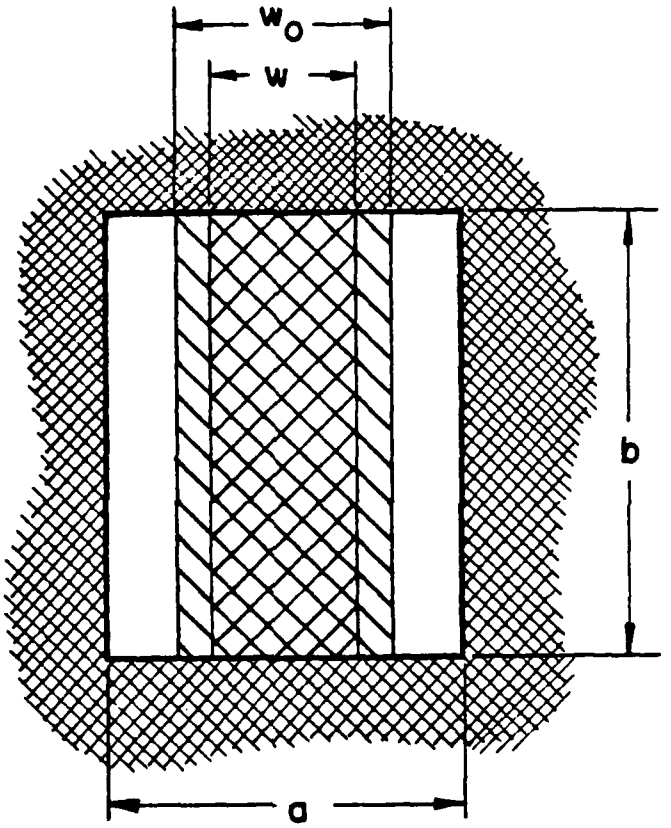
w_o
w
b
a

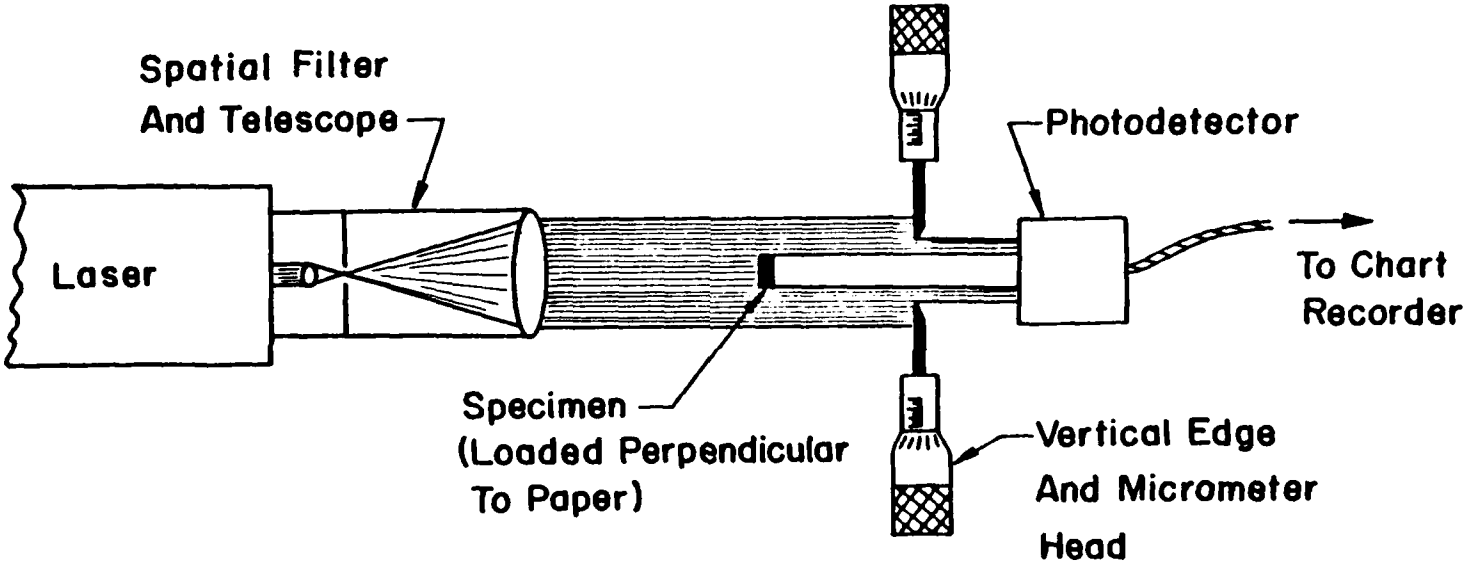
Spatial Filter
And Telescope
Photodetector
Laser
To Chart
Recorder
Specimen
(Loaded Perpendicular
To Paper)
Vertical Edge
And Micrometer
Head

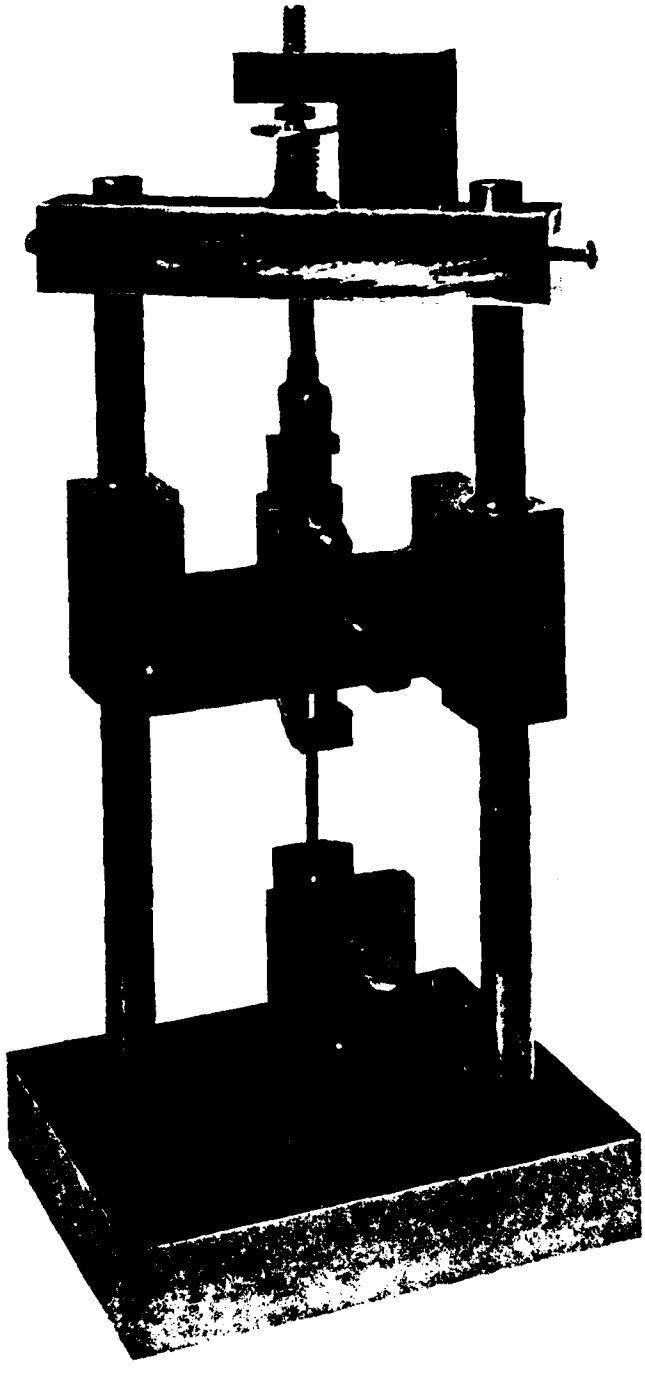

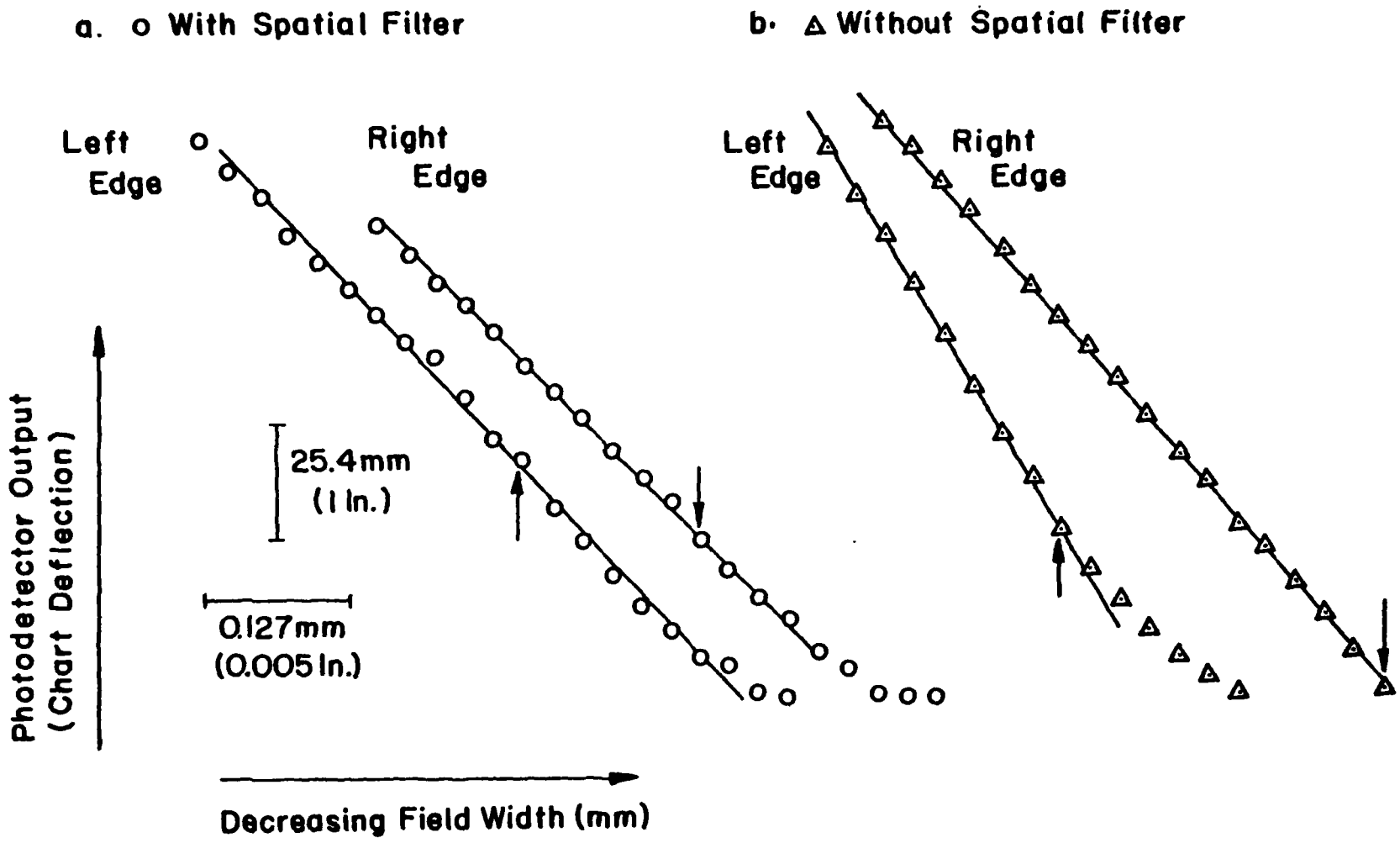
a. o With Spatial Filter
b. Δ Without Spatial Filter
Left Edge
Right Edge
Left Edge
Right Edge
25.4mm (1 In.)
0.127mm (0.005 In.)
Photodetector Output (Chart Deflection)
Decreasing Field Width (mm)

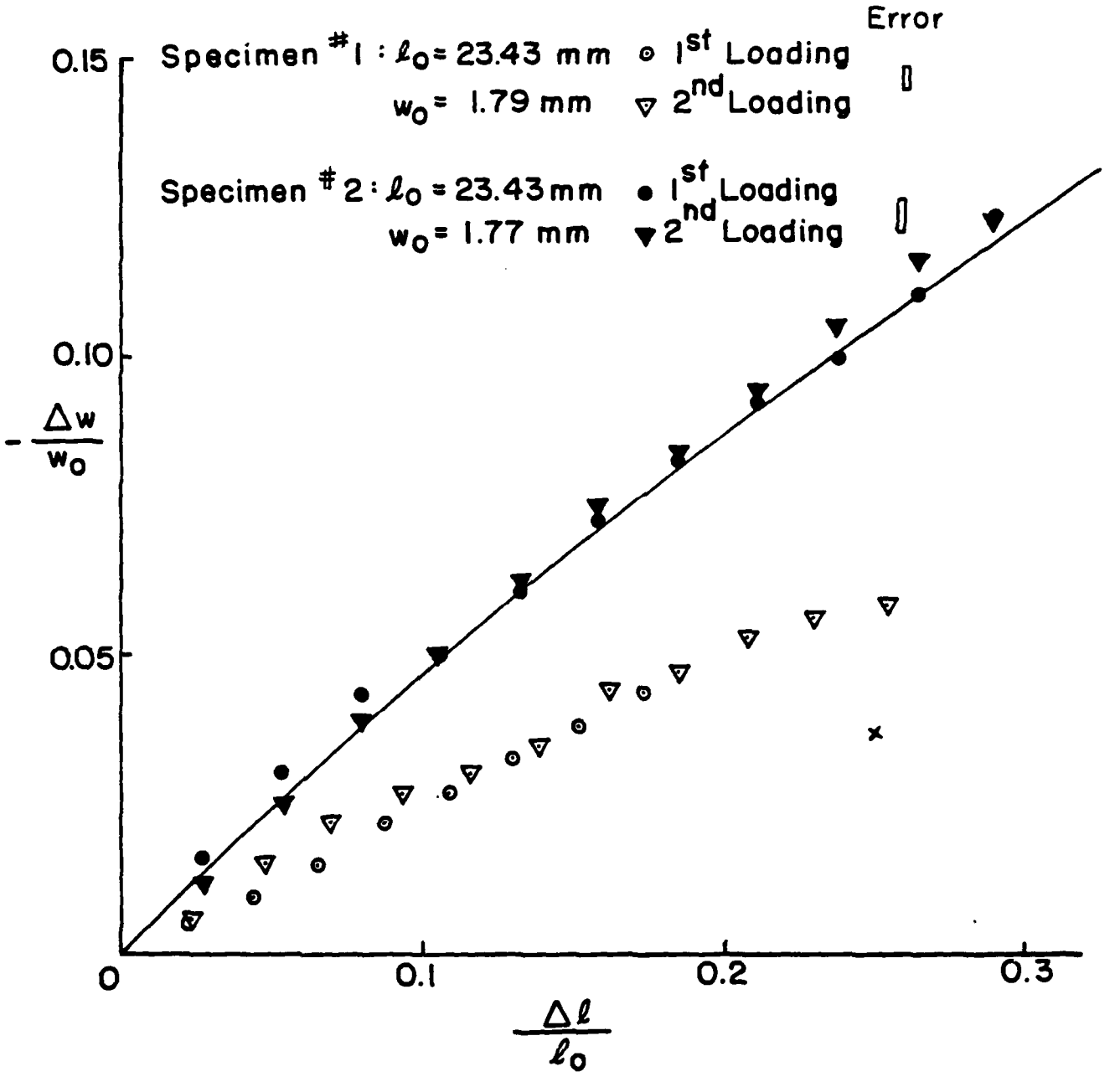
Error
Specimen #1 : ℓ_0 = 23.43 mm
w_0 = 1.79 mm
1st Loading
2nd Loading
Specimen #2 : ℓ_0 = 23.43 mm
w_0 = 1.77 mm
1st Loading
2nd Loading
0.15
0.10
0.05
0
0.1
0.2
0.3
$-\frac{\Delta w}{w_0}$
$\frac{\Delta \ell}{\ell_0}$

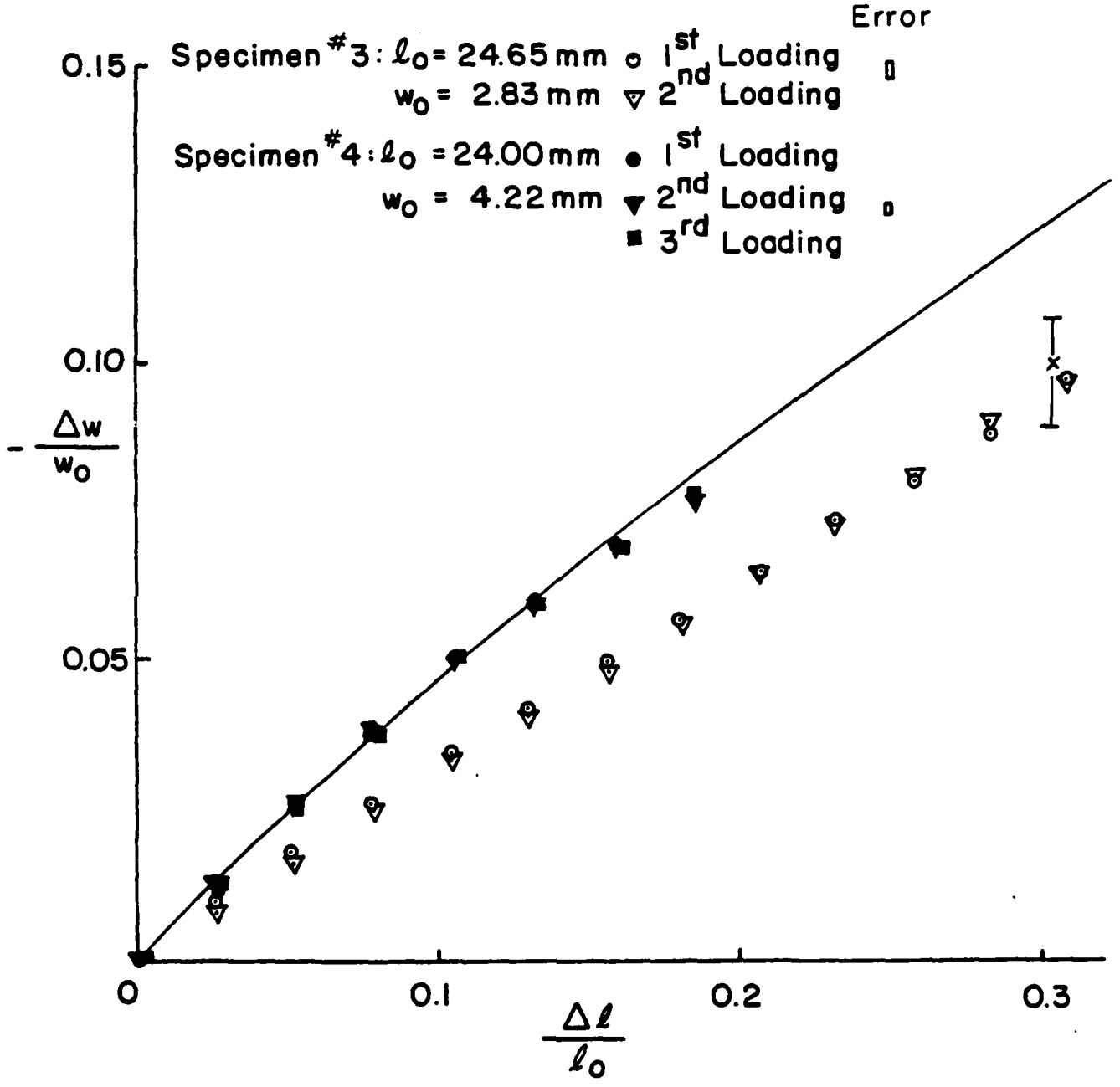
Error
Specimen #3: ℓ_o = 24.65 mm
w_o = 2.83 mm
o 1st Loading
▽ 2nd Loading
Specimen #4: ℓ_o = 24.00 mm
w_o = 4.22 mm
● 1st Loading
▼ 2nd Loading
■ 3rd Loading
0.15
0.10
0.05
0
0.1
0.2
0.3
$-\frac{\Delta w}{w_o}$
$\frac{\Delta \ell}{\ell_o}$

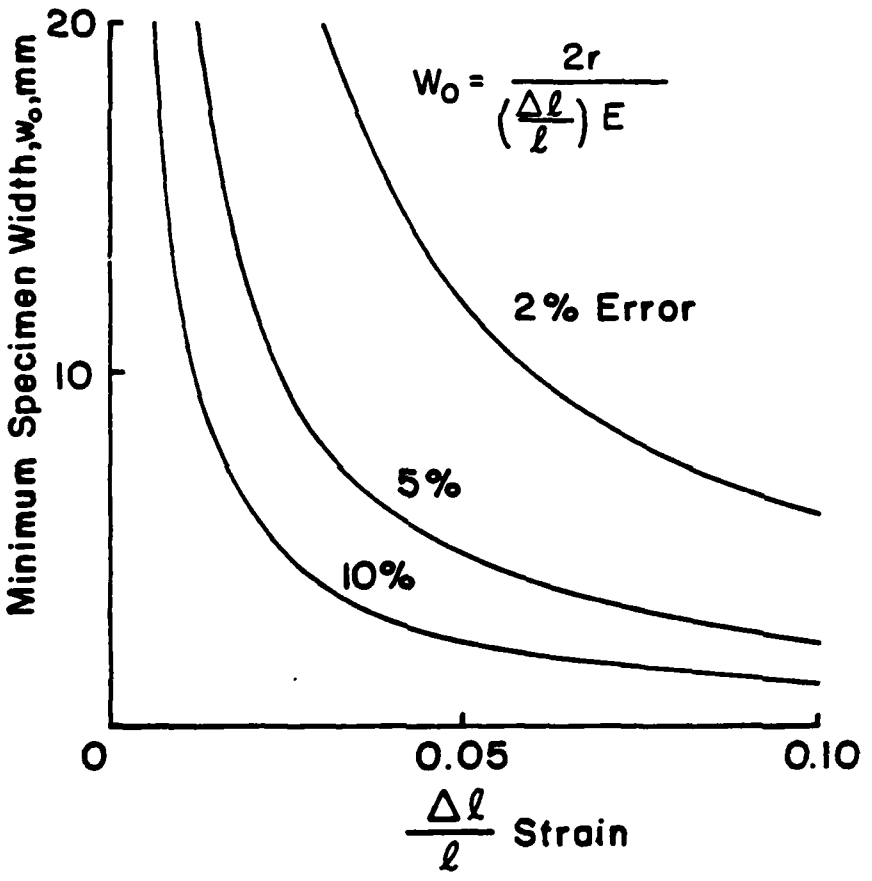
Minimum Specimen Width, w_o, mm
20
10
0
0.05
0.10
$\frac{\Delta \ell}{\ell}$ Strain
$W_o = \frac{2r}{(\frac{\Delta \ell}{\ell}) E}$
2% Error
5%
10%

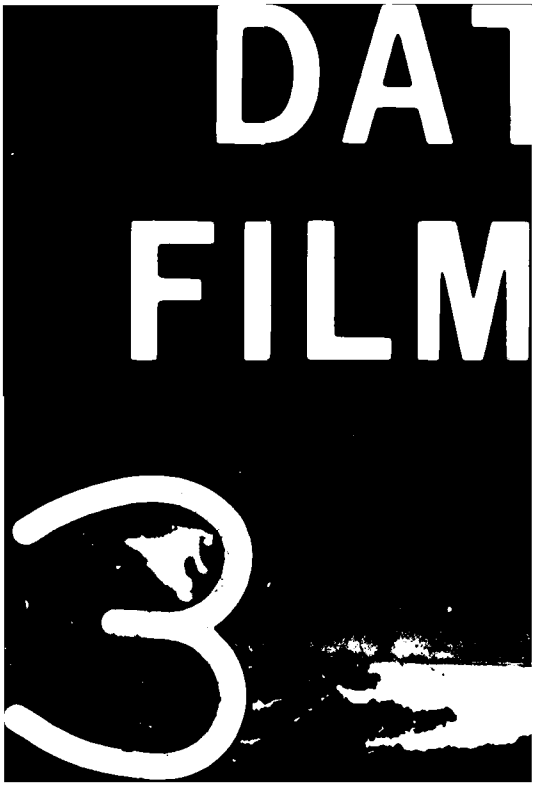
DAT
FILM